Modeling, Control, and Optimization for Diesel-Driven Generator Sets

Knudsen, Jesper Viese

DOI (link to publication from Publisher):
10.5278/vbn.phd.tech.00032

Publication date:
2017

Document Version
Publisher's PDF, also known as Version of record

MODELING, CONTROL, AND OPTIMIZATION FOR DIESEL-DRIVEN GENERATOR SETS

BY
JESPER KNUDSEN

DISSERTATION SUBMITTED 2017

AALBORG UNIVERSITY
DENMARK

Modeling, Control, and Optimization for Diesel-Driven Generator Sets

Ph.D. Dissertation

Jesper Knudsen

AALBORG UNIVERSITY
DENMARK

Dissertation submitted December 22, 2017

Dissertation submitted:	December 22, 2017
PhD supervisor:	Assoc. Prof. Jan D. Bendtsen Aalborg University
Assistant PhD supervisor:	Assoc. Prof. Palle Andersen Aalborg University
Ph.D. Supervisor: (Industrial)	Program Manager Claes H. Sterregaard DEIF
Assistant Ph.D. Supervisor: (Industrial)	Senior Engineer Kjeld K. Madsen DEIF
PhD committee:	Associate Professor Henrik Schiøler (chairman) Aalborg University
	Professor Jan Tommy Gravdahl Norwegian University of Science and Technology
	Director Tommy Mølbak Added Values
PhD Series:	Technical Faculty of IT and Design, Aalborg University
Department:	Department of Electronic Systems

ISSN (online): 2446-1628
ISBN (online): 978-87-7210-117-0

Published by:
Aalborg University Press
Skjernvej 4A, 2nd floor
DK – 9220 Aalborg Ø
Phone: +45 99407140
aauf@forlag.aau.dk
forlag.aau.dk

Printed in Denmark by Rosendahls, 2018

Abstract

Diesel-driven generator sets constitute an important element in a broad spectrum of distributed electrical power generation applications worldwide. Due to their high reliability and low cost, diesel-driven generator sets continue to be the preferred choice whenever the power infrastructure is weak or requires backup; from failsafe applications, such as hospitals, to interim mains establishment and expansion applications. Diesel-driven generator sets are subject to increasing demands regarding efficiency and performance, yet at the same time they must be easy to commission and robust to disturbances. In order to reach these demands, the industry is currently directing its attention towards implementation of more sophisticated control techniques. In light of this, the present thesis addresses the following two important issues in relation to diesel-driven generator set control.

First, current industry-standard control solutions for individual diesel-driven generator sets are based on classical proportional-integral-derivative regulation principles. One drawback of the current solutions is the built-in requirement of time-consuming manual regulator parameter tuning, which to a large extent determines the system performance. Due to this rather decisive human involvement suboptimal and/or inconsistent performance must often be expected. To address this issue, a first principles-based model is derived and a control scheme designed for one of the fundamental operating modes, that is, frequency and voltage regulation, paying particular attention to ease of commissioning and insensitivity to load changes. In addition to simplifying the parameter tuning process, the established solution facilitates a potentially fully automated parameter tuning solution. The control design approach is implemented on two diesel-driven generator sets, demonstrating clear benefits in end-user simplicity and system performance.

Second, improvements in systemwide fuel efficiency hold great potential financial and environmental benefits in applications including large numbers of diesel-driven generator sets operated continuously. Current market-leading solutions utilize a repetitive Unit Commitment scheme based on predefined priority parameters; disregarding live system information, which is becoming increasingly available due to advances in communication and data

gathering technologies. To address this second issue, an optimization algorithm capable of achieving fuel efficiency improvements for applications with a large number of diesel-driven generator sets is proposed. Solving the two-sided problem of Unit Commitment and Economic Dispatch, significant fuel efficiency improvements are obtained through the use of live fuel consumption information. Encouraging results are obtained in simulations where the live fuel consumption variations resemble measurements of fuel consumption during variations in operational conditions.

Resumé

Dieseldrevne generatorer udgør et vigtigt element i et bredt anvendelsesspektrum af distribueret elektricitetsproduktion på verdensplan. Grundet deres høje driftssikkerhed og lave omkostninger fortsætter dieseldrevne generatorer med at være det foretrukne valg, når elektricitetsinfrastrukturen er svag eller kræver støtte - fra fejlsikre applikationer, såsom hospitaler, til midlertidige applikationer med elnetsetablering og -udvidelse. Dieseldrevne generatorer er underlagt stigende krav til effektivitet og ydeevne, men de skal samtidig være nemme at sætte i drift og robuste overfor forstyrrelser. For at opfylde disse krav retter industrien i øjeblikket sin opmærksomhed imod implementation af mere sofistikerede kontrolteknikker. På baggrund af dette omhandler denne afhandling de følgende to vigtige emner, i relation til kontrol af dieseldrevne generatorer.

For det første er nuværende standard industriløsninger til individuelle dieseldrevne generatorer baseret på klassiske proportional-integral-derivative reguleringsprincipper. En ulempe ved de nuværende løsninger er det indbyggede krav om tidskrævende manuel regulatorparameterjustering, som i høj grad afgør systemets ydeevne. På grund af denne ganske afgørende menneskelige involvering bør suboptimal og/eller svingende ydeevne forventes. For at håndtere denne problemstilling udledes en model, baseret på fysiske principper, og et kontrolsystem designes til en af de fundamentale driftssituationer, nemlig frekvens- og spændingsregulering med særlig fokus på idriftsættelsesbyrden og modstandsdygtigheden overfor lastændringer. Udover at simplificere parameterjusteringen muliggør den fremstillede løsning en potentiel fuldautomatisk parameterjusteringsløsning. Kontroldesignet er blevet implementeret på to dieseldrevne generatorer, hvor det demonstrerer klare fordele i enkelheden for slutbrugeren samt systemets ydeevne.

For det andet indeholder forbedringer af den overordnede brændstofseffektivitet potentielt store økonomiske og miljømæssige fordele i applikationer, der inkluderer et stort antal af dieseldrevne generatorer, som kører uafbrudt. De nuværende markedsførende løsninger foretager gentagne overvejelser vedrørende Unit Commitment på baggrund af forudbestemte prioriteringer - og ignorerer aktuel systeminformation, som ellers bliver mere og

mere tilgængeligt grundet fremskridt indenfor kommunikations- og dataopsamlingsteknologier. For at håndtere dette andet problem foreslås en optimeringsalgoritme, som er i stand til at opnå forbedringer af brændstofseffektivitet for applikationer med et stort antal dieseldrevne generatorer. Væsentlige brændstofforbedringer opnås ved brug af aktuelle informationer om brændstofforbrug til at løse det dobblte problem med Unit Commitment og Economic Dispatch. Lovende resultater er opnået i simuleringer, hvor variationen i de aktuelle informationer om brændstofforbrug efterligner målinger af brændstofforbrug, som er taget under varierende driftsforhold.

Acknowledgments

First and foremost, I wish to thank Scanner Software Engineer Frederik Juul at 3Shape and Vice President Jan Aagaard at DEIF for initiating discussions between Aalborg University and DEIF that in the end provided me with the opportunity to take up this Ph.D. study.

I owe my interest in scientific research to the exceptionally contagious enthusiasm and curiosity of Senior Research Scientist Anuradha Annaswamy at Massachusetts Institute of Technology. During my one-year M.Sc. research stay in her Active Adaptive Control Laboratory at MIT, together with Power System Control Engineer Jacob Hansen at Pacific Northwest National Laboratory, Anuradha was a constant inspiration and I am forever grateful for her commitment towards two unacquainted M.Sc. students from the small country of Denmark. I thank Vice Dean and Professor Jakob Stoustrup at Aalborg University for arranging this research stay.

I wish to express my most sincere gratitude and deepest appreciation to my supervisors Associate Professors Jan D. Bendtsen and Palle Andersen at Aalborg University and Program Manager Claes H. Sterregaard and Senior Engineer Kjeld K. Madsen at DEIF. The excellent guidance, support, and encouragement by Jan and Palle, through countless hours of discussions, has been truly essential in the progress of my studies; I could not have hoped for a better pair of supervisors! The everlasting positive attitude and engagement from Claes and Kjeld has been crucial in aligning my studies with the problems and possibilities of the real world; thank you!

I am genuinely thankful for the hospitality extended to me by Reader John Anthony Rossiter at The University of Sheffield in the fall of 2016. Anthony's knowledgeable supervision and personal efforts allowed me to return from Sheffield with wonderful experiences of the beautiful city and countryside in addition to the scientific insights.

Last, but in no regards least, to my girlfriend Line; for showing me how life is meant to be lived, I am forever in your debt.

Jesper Knudsen
Aalborg University, December 22, 2017

Thesis Details

Thesis Title: Modeling, Control, and Optimization for Diesel-Driven Generator Sets

Ph.D. Student: Jesper Knudsen

Supervisors: Assoc. Prof. Jan D. Bendtsen, Aalborg University
Assoc. Prof. Palle Andersen, Aalborg University
Program Manager Claes H. Sterregaard, DEIF
Senior Engineer Kjeld K. Madsen, DEIF

Enclosed Papers: J. Knudsen, J. Bendtsen, P. Andersen, K. Madsen, and C. Sterregaard, "Control-oriented first principles-based model of a diesel generator," in *European Control Conference*, 2016, pp. 321-327

J. Knudsen, J. Bendtsen, P. Andersen, and K. Madsen, "Self-tuning linear quadratic supervisory regulation of a diesel generator using large-signal state estimation," in *Australian Control Conference*, 2016, pp. 32-37

J. Knudsen, J. Bendtsen, P. Andersen, K. Madsen, and C. Sterregaard, "Supervisory control implementation on diesel-driven generator sets," submitted for *IEEE Transactions on Industrial Electronics*, 2017

J. Knudsen, J. Bendtsen, P. Andersen, K. Madsen, C. Sterregaard, and A. Rossiter, "Fuel optimization in multiple diesel driven generator power plants," in *IEEE Conference on Control Technology and Applications (CCTA)*, 2017, pp. 493-498

This thesis has been submitted for assessment in partial fulfillment of the

Ph.D. degree. The thesis is based on the submitted or published scientific papers, which are listed above. Parts of the papers are used directly or indirectly in the extended summary of the thesis. As part of the assessment, co-author statements have been made available to the assessment committee and are also available at the Faculty.

Contents

Preface

This thesis is submitted as a collection of papers in partial fulfillment of a Ph.D. study at the Section for Automation and Control in the Department of Electronic Systems at Aalborg University, Denmark. The work has been conducted in the period from January 2015 to December 2017, supported by Innovation Fund Denmark and DEIF as part of the Industrial Ph.D. Project, Application Number 4135-00108B, under supervision of Associate Professors Jan D. Bendtsen and Palle Andersen, Program Manager Claes H. Sterregaard, and Senior Engineer Kjeld K. Madsen.

The thesis is split in two main parts. Chapters 1 to 6 make up Part I, containing motivation, state of the art, and an extended summary of the study. Part II provides the contributions in detail, through the publications enclosed as Papers A to D. The order of the papers follows the flow of Part I, rather than the exact progression of the study.

Besides modifying the layout, all enclosed publications are presented in the same form as they have been published. This entails minor notational differences between papers, reflecting the refinement of the work throughout the study. Furthermore, the notation employed in Part I will slightly deviate from that of the enclosed papers.

Jesper Knudsen
Aalborg University, December 22, 2017

Part I

Summary

1 Introduction

This chapter concerns the background for the research presented in this thesis by providing the motivation, describing the available laboratory facilities, and stating the research objectives.

The present thesis presents the work of an Industrial Ph.D. study, hence, the research motivation and objectives are to a large extent driven by the market conditions most relevant to the collaborating company, DEIF, and by the state of the current market-leading products. Consequently, the research objectives can be stated prior to examining the related academic state of the art.

1.1 Motivation

Diesel-driven generator sets provide essential reliability in an extensive range of electrical power generation applications worldwide [DEIF, 2016a,b]; with the number of applications only expected to increase in the near future [Johnson, 2014, 2016; Mordor Intelligence, 2016]. Figure 1.1 shows a standard configuration diesel-driven generator set, consisting of a diesel engine driving a synchronous generator with a rating of 40 kVA. Diesel-driven generator sets are interchangeably referred to as diesel generators, gensets, and DGs.

Diesel-Driven Generator Sets

At hospitals, data centers, laboratories, factories, etc., one or a few diesel generators are often installed to provide critical backup supply in the case of mains failure [DEIF, 2016a]. On many ships, offshore, and other installations where no mains connection is available, gensets reliably provide the required electrical power for normal operation [DEIF, 2016b]. Diesel generators in large numbers - occasionally into the hundreds - are installed operating collectively to provide electrical power in areas where an established mains is unavailable or unreliable [DEIF, 2016a, 2017a; MAN Diesel & Turbo, 2017; APR Energy, 2017a,b]. As examples, such conditions might arise in developing regions where no electrical power need has ever previously been present

Figure 1.1: Standard configuration diesel-driven generator set with a rating of 40 kVA.

or when established power plants are taken out of operation due to, e.g., maintenance, expansion, or accidents. Installations of this type are in most cases temporary; with the operational time frame varying from a few months to several years depending on the surrounding circumstances. A number of gensets are also often installed during musical festivals and sporting events, such as the Olympics or the World Cup, to provide electrical power capacity for extraordinary needs in a limited time period. Installations operating without a mains connection are, in general, referred to as island operation; some installations run exclusively in island operation, while others have the possibility to establish connection to an available mains if necessary.

The operational requirements for diesel-driven generator sets depend to a large extent on the type of application in which they are installed. Ensuring sufficient power quality, that is, maintaining satisfactory frequency and voltage levels and transients, is the fundamental objective in applications where one or multiple gensets provide the electrical supply single-handedly. For so-called micro-grid applications, which may consist of various renewable energy resources, energy storage units, and conventional generation units, such as diesel generators, the task of ensuring power quality most often again falls to the conventional generation units. If a connection to a well-established, reliable mains is present, the objective is most likely to provide power generation; at a constant level or varying according to a schedule or intermittent conditions. However, gensets might occasionally be required to aid in ensuring power quality even with a mains connection.

Operation of a diesel-driven generator set according to requirements essentially involves operating its two components; the diesel engine and the electrical generator. Many conceptually different generator designs are utilized worldwide, with the synchronous generator comprising an important portion [Kundur, 1994; ENTSO-E, 2016]. This research specifically considers the salient four-pole, three-phase, brushless excited, synchronous generator as it is used for many industry-standard diesel-driven generator sets. In most genset applications, the angular velocity of the engine shaft is regulated by a so-called governor. The engine shaft connects directly to the synchronous generator and the generated voltage is, correspondingly, regulated by a so-called Automatic Voltage Regulator (AVR). For synchronous generators the electrical frequency of the generated voltage is in steady-state directly proportional to the angular velocity of the driving engine shaft. When features such as synchronization, active and reactive power regulation, or automatic mains failure response are required, an additional supervisory controller is needed; namely, a so-called Automatic Genset Controller (AGC) unit. A conceptual diagram of such a system is shown in Figure 1.2.

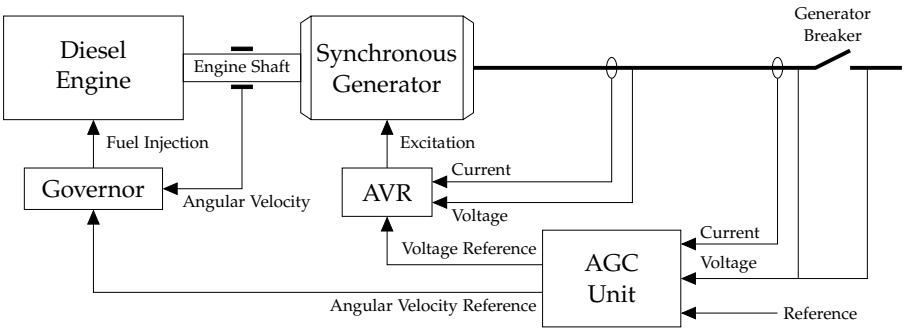

Figure 1.2: Conceptual diagram of a diesel-driven generator set including the control system. The fuel injection regulating governor and the excitation regulating Automatic Voltage Regulator act on references provided by the Automatic Genset Controller unit.

As indicated in Figure 1.2, the governor regulates the fuel injection in order to achieve the required angular velocity of the engine shaft. In a similar manner, the AVR regulates the excitation of the synchronous generator to obtain the required voltage at the generator terminals. Traditionally, governors and AVRs apply one of two characteristic schemes for determining the required angular velocity and voltage, respectively; that is, for determining their respective internal control references. These two schemes are called isochronous and droop operation, respectively. Applying the isochronous scheme entails operating with a constant internal control reference of nominal value irrespectively of the present electrical load situation. Conversely, the droop scheme entails determining the internal control reference based on

the present load situation. For the governor, the droop scheme implies altering the internal angular velocity control reference according to the engine load. The extent to which the internal reference is altered is a variable parameter in droop schemes, usually provided as a percentage. A 4% droop, for example, refers to a characteristic scheme where the internal control reference is lowered 4% of the nominal value at full load. Applying a droop scheme in the AVR implies altering the internal voltage control reference according to the reactive power. The principles of both schemes are shown in Figure 1.3.

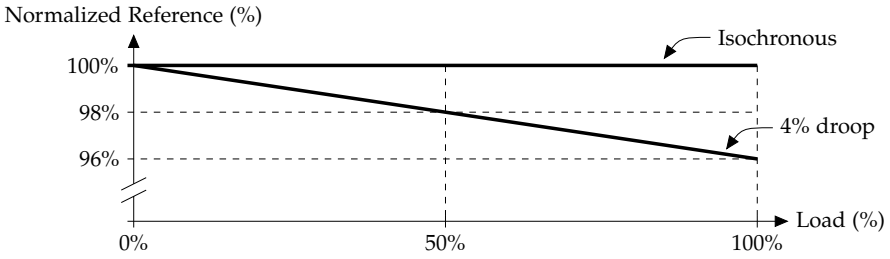

Figure 1.3: Principles of the isochronous and droop characteristic schemes.

Utilizing multiple gensets in parallel without additional supervisory control, such as an AGC, generally requires the droop scheme to be applied in all connected genset governors and AVRs. The diesel generators will then share the load in accordance with the droop settings and thereby reach consensus on the angular velocity and voltage level. If connected while applying the isochronous scheme, even with identical settings, gensets will most likely be unable to settle on a common angular velocity and voltage due to, for example, measurement differences. Ultimately, this will in most cases cause stability issues as gensets start pushing power between each other.

Automatic Genset Controllers

The introduction of an AGC as a supervisory control unit enables additional features, such as controlling the active and reactive power output and synchronizing the voltage across a generator breaker before closing the breaker. The features are implemented, as shown in Figure 1.2, by providing the governor and AVR with external control references, which act as offsets to the internal control references. Although an AGC is generally installed to enable additional features, many diesel generators with AGCs operate in situations where the objective is to ensure power quality. Thus, an AGC usually includes angular velocity and voltage control. It is important to notice that the governor and AVR continue to operate according to either the isochronous or the droop scheme, even when an AGC is providing external control references. This, together with the inherent communication delay between the

governor and AVR and the AGC, entails that an AGC actually risks worsening the control performance on the angular velocity and the voltage if the AGC is inadequately tuned.

The Danish company DEIF is a global market-leading supplier of control solutions for decentralized power production [DEIF, 2017b]. Supervisory control units, such as AGCs, are one of the core businesses for DEIF. Generally, the units implement a large number of features apart from the principal regulation. These additional features can be categorized by protection, monitoring, and instrumentation, just to mention a few. Most, if not all, global manufacturers of AGC units, including DEIF, utilize fundamentally similar principles of control theory for the control of a single genset; namely, the proportional-integral-derivative (PID) regulator. In general, the PID regulator has been the regulator of choice in many industries for the past decades due to its essential qualities of simplicity and applicability. PID regulators offer compelling properties through a simple structure, requiring little system information while at the same time having the capability of stabilizing a wide range of systems. However, regulator parameter tuning must be conducted for each diesel generator during commissioning. Even after such tuning, that is, if the commissioning engineer actually has the time, skill, and opportunity to modify the standard conservative set of regulator parameters provided in an AGC, the regulator is most likely to exhibit suboptimal control performance due to the high complexity of a diesel generator. Utilizing alternative control theoretical principles in the industry of electrical power generation has been considered for many years [Carpentier, 1985]; however, genset controller manufacturers have not until recent years been in a position, in terms of both knowledge and technology, to actually attempt advancements.

Diesel Generator Plants

Diesel-driven generator sets operating collectively to supply reliable electrical power are commonly referred to as a plant. The number of diesel generators in a plant depends on the electrical power needs at the location in which the plant is established; in general, ranging from only a few diesel generators to occasionally more than a hundred [DEIF, 2016a, 2017a]. Typically, each diesel generator in the plant is equipped with an AGC, which acts on references from an additional supervisory control unit performing so-called plant management. Figure 1.4 provides a single-line diagram of a plant consisting of 24 gensets. This plant is structurally made up of four so-called branches, which in Figure 1.4 can be identified as the four columns of diesel generators; each column consisting of six diesel generators. In this example each branch applies a different structure in terms of transformer utilization. Although different structures are rarely implemented across one plant, this is shown in Figure 1.4 to demonstrate how particular plants may differ in other

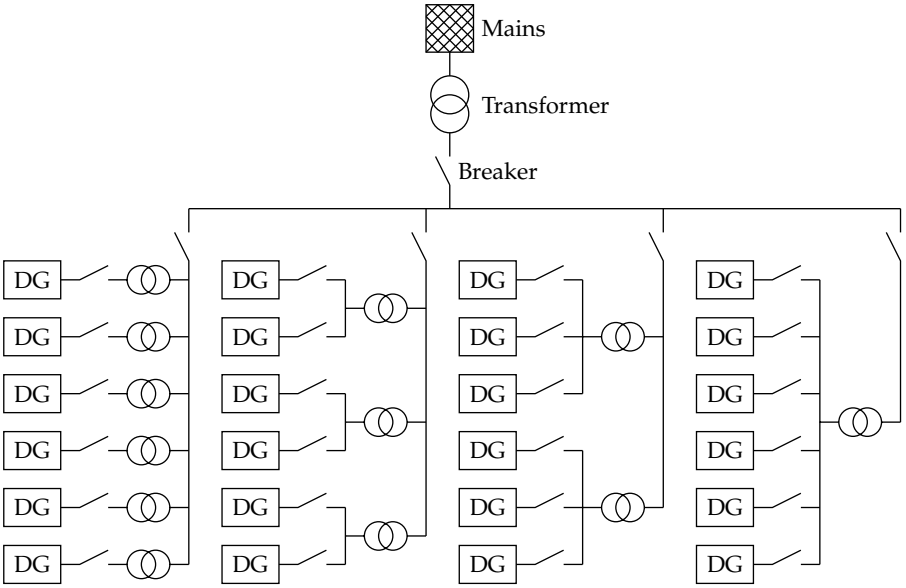

Figure 1.4: Diagram of a 24 genset plant with four branches utilizing different branch structures.

aspects than merely the number of diesel generators. As previously mentioned, a plant does not necessarily have one connection to mains; it could have multiple connection points or none at all.

Plant management controllers are responsible for aligning the operation of a plant with the, for every specific situation, existing requirements. In addition to frequency, voltage, and power concerns, objectives such as fuel optimization have become increasingly important in plant management in recent years. Current market-leading plant management solutions incorporate fuel optimization considerations by determining the number of diesel generators required to run for a given situation. Naturally, in some situations the conditions might prevent such optimization; for example, if the required power generation level of the entire plant dictates all gensets to assist. This type of fuel optimization takes advantage of the fact that diesel generators are most efficient at high load conditions; however, it disregards any efficiency difference that might be observed from one diesel generator to another.

1.2 Laboratory Facilities

In the course of this Industrial Ph.D. study, constantly keeping a close connection to the real world systems and applications has had high priority. Consequently, whenever possible and meaningful, the work has been based on, compared with, and applied to real diesel-driven generator sets.

The facilities utilized for this purpose are located in a designated laboratory at the headquarters of DEIF in Skive, Denmark. The relevant elements and their interconnections are shown in Figure 1.5 as a single-line diagram.

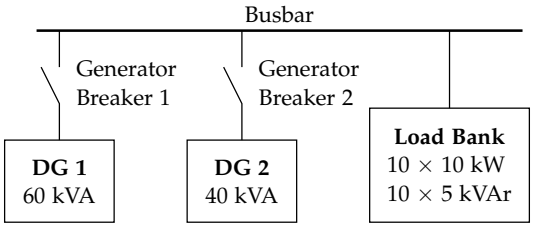

Figure 1.5: Single-line diagram of the laboratory facilities, consisting of two diesel-driven generator sets connected through individual generator breakers to the load bank at the busbar.

The laboratory contains two diesel generators of different ratings and a controllable load bank with both resistive and inductive load elements. As shown in Figure 1.5, each diesel generator connects to the load bank on a common busbar through individual generator breakers. These generator breakers are operated by AGCs installed on each genset; if both breakers should be closed for a load-sharing application experiment, the AGC closing the breaker last must synchronize its diesel generator to the busbar frequency and voltage before closing the breaker.

Diesel Generator 1

This diesel generator is made up of a turbocharged, four-stroke, four-cylinder Deutz BF4M2012 diesel engine and a salient four-pole, three-phase, brushless excited, synchronous, 60 kVA/48 kW at 50 Hz Leroy-Somer LSA 42.3 L9 C6/4 generator. The diesel engine is controlled by a Deutz EMR 2 governor and the synchronous generator is controlled by a DEIF DVC310 Automatic Voltage Regulator. For verification of the fuel consumption estimate provided by the governor, a Titan/RS Pro OG1-SSS-SSQ-B oval gear flowmeter has been mounted in the fuel supply path. Diesel Generator 1 is shown in Figure 1.6.

Diesel Generator 2

Shown previously in Figure 1.1, Diesel Generator 2 is the smaller of the available gensets. It consists of a turbocharged, four-stroke, four-cylinder Deutz BF4M1011F diesel engine and a salient four-pole, three-phase, brushless excited, synchronous, 40 kVA/32 kW at 50 Hz Mecc Alte Spa ECO 32-3S/4 generator. The diesel engine is controlled by a Huegli Tech HT-SG-100 governor while the synchronous generator is controlled by a DEIF DVC310 Automatic Voltage Regulator, similarly to the generator on Diesel Generator 1.

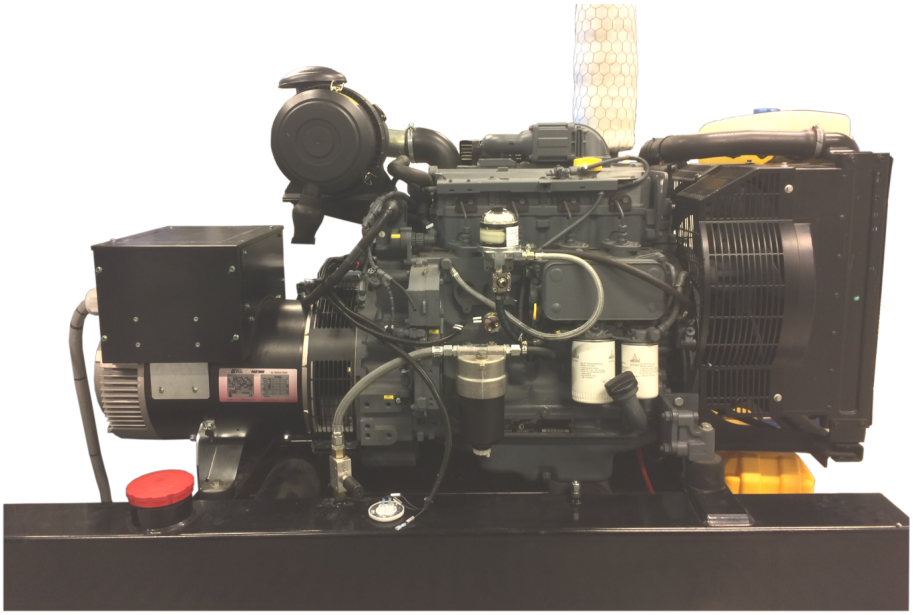

Figure 1.6: 60 kVA/48 kW diesel-driven generator set available at the laboratory facilities at the headquarters of DEIF in Skive, Denmark.

Load Bank

The load bank is a controllable system of active and reactive load elements, which can be connected in parallel. The active load elements are ten resistive JEVI heating elements placed in a 10 m^3 water tank. With a 400 V phase-to-phase RMS voltage each heating element is a 10 kW three-phase load, which enables an applied active load from 0 to 100 kW in steps of 10 kW. The actual per phase resistance is 16 Ω for each heating element. The reactive load elements are ten custom-built DANTRAFO inductors. With a 400 V phase-to-phase RMS voltage at 50 Hz each inductor is a 5 kVAr three-phase load, which enables an applied reactive load from 0 to 50 kVAr in steps of 5 kVAr. The actual per phase inductance is roughly 102 mH for each inductor.

Rapid Control Prototyping System

To enable time-efficient testing a Rapid Control Prototyping (RCP) system based on a dSPACE DS1103-07 400 MHz PPC controller board is available in the laboratory facilities by collaboration with the Section for Automation and Control at Aalborg University, Denmark. Shown in Figure 1.7, the RCP system uses dSPACE Release 2015-A 64-bit software on a Microsoft Windows® 7 SP1 64-bit desktop PC with MATLAB Simulink® R2015a software.

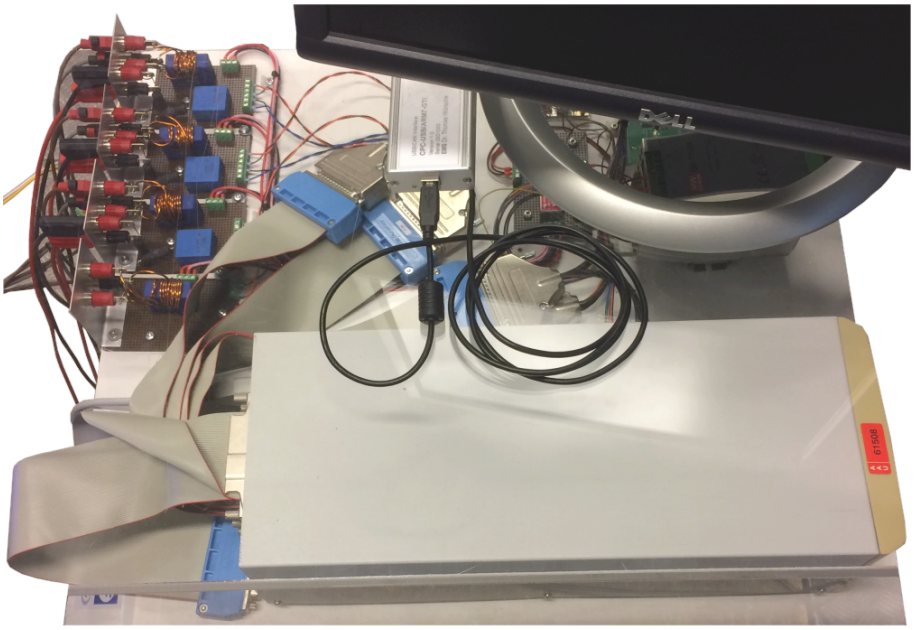

Figure 1.7: Rapid Control Prototyping system based on a dSPACE DS1103-07 400 MHz PPC controller board available in the laboratory by collaboration with Aalborg University.

Each of the three phase currents and voltages, used during RCP for load estimation and RMS voltage calculations, are obtained through LEM® LA 25-P current transducers and LEM® LV 25-P voltage transducers, respectively. The frequency measurement is a calculated value based on timestamped interrupt signals from a magnetic pick-up on the engine shaft giving 129 pulses per revolution, both on DG 1 and DG 2. The RCP system is executed at a 10 kHz base frequency with measurement intervals determined by the rotational speed of the engine shaft to provide 16 samples per period.

The control commands from any AGC control algorithm subject to testing is sent to the governor and AVR as a 40 ms Controller Area Network (CAN) J1939 message, resembling a typical communication speed and protocol of industrial AGC units.

Data Collection System

Measurements obtained throughout this Industrial Ph.D. study come from a separate system to that of the RCP system, allowing for a high sampling rate without putting an additional computational load on the RCP system. Data collection is done using a HIOKI Memory HiCorder 8861 with High Resolution Unit 8957 input modules. During every test all three phase currents and

voltages are measured by three HIOKI 9667 Flexible Clamp On Sensors and three Metrix MX9030-Z differential probes, respectively. Further, the signals from the magnetic pick-up on the diesel engine shaft and the fuel flowmeter, mounted on Diesel Generator 1, are collected through Tektronix P2220 voltage probes. All measurements from the HIOKI data collection system are taken at a 50 kHz sampling rate; except the fuel flowmeter on Diesel Generator 1, which is sampled at 1 kHz.

1.3 Research Objectives

The ambitions for this Industrial Ph.D. study are founded on an identified potential for improvements to the current market-leading control solutions for decentralized power production. Additionally, acquiring fundamental knowledge about the involved systems and anchoring that knowledge in the collaborating company, DEIF, is crucial. Demonstrating a proof of concept solution is a vital step in that process.

The following research objectives have been formulated to determine the aspired outcome of this Industrial Ph.D. study:

- **Form a simulation model based on relevant physical principles of a diesel engine driving a synchronous generator suitable for applying supervisory control algorithms.**
  The availability of a simulation model will facilitate analysis of new control algorithms as part of the process of improving on the current solution with PID regulators. Besides accommodating the inherent need for a model in any model-based control design, simulation can be a powerful tool in general problem analysis and by revealing details of a new solution before it is implemented. Further, a simulation model can act as a source of information; especially if it is based on physical principles and quantities.

- **Propose an adaptive supervisory control algorithm for the Automatic Genset Controller, which reduces parameter tuning complexity during commissioning of a diesel-driven generator set.**
  Any alternative supervisory control algorithm must be capable of providing, at least, a similar level of control performance to that of the current PID regulator. Additionally, it must address the issue of parameter tuning in an effort to reduce the time that should be spent during commissioning; thereby, reducing the number of diesel generators in operation lacking proper parameter tuning.

- **Obtain a proof of concept solution for the proposed supervisory control algorithm in the available laboratory.**
  Anchoring the knowledge gained throughout this Industrial Ph.D. study in DEIF, is a crucial element for the future successful implementation of a new control algorithm in the Automatic Genset Controllers by DEIF. Tangible results, such as a proof of concept, is the best method for creating the required attention within the company. Furthermore, experiences gained from working closely with actual diesel generators can be used to improve and validate the characteristics of the simulation model.

- **Propose an optimization algorithm based on available fuel consumption data capable of optimizing the fuel consumption of a diesel generator plant complying to a power reference.**
  Considering the amount of fuel consumed by large diesel generator plants, any improvement in terms of fuel optimization is highly valuable. Current market-leading plant management units implement a fuel optimization method limited to determination of the required number of running diesel generators for a specific plant power reference. The extent of fuel savings obtainable for a typical diesel generator plant through utilization of available fuel consumption information by distributing the load to the most efficient gensets is to be investigated.

Establishing the above research objectives concludes the introductory chapter of the present thesis, by gathering the essential aspects of the motivation behind this Industrial Ph.D. study. Additionally, the research objectives set the direction for the following state of the art analysis.

2 State of the Art and Contributions

This chapter provides an overview of related work before emphasizing how the contributions of this thesis expand upon the state of the art.

The application of Automatic Genset Controllers has seemingly caught rather limited academic attention; therefore, a large portion of the related work only partially coincides with the research objectives of this Industrial Ph.D. study.

Plant management in the context of diesel-driven generator sets focusing on fuel optimization has to the best of my knowledge escaped academic attention. Pertaining to so-called microgrids, considerations regarding fuel consumption of diesel generators come into play; however, the primary attention in such works is naturally directed at the utilization of renewable energy resources and energy storage units rather than the diesel generators. Although at a different scale than management of diesel generator plants, works related to the traditional so-called macrogrid or mains include considerations and approaches, which to some extent coincide.

2.1 Diesel Generator Modeling and Control

A diesel engine driving a synchronous generator is altogether a truly complex machine. Naturally, many different approaches can be taken to modeling of such a machine; aligning the approach with the purpose is essential.

[Guzzella and Amstutz, 1998] presents modeling of diesel engines with emphasis on torque generation, which includes nonlinear models of the turbocharger, the injection system, and more. However, the authors point out that such models usually are too complex for control purposes and suggest using linear low-order models instead. Applying that argument, [Guermouche et al., 2015] presents a seventh-order diesel engine model including, e.g., turbocharger and manifold states, which is reduced to a third-order model explicitly to obtain a simpler control law for a sliding mode controller. [Lyshevski, 2000] presents a nonlinear so-called cylinder-by-cylinder fourth-

order diesel engine model involving cylinder volume, cylinder gas pressure, crankshaft angular velocity, and crankshaft displacement. Both [Gasparjan et al., 2015] and [Sivertsson and Eriksson, 2015] present fourth-order diesel engine models, which include crankshaft, turbocharger, and intake and exhaust manifold states. Demonstrating a different approach, [Sakamoto, 2015] uses measurements of the fluctuating engine torque in her analysis of cylinder misfire effects. The above examples relate closely to the fundamental principles of internal combustion diesel engines as provided in reference books such as [Heywood, 1988; Challen and Baranescu, 1999; Kiencke and Nielsen, 2005; Rakopoulos and Giakoumis, 2009], in which the number and dimensions of the cylinders, the different stages of the combustion cycle, the properties of the fuel and air, and much more are considered.

The dynamics of diesel engines are often approximated in alignment with the modeling purpose. [Roy et al., 1991; Chen, 2010; Zhang, 2010] present models of diesel engines comprising first-order linear differential equations and a time delay, which are used for control design and running simulations of a model-based adaptive, model-free adaptive, and sliding mode governor, respectively. [Tuffaha and Gravdahl, 2014] presents a diesel engine model consisting of first-order linear differential equations and a time delay for proposing governor control designs based on feedback linearization, which is utilized to handle nonlinearities of the synchronous generator. The same authors include nonlinearities in their diesel engine model in [Tuffaha and Gravdahl, 2015]. Utilized in cooperation with an energy storage unit, [Perahia and Nayar, 1998] presents a model consisting of first and second-order linear differential equations of the diesel engine. Similar engine modeling concepts are presented for low voltage ride through analysis of mains-connected diesel generators in [Keerti et al., 2016]. [Singh and Singh, 2010] utilizes a diesel engine model based on second-order linear differential equations and a time delay in their research on control design for a system including a distribution static compensator. Additional different applications of diesel engine models consisting of combinations of first-order linear differential equations are found in [Yasin et al., 2006; Torres and Lopes, 2010; Mirosevic and Maljkovic, 2012; Theubou et al., 2012; Shi et al., 2016]. The parameters of engine models based on first and/or second-order differential equation approximations are rarely readily available from engine datasheets. [McGowan et al., 2003] obtains parameters for a second-order exponential diesel engine model using a least squares method on measurements of an engine speed step response before utilizing the model in the design of a PID governor.

The fundamentals of synchronous generator modeling are provided in reference books such as [Kundur, 1994; Machowski et al., 2008; Krause et al., 2013; Eremia and Shahidehpour, 2013]. Reference books commonly present synchronous generators both in the physical three-phase representation, often referred to as *abc*, and the frequently utilized mathematically transformed

representation introduced by [Park, 1929], often referred to as *dq*, which is presented in greater detail in Section 3.3.

[Yasin et al., 2006; Kassem and Yousef, 2011] present first-order nonlinear differential equations for *dq* generator models, which are linearized in order to design optimal controllers for frequency and voltage stabilization. [Abdin et al., 1999] utilizes an identical modeling approach in the design of an optimal controller for frequency and voltage stabilization in cooperation with photovoltaic generation. [Tuffaha and Gravdahl, 2014, 2015] utilize a first-order nonlinear differential equation *dq* generator model in the design of a robust governor controller. [Mirosevic and Maljkovic, 2012] presents the fundamental first-order nonlinear differential *dq* generator equations in their analysis of varying AVR PI gains, while [Singh and Singh, 2010] mentions a sixth-order state-space synchronous generator model; however, the equations are never presented. [Theubou et al., 2012] linearizes a model of the fundamental first-order nonlinear differential *dq* generator equations; similarly, [Perahia and Nayar, 1998] investigates the cooperation of a genset and an energy storage unit, utilizing a linearized *dq* generator model. [Zhang, 2011] presents online tuning of the PID regulator in an AVR using a genetic algorithm on the basis of a *dq* generator model, which consists of a first order differential equation for excitation dynamics utilizing voltage and current measurements. [Torres and Lopes, 2010] provides first-order nonlinear differential *dq* generator equations in their modeling of a diesel generator, whereas [Gasparjan et al., 2015] uses a rarely encountered combination of *abc* and *dq* generator equations in their analysis of diesel generators. Based on the fundamental equations, the synchronous generator simulation blocks provided by the Simscape Power Systems™ [MathWorks, 2017] in MATLAB Simulink® are used in simulation studies, see for example [Singh et al., 2005; Cooper et al., 2009; Singh and Solanki, 2011; Benhamed et al., 2016]. An alternative modeling approach is utilized by [Lin et al., 2016] in presentation of a synchronous generator as an active and reactive power source by nonlinear functions of terminal voltage, excitation voltage, and torque angle, which they utilize for experiments of mains-connected operation of a diesel generator. As additional examples of alternatives, [Shi et al., 2005; Jiang et al., 2014] use measurements for offline model training of a radial basis function neural network model and a nonlinear autoregressive with exogenous inputs model of a diesel generator, respectively. The use of commercial software packages for modeling synchronous generators are also encountered, see for example [Hassan et al., 1992; Guo et al., 2012; Voroshilov et al., 2013], which utilize the EMTP, PSCAD, and PSIM software packages, respectively.

Utilizing synchronous generator models closely related to the fundamental equations, as provided by reference books [Kundur, 1994; Machowski et al., 2008; Krause et al., 2013; Eremia and Shahidehpour, 2013], with an appropriate degree of simplifying assumptions, most often entails the avail-

ability of some model parameters in generator datasheets; however, not all of the model parameters can be assumed available since datasheets usually provide only a subset of the system parameters, in accordance with the standardized test procedures specified by [IEEE Power Engineering Society, 1983, 2010]. Consequently, works on parameter identification of synchronous generators such as the following examples are relevant. [Mamboundou and Langlois, 2011] identifies the parameters of a fourth-order generic transfer function from actuator voltage to generated active power using a recursive least squares method, followed by the design of an adaptive model predictive active power controller. Similarly, [Cheong et al., 2010] uses recursive least squares methods in the identification of parameters for their presented diesel generator model. [Karrari and Malik, 2004] identifies the parameters of a third-order linear model of a synchronous generator based on measurements of the generated power, the terminal voltage, and the excitation voltage. [Wamkeue et al., 2008] utilizes an asymptotic weighted least-squares estimator to obtain parameters for a generator model formed by the fundamental first-order nonlinear differential dq equations, while [Huang et al., 2013] presents a generator model with a combination of abc and dq nonlinear equations and utilizes a least squares method to identify parameters.

Control of diesel-driven generator sets involves, as briefly introduced in Section 1.1, regulation of both the angular velocity of the engine and the terminal voltage of the generator. Exclusively concerning diesel engine control design, also known as governor design, [Guzzella and Amstutz, 1998] provides references of PID, adaptive, self-tuning, optimal, gain scheduling, and sliding mode control results; all of those obtained two decades ago. Additional examples are found among the references discussed above, such as [Roy et al., 1991; Chen, 2010; Zhang, 2010, 2011]. Further, [Goh et al., 2003] presents a higher-order sliding mode governor controller, which is experimentally analyzed using a Rapid Control Prototyping system with a 65 kW diesel generator. [McGowan et al., 2006] presents a fuzzy logic governor controller, which utilizes angular velocity and voltage information, based on PID regulation structures, and tests it through a Rapid Control Prototyping system on a 50 kVA diesel generator. Further, [McGowan et al., 2008] advances the performance by including the additional information of power factor in the governor control design. [Best et al., 2007] presents and experimentally demonstrates, using a RPC system, a fuzzy logic governor controller that aligns the electrical phase of an islanded diesel generator subject to load variations to the nearby mains. [Broomhead et al., 2017] designs an economic model predictive governor controller for active power tracking with fuel and emissions minimization, which is experimentally demonstrated using a Rapid Control Prototyping system. Alternatively, [Cooper et al., 2012] designs a temperature-dependent PID AVR controller, which through experiments is shown to improve load acceptance performance during cold starts

of a 375 kVA diesel-driven generator set. Finally, [Hilal et al., 2016] presents the development and implementation of governor droop adjustments and supervisory PI regulators, implemented in a programmable logic controller, that changes the references for the governor and AVR on a diesel generator in a case study system in Indonesia including photovoltaic generation. This implementation in [Hilal et al., 2016] represents one operation mode of an Automatic Genset Controller; note however, this is the only contribution from all of the references provided above that relates directly to AGC design.

2.2 Fuel Optimization as Plant Management

Minimizing the fuel consumption of one diesel-driven generator set operating in steady-state is in essence the business of the engine and generator manufacturers. Operating under varying conditions, fuel optimization of one diesel generator is furthermore affected by the control characteristics. One example of a governor control design that minimizes the fuel consumption of one diesel-driven generator set during variations in produced power is provided by [Broomhead et al., 2017].

From a plant management perspective, that is, when concerned with the total power production of a number of gensets, fuel optimization fundamentally relates to the so-called Unit Commitment and Economic Dispatch problems. Generally, solving the Unit Commitment problem refers to the determination of a generation unit startup and shutdown schedule for a given consumption forecast period, while the Economic Dispatch problem covers determination of generation levels for each generation unit in operation, such that the load is supplied at the lowest possible cost [Wood et al., 2014]. The Economic Dispatch problem is often, implicitly or explicitly, incorporated in the Unit Commitment problem, since the costs associated with Economic Dispatch affect the solution to Unit Commitment.

For the macrogrid, or simply mains, these problems traditionally concerned a large geographical area with a small portfolio of conventional power plants. At that scale, the problems can involve power transmission and distribution networks, fuel availability and cost, substantial startup and shutdown periods and costs, etc., and the solution has been pursued using many different methodologies, as comprehensively documented in the survey by [Padhy, 2004]. Particularly, [Tong et al., 1991] discusses an approach that in many aspects relates to the industrial state of the art of today with their combination of Priority Listing and the so-called Expert System. An Expert System is characterized by [Tong et al., 1991] as the implementation of a heuristic set of rules based on the experience and judgment of human experts. Priority Listing entails determining the solution with the lowest cost based on a predetermined ranking of the available generation units according to cost characteristics.

[Senjyu et al., 2003] presents an approach utilizing an Extended Priority Listing, which solves Unit Commitment in a two-step process of Priority Listing and heuristics. [Sheblé and Maifeld, 1994] enhances a Genetic Algorithm approach by applying an Expert System to the proposed solutions of the Genetic Algorithm. [Kazarlis et al., 1996] presents an alternative Genetic Algorithm approach that finds the optimal solution by utilizing varying penalty terms for constraint violations. By reducing the required number of integer variables, [Carrion and Arroyo, 2006] obtains an efficient Mixed-Integer Linear Programming approach, whereas [Wu et al., 2007] utilizes Lagrangian relaxation to decompose a Unit Commitment problem into subproblems solvable by Mixed-Integer Programming. Alternatively, [Tuffaha and Gravdahl, 2017] presents a Mixed-Integer Programming state-space model for solving the combined Unit Commitment and Economic Dispatch problem.

In the above paragraph, publications of a limited selection of the different methodologies utilized for finding a solution to the Unit Commitment problem has been presented. The reader is referred to the extensive survey by [Padhy, 2004] for a more comprehensive analysis.

Looking at microgrid applications involving diesel generators, which is most often where fuel consumption of individual generation units is considered, the academic attention has primarily fallen upon hybrid systems with a focus on the utilization of renewable energy resources and energy storage systems. [Ashari et al., 2001; Ameen et al., 2015; Ghenai et al., 2017; Askarzadeh, 2017] all utilize affine functions of produced power and power rating to model the fuel consumption of diesel-driven generator sets as one of the generation unit types in hybrid systems. [Ashari et al., 2001] designs an operation strategy and performs an economic analysis of a mains-connected hybrid system containing a battery system, a diesel generator, and photovoltaic generation. [Ameen et al., 2015] presents models under consideration of control strategies for a similar hybrid system consisting of a battery system, a diesel generator, and photovoltaic generation. Such a hybrid system is also investigated by [Ghenai et al., 2017] in the design of fuel optimizing control strategies. [Askarzadeh, 2017] uses the affine fuel consumption characteristics in his presentation of an approach for optimal sizing of photovoltaic and diesel generator hybrid systems. Alternatively, [Pandiaraj et al., 2002; Bokabo and Kusakana, 2016; Kusakana, 2017] utilize quadratic functions of produced power to model the diesel generator fuel consumption. [Pandiaraj et al., 2002] presents a centralized fuel optimization controller for decentralized diesel generators, while [Bokabo and Kusakana, 2016] minimizes the operation costs of a hybrid system consisting of wind generation, photovoltaic generation, and a diesel generator with pumped hydro storage. [Kusakana, 2017] analyzes the obtainable fuel savings by operating multiple diesel generators in parallel. Finally, [Rao et al., 2015] utilizes piecewise second-order polynomial fits of datasheet information as a model for the fuel

consumption of diesel generators in their development of a fuel optimization control design for the operation of parallel diesel generators on an offshore vessel. The authors present fuel optimization results for the entire power production range of two system configurations; (i) four identical 2 MW gensets operating in parallel and (ii) three identical 2 MW gensets operating in parallel together with two identical 1 MW gensets. Due to the simplicity of the configurations, Unit Commitment is solved by hand prior to the utilization of a Genetic Algorithm, which finds the power level of each diesel generator that minimizes fuel consumption for a given common load requirement.

Out of all the references provided above, only the contributions by [Rao et al., 2015; Tuffaha and Gravdahl, 2017] relate, in their entirety, closely to the problem concerning fuel optimization as plant management in applications of diesel-driven generator set plants.

2.3 Contributions of This Thesis

Considering the state of the art, as it is documented in Section 2.1 and Section 2.2, this Industrial Ph.D. study adds to the state of the art within both of the accentuated areas. This section highlights the contributions through the associated papers, emphasizing the specific contributions of each paper. All the papers are provided in full in Part II of this thesis.

Diesel-Driven Generator Set Modeling and Control

The area of individual diesel-driven generator set modeling and control has been the topic of three papers:

Paper A
J. Knudsen, J. Bendtsen, P. Andersen, K. Madsen, and C. Sterregaard, "Control-oriented first principles-based model of a diesel generator," in *European Control Conference*, 2016, pp. 321-327.

Paper A presents the development of a diesel-driven generator set model. With the application of an Automatic Genset Controller in mind, the diesel engine is modeled according to the mean value modeling approach, while the synchronous generator is modeled utilizing first principles. The usage of first principles and a limited adoption of assumptions entail that the model is valid through every stage of transient and steady-state conditions. Including the governor and AVR as PI regulators, the model is validated for steps in supplied active load during island operation with measurements from Diesel Generator 1, which was introduced in Section 1.2.

This paper contributes to the state of the art by explicitly presenting a nonlinear dynamical diesel generator model, which includes the governor

and AVR and which is valid in subtransient, transient, and steady-state conditions. By including the governor and AVR as part of the diesel-driven generator set, this model is applicable in the scenarios that many industry controllers face. Paper A has been published as [Knudsen et al., 2016a].

Paper B

J. Knudsen, J. Bendtsen, P. Andersen, and K. Madsen, "Self-tuning linear quadratic supervisory regulation of a diesel generator using large-signal state estimation," in *Australian Control Conference*, 2016, pp. 32-37.

Paper B presents the formulation of an Automatic Genset Controller design based on the Linear Quadratic Regulator (LQR) theory for the diesel generator model presented in Paper A. The design includes a large-signal state estimator and a simple, linear parameter identification method, which facilitates a self-tuning regulator implementation.

Comparing, through simulations, the proposed design to a PID regulator solution, this paper represents a novel investigation of a multiple-input multiple-output (MIMO) AGC regulator design for diesel-driven generator sets resembling the reality faced by industrial AGC solutions. Paper B has been published as [Knudsen et al., 2016b].

Paper C

J. Knudsen, J. Bendtsen, P. Andersen, K. Madsen, and C. Sterregaard, "Supervisory control implementation on diesel-driven generator sets," submitted for *IEEE Transactions on Industrial Electronics*, 2017.

Paper C presents an enhanced diesel-driven generator set model, which improves on the validity and the generic nature of the model presented and utilized in Papers A and B. Additionally, utilizing the AGC design approach introduced in Paper B, Paper C presents a series of experimental implementation results on Diesel Generators 1 and 2, that convincingly demonstrates the advantages of the proposed LQR-based AGC design.

By enhancing and extending the works in previous publications, primarily through experimental demonstrations, this paper contributes to the state of the art. Paper C has been submitted as [Knudsen et al., 2017a].

Fuel Optimization as Plant Management

The area of fuel optimization as plant management of diesel-driven generator set plants has been the topic of one paper:

Paper D

J. Knudsen, J. Bendtsen, P. Andersen, K. Madsen, C. Sterregaard, and A. Rossiter, "Fuel optimization in multiple diesel driven generator power plants," in *IEEE Conference on Control Technology and Applications (CCTA)*, 2017, pp. 493-498.

Paper D presents an investigation of fuel consumption characteristics on a diesel-driven generator set subject to different operational conditions. Utilizing the results of that investigation, Paper D additionally propose a Genetic Algorithm for fuel optimization in a genset plant producing a steady power output. The algorithm achieves significant fuel savings through the usage of live information regarding individual diesel generator conditions.

This paper represents a novel contribution to the state of the art by considering the influence of changing fuel consumption characteristics in the plant management solution for plants of diesel-driven generator sets. Paper D has been published as [Knudsen et al., 2017b].

Note, that these contributions align with the research objectives presented in Section 1.3 with only one exception; relating to the objective of an adaptive AGC design. The remaining chapters of Part I provide an extended summary of the contributions described above.

3 Diesel-Driven Generator Set Modeling

This chapter provides specific models of each diesel-driven generator set element considered in this study, prior to formulating the complete nonlinear state-space model. Measurements are utilized for the model validation, which concludes this chapter.

The first section of this chapter provides a functional description of a diesel-driven generator set, while the subsequent sections present mathematical characterizations of each element. This functional description is a more in-depth exposition than the introduction provided in Section 1.1; however, it relates closely to the conceptual diagram in Figure 1.2. The diagram is provided again here in Figure 3.1, for the convenience of the reader.

While the majority of this chapter deals with the final formulations of the model elements, comments are included to show and review the progression of the work through the timespan of this Industrial Ph.D. study.

The explicit time dependency of variables is suppressed throughout this thesis when it is not of specific interest. Furthermore, all variables, constants, etc., are assumed scalar and real unless stated otherwise.

Per Unit System Representation

The mathematical models of each system element are stated using a so-called per unit (p.u.) system. Quantities in p.u. are normalized versions of physical unit quantities, which could be provided in hertz, volts, ohms, radians per second, etc. The normalization is given by [Kundur, 1994]

$$\text{quantity in p.u.} = \frac{\text{quantity in physical unit}}{\text{base value of quantity}}$$

where the base value is the nominal or rated value of the corresponding quantity, such that the p.u. quantity equals one under nominal or rated conditions. That is, for a nominal frequency base, the p.u. frequency equals one when the actual frequency equals the desired frequency; whereas, for a

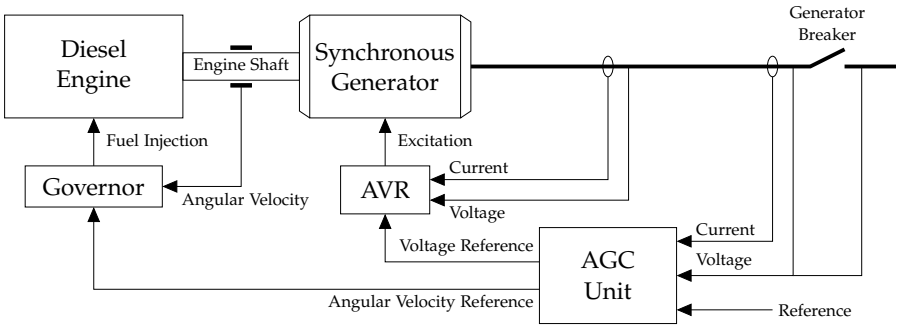

Figure 3.1: Conceptual diagram of a diesel-driven generator set including the control system. The fuel injection regulating governor and the excitation regulating Automatic Voltage Regulator act on references provided by the Automatic Genset Controller unit.

rated engine torque base, the p.u. engine torque equals one when the engine produces its maximum torque.

In general, utilizing a per unit system offers computational simplicity [Kundur, 1994] and, for control design, it is most often preferable to have a system representation in which the domains of the variables are aligned. Various per unit systems exist for synchronous machines, offering different properties; however, this work considers only the so-called L_{ad}-base reciprocal per unit system [Kundur, 1994]. In the following formulation of a diesel engine model, one additional base value is introduced. This base value incorporates a separate rated torque for the diesel engine, which accommodates the possibility of unequal engine and generator sizing.

3.1 Functional System Description

The prime-mover of a diesel-driven generator set is the diesel engine, of which the most common type is the four-stroke cycle diesel engine [Kiencke and Nielsen, 2005]. A stroke is the full movement of the piston, upwards or downwards, inside the engine cylinder. The piston is connected to the crankshaft through a connecting rod, which converts the linear motion into rotational movement. Every piston connects to the crankshaft, combining the total produced engine torque at one shaft. In single-cylinder engines the torque delivered to the shaft comes in periodic peaks, whereas multiple-cylinder engines deliver a more steady torque, most often smoothened further by way of a flywheel [Goering et al., 2003]. Diesel Generators 1 and 2 in the available laboratory facilities, as presented in Section 1.2, both have turbocharged, four-stroke, four-cylinder diesel engines with flywheels.

The shaft of the diesel engine drives the connected electrical generator. Synchronous generators comprise an important source of electrical power

worldwide [Kundur, 1994; ENTSO-E, 2016] and many designs are in active use; however, this study considers the salient four-pole, three-phase, brushless excited, synchronous generator as it is used for many industry-standard diesel generators. In particular, Diesel Generators 1 and 2 are of this type. Synchronous generators consist essentially of two components; the rotor and the stator. An example of a salient four-pole, three-phase, brushless excited, synchronous generator, where the rotor and stator have been detached, is shown in Figure 3.2 with indication of different elements.

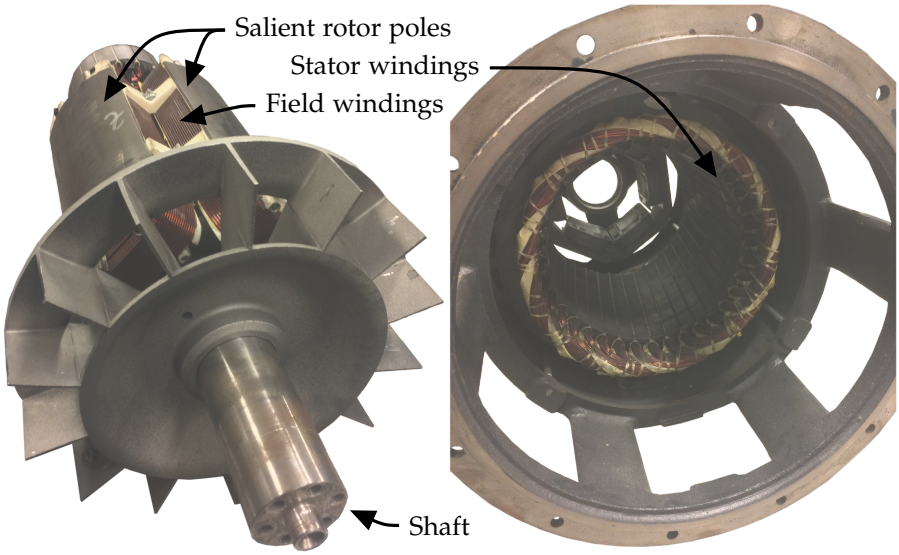

Figure 3.2: Salient four-pole, three-phase, synchronous generator rotor (left) and stator (right).

Indicated for the rotor on the left in Figure 3.2, the diesel engine shaft connects directly to the rotor, causing it to rotate inside the stator. Supplied by the excitation system, the field excitation windings basically turn the rotor into an electromagnet that, when rotating, induces alternating voltages in the stator windings, indicated for the stator on the right in Figure 3.2; thus providing the electrical output of the genset. A brushless excitation system can be identified in the back both on the rotor and in the stator in Figure 3.2. The angular velocity of the shaft and, thereby, the magnetic field of the field excitation windings determine the electrical frequency of the generated electrical output. The exact relation depends on the number of magnetic poles in the rotor. In Figure 3.2, two salient poles are visible on the four-pole rotor. Diesel Generators 1 and 2 both have four magnetic poles in the rotor, implying a requirement for the diesel engine of running the shaft at 1500 rpm, which is equivalent to 25 Hz, to obtain an electrical frequency of the 50 Hz utilized in Denmark and many other parts of the world.

As evident in Figure 3.1, regulating the frequency and voltage of the electrical output of a diesel-driven generator set fundamentally involves two tasks; fuel injection regulation and rotor excitation regulation. Generally in industry-standard diesel generator configurations, two separate regulators are installed to handle the first level of this control assignment. The fuel injection regulator, commonly denoted governor, uses measurements of the angular velocity of the shaft to adjust the fuel injection for the diesel engine, while the so-called Automatic Voltage Regulator uses measurements of the output voltages to adjust the rotor excitation and, thereby, the strength of the rotating magnetic field. Most often, the governor and AVR employ one of two characteristic schemes for determining their respective internal control references. The present study exclusively considers governors and AVRs applying the so-called isochronous scheme, which entails operating with a constant internal control reference of nominal value. The alternative to the isochronous characteristic scheme is referred to as the droop scheme, which is described in detail in Section 1.1.

An AGC unit is installed to add supervisory control capabilities, by providing external control reference offsets for the regulators of the governor and AVR. Utilizing supplementary voltage and current measurements enables features, such as the so-called synchronization, active and reactive power control, and automatic mains failure response. Synchronization is obtained by matching the amplitude, frequency, and phase of the generated electrical output to the conditions on the other side of the generator breaker before closing that breaker. Alternatively, automatic mains failure entails starting up the genset if the other side of the generator breaker goes black, that is, if the voltage level drops to zero. Simply operating in traditional frequency and voltage regulation conditions, the AGC is capable of affecting the control performance; for better or worse, depending on the regulator in the AGC.

3.2 Diesel Engine and Governor

Maintaining nominal angular velocity of the engine shaft, which determines the electrical frequency of the genset, requires applying a torque to the shaft that balances the torque exerted by the synchronous generator. Referred to as the swing equation, the equation of this rotational motion is given by

$$J\underline{\omega}_m\dot{\omega}_m = \underline{T}_m T_m - \underline{T}_e T_e - D\underline{\omega}_m\omega_m \tag{3.1}$$

where ω_m is the p.u. angular velocity of the shaft, $\dot{\omega}_m$ is its time derivative, T_m and T_e are the p.u. mechanical and electrical torques applied to the shaft by the engine and generator, respectively, J and D are the total system inertia and damping, and $\underline{\omega}_m$, $\underline{T}_m$, and $\underline{T}_e$ are the mechanical angular velocity base, mechanical torque base, and electrical torque base, respectively. To remove

ambiguity, these base values denote the nominal angular velocity of the shaft, the rated engine torque at nominal angular velocity, and the rated electrical torque at nominal voltage and electrical frequency, respectively.

This per unit version of the swing equation, provided in Equation 3.1, allows the usage of datasheets for determining the total system inertia, J, in kg·m^2 as commonly provided. Conversely, determination of the total system damping, D, is non-obvious. After considering the meaning and effect of the term, a value of 0.1 N·m·s/rad has been chosen and utilized throughout this study. Both $\underline{T}_m$ and $\underline{T}_e$ are found in N·m utilizing datasheets for a specific genset, while $\underline{\omega}_m$ in rad/s is determined as

$$\underline{\omega}_m = \underline{\omega}_e \frac{2}{p_f}$$

where $\underline{\omega}_e$ is the electrical angular velocity base and p_f is the number of magnetic poles in the rotor, which for this study utilizing Diesel Generators 1 and 2 are 100π rad/s and four, respectively.

For control purposes, it is sufficient and appropriate to model the applied mechanical torque as a mean value function of the injected fuel; rather than establishing a cylinder-by-cylinder dynamical model [Karlsson and Fredriksson, 1999]. Predominantly of a retarding nature, the non-negligible dynamics of the turbocharger, the fuel injection system, etc., can be represented by a first-order low-pass filter. During experiments, it has been observed that this retarding is more pronounced at increased torque levels; therefore, the time constant of the filter is implemented as a function of the torque itself. The time derivative of the p.u. mechanical torque, $\dot{T}_m$, is then given by

$$\dot{T}_m = \frac{1}{\tau_m(\sigma + T_m)}(\mu - T_m) \tag{3.2}$$

where T_m is the p.u. mechanical torque, τ_m is the constant term of the engine time constant, μ is the p.u. fuel injection requested by the governor, which has a range of zero to one, and σ describes the degree of increased retarding. The exact value of τ_m depends on the specific diesel engine. In the present study, its value has been identified as discussed later in this chapter. A $\sigma = 1$ has been found experimentally to be an appropriate value for describing the increased retarding behavior of the available diesel generators.

A governor is included in the model as a PI regulator operating according to the isochronous characteristic scheme, i.e., attempting to maintain nominal angular velocity of the shaft. The governor equations are given by

$$\begin{aligned} \dot{e}_{i\omega} &= r_\omega + u_\omega - \omega_m \\ \mu &= k_{p\omega}(r_\omega + u_\omega - \omega_m) + k_{i\omega} e_{i\omega} \end{aligned} \tag{3.3}$$

where $e_{i\omega}$ is the governor integral error state, $\dot{e}_{i\omega}$ is its time derivative, r_ω is the p.u. angular velocity internal governor reference, which remains at

nominal value of the p.u. angular velocity, u_ω is the p.u. angular velocity governor reference offset, which is one of the two control variables of the supervisory AGC regulator, and $k_{p\omega}$ and $k_{i\omega}$ are the proportional and integral governor regulator gains, whose values depend on the specific governor. The gains are identified as discussed later in this chapter. Given that the p.u. fuel injection, μ, is naturally limited to attain positive values less than or equal to one, integrator anti-windup is implemented in the governor.

As presented in [Knudsen et al., 2016a], the original formulation of the diesel engine model did not utilize a per unit system. Instead, it contained a number of engine and fuel specific constants; however, the assumptions applied to obtain a mean value torque model effectively lead to a formulation of the same form as the one provided above.

3.3 Synchronous Generator and Automatic Voltage Regulator

As introduced in Section 3.1, a synchronous generator consists essentially of two elements; rotor and stator. Figure 3.3 shows a simplifying cross section schematic of a salient two-pole, three-phase, synchronous generator.

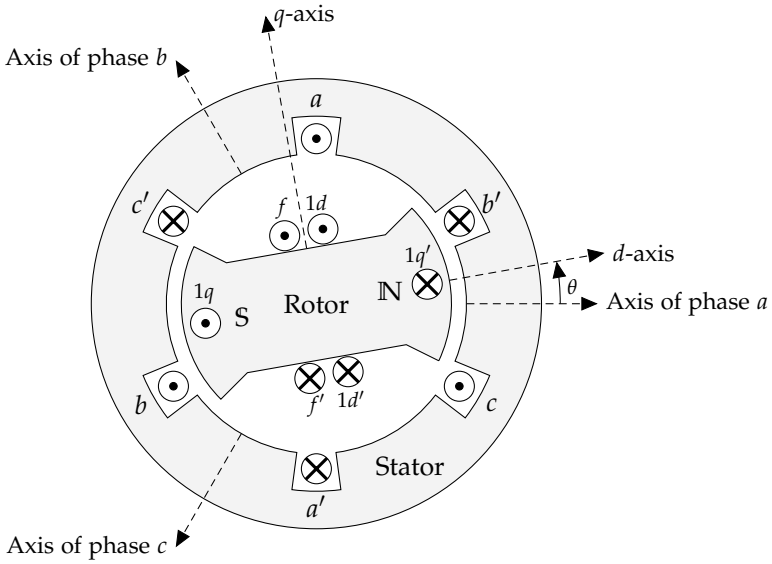

Figure 3.3: Simplifying cross section schematic of a salient two-pole, three-phase, synchronous generator consisting of rotor, stator, and windings [Kundur, 1994].

In Figure 3.3, the north and south poles, $\mathbb{N}$ and $\mathbb{S}$, of the rotor are salient, unlike a round rotor. The field winding, f, is spun around the rotor, carrying

a direct current, supplied by the field excitation system, which generates the necessary magnetic field. Furthermore, two damper windings, $1d$ and $1q$, represent the effects of short-circuited metal bars, typically copper, mounted on the rotor to dampen transient oscillations by providing short-circuited paths for eddy currents. The two damper windings are modeled as spun perpendicular to each other [Kundur, 1994]. When rotated by the diesel engine, the magnetic field of the rotor induces alternating voltages in the three stator windings, a, b, and c, which are separated by 120 degrees in space. Under a uniform rotation of the magnetic field, this spatial separation causes voltages with 120 degrees phase separation to be generated in the stator windings. Producing a steady torque requires the rotor to run at synchronous speed, i.e., the rotor and stator fields must rotate at the same speed.

Indicated by dashed lines in Figure 3.3, two different reference frames linked by the angle θ are utilized in relation to synchronous generators; the stator-anchored abc reference frame and the rotor-anchored $dq0$ reference frame. Commonly known as the direct-quadrature-zero transformation or simply the Park transformation, the transformation from the abc reference frame to the $dq0$ reference frame is given by [Park, 1929]

$$\begin{bmatrix} i_d \\ i_q \\ i_0 \end{bmatrix} = \begin{bmatrix} k_d \cos\theta & k_d \cos\left(\theta - \frac{2\pi}{3}\right) & k_d \cos\left(\theta + \frac{2\pi}{3}\right) \\ -k_q \sin\theta & -k_q \sin\left(\theta - \frac{2\pi}{3}\right) & -k_q \sin\left(\theta + \frac{2\pi}{3}\right) \\ \frac{1}{3} & \frac{1}{3} & \frac{1}{3} \end{bmatrix} \begin{bmatrix} i_a \\ i_b \\ i_c \end{bmatrix}$$

where k_d and k_q are transformation coefficients, θ is the angle between the direct axis and the magnetic axis of the phase a winding in the stator, as indicated in Figure 3.3, and i_a, i_b, and i_c are the alternating currents of phase a, b, and c, respectively. The transformation is similar for voltages and stator flux linkages. With transformation coefficients $k_d = k_q = 2/3$, as used in the present work, equal peak values of the abc and $dq0$ quantities are obtained. Nevertheless, the coefficients are basically arbitrary and can be set differently to obtain alternative transformation properties if desirable, such as power invariance [Kundur, 1994].

The 0 quantities are constantly zero in balanced systems; consequently they are omitted in the present model development. The most significant advantage of the transformation is that it turns alternating quantities in the stator frame into constant quantities during synchronous operation, implying that only slow variations appear in the rotor frame, which is advantageous in stability studies [Kundur, 1994]. However, one disadvantage of the transformation relates to the interfacing of synchronous generators with electrical load, which is a well-known open problem surveyed in, for example, [Wang et al., 2010]. Although alternative modeling approaches, such as the voltage-behind-reactance representation [Pekarek et al., 1998], have been proposed to alleviate issues in relation to the usage of dq, those alternatives are not investigated in the present study.

Utilizing the dq reference frame, the electrical equivalent circuit of the rotor is provided on the left in Figure 3.4, while the electrical equivalent circuit of the stator is provided on the right using the abc reference frame.

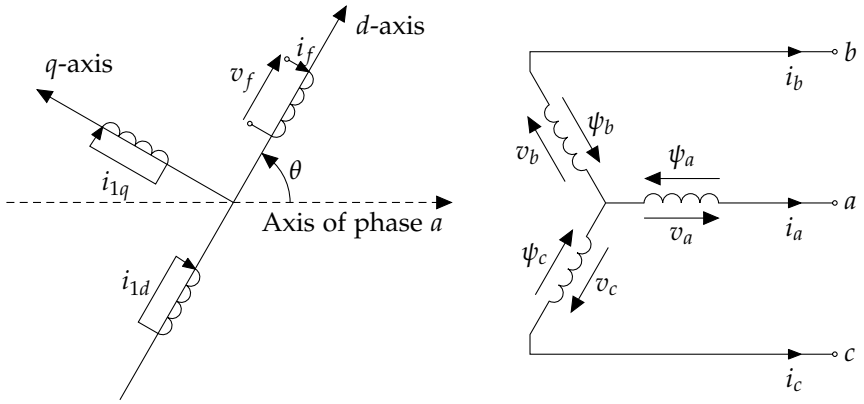

Figure 3.4: Electrical equivalent circuits for the rotor (left) and stator (right) [Kundur, 1994].

In Figure 3.4, i_f, i_{1d}, and i_{1q} are the field excitation, d-axis damper, and q-axis damper currents, respectively, and v_f is the field excitation voltage applied by the field excitation system. The dynamics of the brushless field excitation system are in this study assumed to be on a timescale that makes them negligible; in other words, the field excitation system is assumed to apply any desired field excitation voltage instantaneously. Additionally in Figure 3.4, i_a, i_b, and i_c are the phase a, b, and c alternating stator currents, respectively, v_a, v_b, and v_c are the alternating stator abc phase voltages, and ψ_a, ψ_b, and ψ_c are the stator flux linkages.

Under the reasonable and common assumptions that (i) the stator windings are sinusoidally distributed along the air-gap as far as the mutual effects with the rotor are concerned, (ii) the stator slots cause no appreciable variation of the rotor inductances with rotor position, (iii) magnetic hysteresis is negligible, and (iv) magnetic saturation effects are negligible, the p.u. electrical torque on the shaft, T_e, is given by [Kundur, 1994]

$$T_e = \psi_d i_q - \psi_q i_d$$

where ψ_d and ψ_q are the d and q-axis p.u. stator flux linkages, while i_d and i_q are the d and q-axis p.u. stator currents. The d and q-axis p.u. stator flux linkages are given by [Kundur, 1994]

$$\psi_d = -L_d i_d + L_{ad} i_f + L_{ad} i_{1d}$$
$$\psi_q = -L_q i_q + L_{aq} i_{1q}$$

where i_f, i_{1d}, and i_{1q} are the field excitation, d-axis damper, and q-axis damper p.u. currents, respectively, L_d and L_q are the d and q-axis p.u. synchronous

inductances, and L_{ad} and L_{aq} are the d and q-axis p.u. mutual inductances, given by subtraction of the p.u. leakage inductance, L_l, from the d and q-axis p.u. synchronous inductances as [Kundur, 1994]

$$L_{ad} = L_d - L_l$$
$$L_{aq} = L_q - L_l$$

The p.u. synchronous inductances, L_d and L_q, can be determined from datasheets, whereas the p.u. leakage inductance, L_l, has been chosen based on example values found in literature.

In the present study, the dynamics of the synchronous generator are expressed using per unit time, for which the time base, $\underline{t}$, is the time it takes the rotor to rotate one electrical radian at nominal angular velocity; that is, the time base is $1/100\pi$ s [Kundur, 1994]. Accordingly, the change in d and q-axis p.u. stator flux linkages are given by their p.u. time derivatives, $\dot{\psi}_d$ and $\dot{\psi}_q$, as [Kundur, 1994]

$$\dot{\psi}_d = v_d + \psi_q \omega_e + R_a i_d \tag{3.4}$$
$$\dot{\psi}_q = v_q - \psi_d \omega_e + R_a i_q \tag{3.5}$$

where v_d and v_q are the d and q-axis p.u. stator voltages, R_a is the p.u. armature resistance per phase, which can be determined through datasheets, and ω_e is the p.u. electrical angular velocity of the rotor, which in this work is assumed equal to ω_m, the p.u. angular velocity of the shaft. The field excitation, d-axis damper, and q-axis damper p.u. flux linkages, ψ_f, ψ_{1d}, and ψ_{1q}, are given by [Kundur, 1994]

$$\psi_f = L_{ffd} i_f + L_{f1d} i_{1d} - L_{ad} i_d$$
$$\psi_{1d} = L_{11d} i_{1d} + L_{f1d} i_f - L_{ad} i_d$$
$$\psi_{1q} = L_{11q} i_{1q} - L_{aq} i_q$$

where L_{ffd}, L_{11d}, and L_{11q} are the field excitation, d-axis damper, and q-axis damper p.u. self-inductances, respectively, and L_{f1d} is the field excitation and d-axis damper p.u. mutual inductance. None of these four rotor p.u. inductances are, generally, provided in datasheets, but have been determined as discussed later in this chapter. The associated p.u. time derivatives, $\dot{\psi}_f$, $\dot{\psi}_{1d}$, and $\dot{\psi}_{1q}$, respectively, are [Kundur, 1994]

$$\dot{\psi}_f = v_f - R_f i_f \tag{3.6}$$
$$\dot{\psi}_{1d} = -R_{1d} i_{1d} \tag{3.7}$$
$$\dot{\psi}_{1q} = -R_{1q} i_{1q} \tag{3.8}$$

where v_f is the field excitation p.u. voltage, regulated by the Automatic Voltage Regulator, and R_f, R_{1d}, and R_{1q} are the field excitation, d-axis damper,

and q-axis damper p.u. resistances, respectively. As in the case of the four rotor p.u. inductances, these three rotor p.u. resistances have been determined as discussed later in the chapter.

Similarly to the governor given in Section 3.2, an AVR is included in the model as a PI regulator operating according to the isochronous characteristic scheme, that is, attempting to maintain nominal three-phase phase-to-neutral RMS voltage. The dynamics of the AVR are

$$\begin{aligned} \dot{e}_{iv} &= r_v + u_v - v_{rms} \\ v_f &= k_{pv}(r_v + u_v - v_{rms}) + k_{iv} e_{iv} \end{aligned} \tag{3.9}$$

where e_{iv} is the AVR integral error state, $\dot{e}_{iv}$ is its time derivative, r_v is the three-phase phase-to-neutral p.u. RMS internal AVR voltage reference, which remains at the nominal value of the three-phase phase-to-neutral p.u. RMS voltage, u_v is the three-phase phase-to-neutral p.u. RMS voltage offset, which is the second of the two control variables of the supervisory AGC regulator, v_{rms} is the three-phase phase-to-neutral p.u. RMS voltage, and k_{pv} and k_{iv} are the proportional and integral AVR regulator gains, whose values depend on the specific AVR. Similarly to the governor gains, these gains are identified as discussed later in this chapter. In practice, calculations of RMS values are based on measurements of the latest full time period of the alternating signal. For balanced systems, this effectively amounts to a filtering of an instantaneous RMS value. In the present work, this filtering is approximated as a first-order low-pass filter, providing the time derivative of the three-phase phase-to-neutral p.u. RMS voltage as

$$\dot{v}_{rms} = \frac{1}{\tau_v}\sqrt{\frac{1}{2}\left(v_d^2 + v_q^2\right)} - \frac{1}{\tau_v} v_{rms} \tag{3.10}$$

where τ_v is the filter time constant of twice the p.u. time period of the nominal frequency, while the square root term represents the calculation of an instantaneous p.u. RMS voltage.

3.4 Complete State-Space Model

Equations (3.1) to (3.10) define the dynamics of a diesel-driven generator set, including governor and AVR PI regulators, as a tenth-order nonlinear model. On state-space form, the complete model can be written as

$$\begin{aligned} \dot{x} = {} & A(x_2)x + x_1 F_1 x + x_3 F_3 x + x_4 F_4 x \\ & + B_1 w + B_2 \sqrt{\frac{1}{2}\left(w_1^2 + w_2^2\right)} + B_3(x_2)(r + u) \end{aligned} \tag{3.11a}$$

$$y = Cx \tag{3.11b}$$

where $x \in \mathbb{R}^{10\times 1}$, $w \in \mathbb{R}^{2\times 1}$, $r \in \mathbb{R}^{2\times 1}$, $u \in \mathbb{R}^{2\times 1}$, and $y \in \mathbb{R}^{2\times 1}$ are the state, stator voltage, internal reference, supervisory control variable, and output vectors, respectively. These vectors are given by

$$
\begin{aligned}
x &= \begin{bmatrix} \omega_m & T_m & \psi_d & \psi_q & \psi_f & \psi_{1d} & \psi_{1q} & e_{i\omega} & e_{iv} & v_{rms} \end{bmatrix}^T \\
w &= \begin{bmatrix} v_d & v_q \end{bmatrix}^T \\
r &= \begin{bmatrix} r_\omega & r_v \end{bmatrix}^T \\
u &= \begin{bmatrix} u_\omega & u_v \end{bmatrix}^T \\
y &= \begin{bmatrix} \omega_m & v_{rms} \end{bmatrix}^T
\end{aligned}
$$

Furthermore, the matrices $A(x_2) \in \mathbb{R}^{10\times 10}$, $B_1 \in \mathbb{R}^{10\times 2}$, $B_2 \in \mathbb{R}^{10\times 1}$, $B_3(x_2) \in \mathbb{R}^{10\times 2}$, $C \in \mathbb{R}^{2\times 10}$, $F_1 \in \mathbb{R}^{10\times 10}$, $F_3 \in \mathbb{R}^{10\times 10}$, and $F_4 \in \mathbb{R}^{10\times 10}$ are

$$
A(x_2) = \begin{bmatrix}
-c_1 & c_2 & 0 & 0 & 0 & 0 & 0 & 0 & 0 & 0 \\
-c_3(x_2) & -c_4(x_2) & 0 & 0 & 0 & 0 & 0 & c_5(x_2) & 0 & 0 \\
0 & 0 & c_6 & 0 & -c_7 & -c_8 & 0 & 0 & 0 & 0 \\
0 & 0 & 0 & c_9 & 0 & 0 & -c_{10} & 0 & 0 & 0 \\
0 & 0 & -c_{11} & 0 & -c_{12} & -c_{13} & 0 & 0 & c_{14} & -c_{15} \\
0 & 0 & -c_{16} & 0 & -c_{17} & -c_{18} & 0 & 0 & 0 & 0 \\
0 & 0 & 0 & -c_{19} & 0 & 0 & -c_{20} & 0 & 0 & 0 \\
-1 & 0 & 0 & 0 & 0 & 0 & 0 & 0 & 0 & 0 \\
0 & 0 & 0 & 0 & 0 & 0 & 0 & 0 & 0 & -1 \\
0 & 0 & 0 & 0 & 0 & 0 & 0 & 0 & 0 & -c_{21}
\end{bmatrix}
$$

$$
B_1 = \begin{bmatrix}
0 & 0 & c_{22} & 0 & 0 & 0 & 0 & 0 & 0 & 0 \\
0 & 0 & 0 & c_{22} & 0 & 0 & 0 & 0 & 0 & 0
\end{bmatrix}^T
$$

$$
B_2 = \begin{bmatrix} 0 & 0 & 0 & 0 & 0 & 0 & 0 & 0 & 0 & c_{21} \end{bmatrix}^T
$$

$$
B_3(x_2) = \begin{bmatrix}
0 & c_3(x_2) & 0 & 0 & 0 & 0 & 0 & 1 & 0 & 0 \\
0 & 0 & 0 & 0 & c_{15} & 0 & 0 & 0 & 1 & 0
\end{bmatrix}^T
$$

$$
F_1 = \begin{bmatrix}
0 & 0 & 0 & 0 & 0 & \cdots & 0 \\
0 & 0 & 0 & 0 & 0 & & \\
0 & 0 & 0 & c_{22} & 0 & & \\
0 & 0 & -c_{22} & 0 & 0 & & \vdots \\
0 & 0 & 0 & 0 & 0 & & \\
\vdots & & & & & \ddots & \\
0 & & & \cdots & & & 0
\end{bmatrix}
$$

$$
F_3 = \begin{bmatrix}
0 & 0 & 0 & -c_{23} & 0 & 0 & c_{24} & 0 & 0 & 0 \\
0 & & & & \cdots & & & & & 0 \\
\vdots & & & & \ddots & & & & & \vdots \\
0 & & & & \cdots & & & & & 0
\end{bmatrix}
$$

$$F_4 = \begin{bmatrix} 0 & 0 & c_{25} & 0 & -c_{26} & -c_{27} & 0 & 0 & 0 & 0 \\ 0 & & & & \cdots & & & & & 0 \\ \vdots & & & & \ddots & & & & & \vdots \\ 0 & & & & \cdots & & & & & 0 \end{bmatrix}$$

$$C = \begin{bmatrix} 1 & 0 & 0 & 0 & 0 & 0 & 0 & 0 & 0 & 0 \\ 0 & 0 & 0 & 0 & 0 & 0 & 0 & 0 & 0 & 1 \end{bmatrix}$$

Please note that x_2 refers to the second element in the state vector; the p.u. mechanical torque, T_m. The elements c_1 to c_{27}, including those that are functions of x_2, are defined as

$$c_1 = \frac{D}{J}, \qquad c_2 = \frac{\underline{T}_m}{J\underline{\omega}_m}, \qquad c_3(x_2) = k_{p\omega}c_4(x_2), \; c_4(x_2) = \frac{1}{\tau_m(\sigma + x_2)},$$

$$c_5(x_2) = k_{i\omega}c_4(x_2), \quad c_6 = \frac{R_a c_{30}}{\underline{t}c_{28}}, \qquad c_7 = \frac{R_a c_{31}}{\underline{t}c_{28}}, \qquad c_8 = \frac{R_a c_{32}}{\underline{t}c_{28}},$$

$$c_9 = \frac{R_a L_{11q}}{\underline{t}c_{29}}, \quad c_{10} = \frac{R_a L_{aq}}{\underline{t}c_{29}}, \qquad c_{11} = \frac{R_f c_{31}}{\underline{t}c_{28}}, \qquad c_{12} = \frac{R_f c_{33}}{\underline{t}c_{28}},$$

$$c_{13} = \frac{R_f c_{34}}{\underline{t}c_{28}}, \quad c_{14} = \frac{k_{iv}}{\underline{t}}, \qquad c_{15} = \frac{k_{pv}}{\underline{t}}, \qquad c_{16} = \frac{R_{1d} c_{32}}{\underline{t}c_{28}},$$

$$c_{17} = \frac{R_{1d} c_{34}}{\underline{t}c_{28}}, \quad c_{18} = \frac{R_{1d} c_{35}}{\underline{t}c_{28}}, \qquad c_{19} = \frac{R_{1q} L_{aq}}{\underline{t}c_{29}}, \qquad c_{20} = \frac{R_{1q} L_q}{\underline{t}c_{29}},$$

$$c_{21} = \frac{1}{\tau_v}, \qquad c_{22} = \frac{1}{\underline{t}}, \qquad c_{23} = \frac{\underline{T}_e L_{11q}}{J\underline{\omega}_m c_{29}}, \qquad c_{24} = \frac{\underline{T}_e L_{aq}}{J\underline{\omega}_m c_{29}},$$

$$c_{25} = \frac{\underline{T}_e c_{30}}{J\underline{\omega}_m c_{28}}, \quad c_{26} = \frac{\underline{T}_e c_{31}}{J\underline{\omega}_m c_{28}}, \qquad c_{27} = \frac{\underline{T}_e c_{32}}{J\underline{\omega}_m c_{28}}$$

where the additional elements , c_{28} to c_{35}, are defined as

$$c_{28} = L_{ad}^2 L_{ffd} + L_d L_{f1d}^2 + L_{ffd} L_{ad}^2 - 2L_{ad}^2 L_{f1d} - L_{11d} L_d L_{ffd},$$

$$c_{29} = L_{aq}^2 - L_{11q} L_q, \qquad c_{30} = L_{11d} L_{ffd} - L_{f1d}^2, \quad c_{31} = L_{11d} L_{ad} - L_{ad} L_{f1d},$$

$$c_{32} = L_{ffd} L_{ad} - L_{ad} L_{f1d}, \quad c_{33} = L_{ad}^2 - L_{11d} L_d, \qquad c_{34} = L_{f1d} L_d - L_{ad}^2,$$

$$c_{35} = L_{ad}^2 - L_{ffd} L_d$$

Equations (3.11) represent a formulation of a genset model, which is completely disconnected from electrical load, in the sense that the stator voltages, v_d and v_q, are incorporated as uncontrollable inputs, w. Naturally, stator voltages depend to a great extent on what is connected to the generator terminals. With a connection to a well-established mains, the voltages are basically stiff, whereas the genset has the capability to regulate the voltages in various other conditions, such as island operation. Although Figure 3.5 is not a strictly conventional block diagram, due to the nonlinearities, it does provide a visual overview of the tenth-order nonlinear diesel generator model.

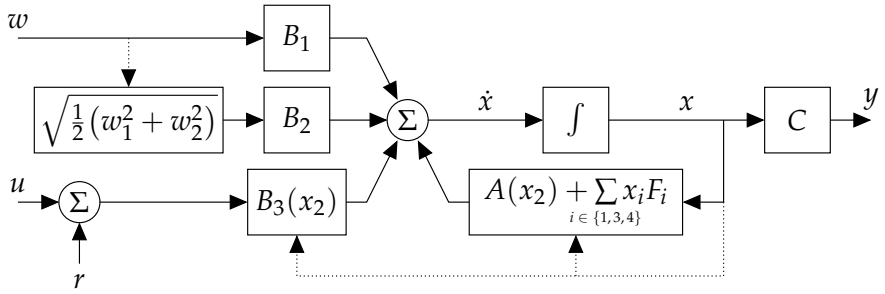

Figure 3.5: Block diagram of the complete tenth-order nonlinear state-space diesel-driven generator set model provided in Equations (3.11). Dotted lines indicate that signals appear in a nonlinear fashion in the corresponding blocks.

The original formulation, presented in [Knudsen et al., 2016a], utilized the p.u. currents as generator states, rather than the p.u. flux linkages. In terms of computational efficiency, usage of flux linkages has provided better performance, which is also suggested in [Pekarek et al., 1998]. Investigations in relation to [Knudsen et al., 2016a] revealed significant improvements concerning the validity of the model in transient conditions by including the two damper windings, which have been included ever since.

3.5 Model Validation

Considering frequency and voltage stabilization in island operation as one of the most fundamental operating modes on a diesel-driven generator set, the model is validated utilizing the laboratory facilities in that setting. That is, one diesel generator is connected to the busbar, supplying the load bank during changing load conditions. Validating the model during load changes, entails modeling the load in the interest of determining the resulting stator voltages. As introduced in Section 1.2, the load bank consists of resistive and inductive load elements, which can be connected in parallel as a balanced phase-to-neutral load on all three *abc* phases. The impedance, Z, of a parallel resistor and inductor circuit is given by [Irwin and Nelms, 2008]

$$Z = \frac{RsL}{R + sL} = \frac{V}{I}$$

where s is the Laplace variable, R is the resistance, L is the inductance, V is the voltage across the impedance, and I is the current running through the impedance. Applying the inverse Laplace transform, to obtain an expression in the time domain, and simple rearranging yields

$$V = RI - \frac{R}{L} \int V \, dt \tag{3.12}$$

For a balanced phase-to-neutral parallel resistor and inductor circuit on all three *abc* phases, utilizing Equation (3.12) in the $dq0$ transformation, the p.u. stator voltages, v_d and v_q, can be found as

$$\begin{aligned} v_d = R_L i_d - \frac{2R_L}{3L_L}\Bigg(&\cos(\theta)\int v_d\cos(\theta) - v_q\sin(\theta)\,dt \\ &+ \cos(\theta-\frac{2\pi}{3})\int v_d\cos(\theta-\frac{2\pi}{3}) - v_q\sin(\theta-\frac{2\pi}{3})\,dt \\ &+ \cos(\theta+\frac{2\pi}{3})\int v_d\cos(\theta+\frac{2\pi}{3}) - v_q\sin(\theta+\frac{2\pi}{3})\,dt\Bigg) \end{aligned} \tag{3.13a}$$

$$\begin{aligned} v_q = R_L i_q + \frac{2R_L}{3L_L}\Bigg(&\sin\theta\int v_d\cos\theta - v_q\sin\theta\,dt \\ &+ \sin(\theta-\frac{2\pi}{3})\int v_d\cos(\theta-\frac{2\pi}{3}) - v_q\sin(\theta-\frac{2\pi}{3})\,dt \\ &+ \sin(\theta+\frac{2\pi}{3})\int v_d\cos(\theta+\frac{2\pi}{3}) - v_q\sin(\theta+\frac{2\pi}{3})\,dt\Bigg) \end{aligned} \tag{3.13b}$$

where θ is the angle between the d-axis and the magnetic axis of the phase a winding in the stator, which is found as the p.u. time integral of ω_m assumed to start from zero, R_L is the per phase p.u. load resistance, L_L is the per phase p.u. load inductance, and i_d and i_q are the d and q-axis p.u. stator currents, which can be expressed by the p.u. flux linkage states of the diesel generator model as [Kundur, 1994]

$$i_d = \frac{c_{30}}{c_{28}}\psi_d - \frac{c_{31}}{c_{28}}\psi_f - \frac{c_{32}}{c_{28}}\psi_{1d} \tag{3.14a}$$

$$i_q = \frac{L_{11q}}{c_{29}}\psi_q - \frac{L_{aq}}{c_{29}}\psi_{1q} \tag{3.14b}$$

For a known electrical load described by a parallel per phase p.u. resistance and inductance, Equations (3.13) and (3.14) enable the calculation of the stator voltages, v_d and v_q. In general, the active and reactive powers consumed by a balanced three-phase phase-to-neutral load are given by

$$P = \frac{V^2}{R} \tag{3.15a}$$

$$Q = \frac{V^2}{\omega L} \tag{3.15b}$$

where P is the active power, V is the phase-to-phase RMS voltage, R is the per phase load resistance, Q is the reactive power, ω is the electrical angular velocity of the supply, and L is the per phase load inductance.

A simple analysis of Equations (3.15) shows that, for nominal V and ω, R approaches infinity as P approaches zero watt and L approaches infinity as Q approaches zero volt-ampere reactive. Applying this analysis to Equations

(3.13), for the latter, both Equation (3.13a) and Equation (3.13b) are effectively reduced to the first term; whereas, for the former, Equations (3.13) become practically unimplementable with the multiplication by infinity. Conditions of zero active load represent a specific case, however, which is of little interest and has not been investigated in the present study.

Figure 3.6 presents measurements and simulations of Diesel Generator 1 for increasing active load elements; in steps of 10 kW, from 10 kW to 50 kW, which represents what is possible in the laboratory facilities and within the capabilities of this 60 kVA genset.

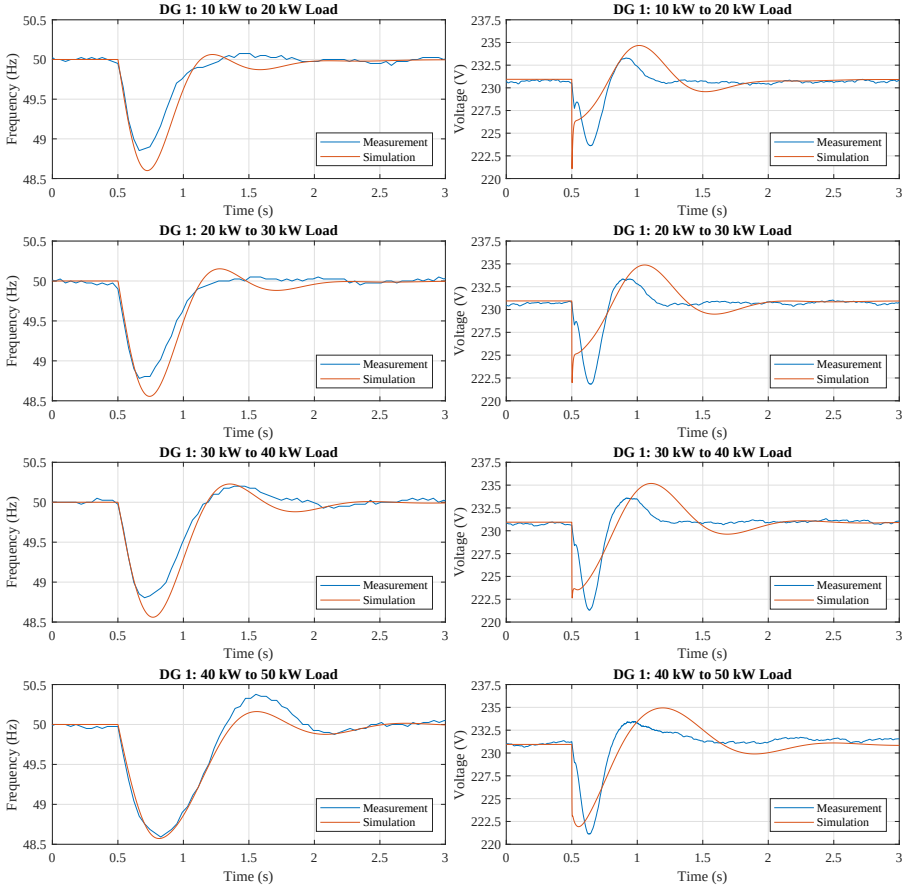

Figure 3.6: Frequency (left) and voltage (right) transients following steps of increasing active load on Diesel Generator 1 with isochronous governor and AVR but no AGC.

Generally, both the frequency and the voltage transients, on the left and right in Figure 3.6, respectively, show a satisfactory match between measurements and simulations. The small flicker in the voltages within the first tenths

of milliseconds after the load steps, relates to the calculation of RMS values. As shown in Figure 3.7, equally satisfying results are obtained for steps of increasing parallel active and reactive load elements on Diesel Generator 1; with the steps consisting of 10 kW and 5 kVAr load elements connected simultaneously in the load bank to the busbar.

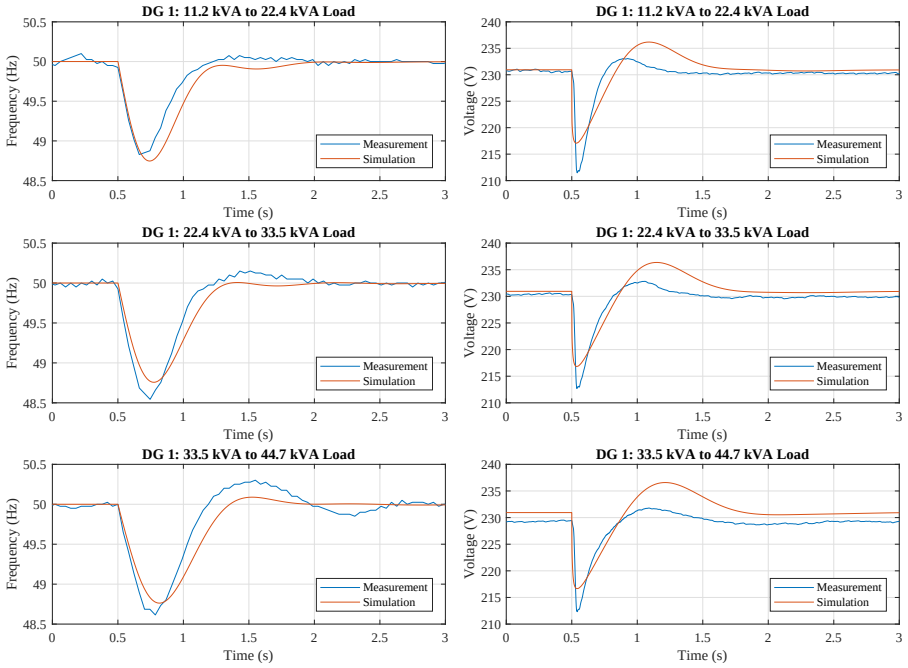

Figure 3.7: Frequency (left) and voltage (right) transients following steps of increasing active and reactive load on Diesel Generator 1 with isochronous governor and AVR but no AGC.

Contrary to the steps in active load, only three steps are possible with simultaneous active and reactive load elements. Although the fourth step, which would consists of 50 kW and 25 kVAr, seemingly lies within the 60 kVA rating of Diesel Generator 1, gensets are rated at a specific ratio between active and reactive power; denoted power factor. Rated at a power factor of 0.8, as is most often the case, Diesel Generator 1 has a rating of 60 kVA/48 kW, which means that the previous step to 50 kW is actually above the rated output, even without the additional load of the reactive elements. However, as evident in Figure 3.6, the diesel generator is capable of supplying a 50 kW load, at least for a limited time period, whereas a load of 50 kW and 25 kVAr is more than Diesel Generator 1 can handle even for a short time period. If such a load is connected regardless, the diesel-driven generator set will simply be unable to reestablish nominal frequency and voltage; quickly leading to a complete shutdown.

Figure 3.8 presents measurements and simulations of Diesel Generator 2 for steps of increasing active load elements, which for the 40 kVA/32 kW genset is limited to a maximum of 30 kW.

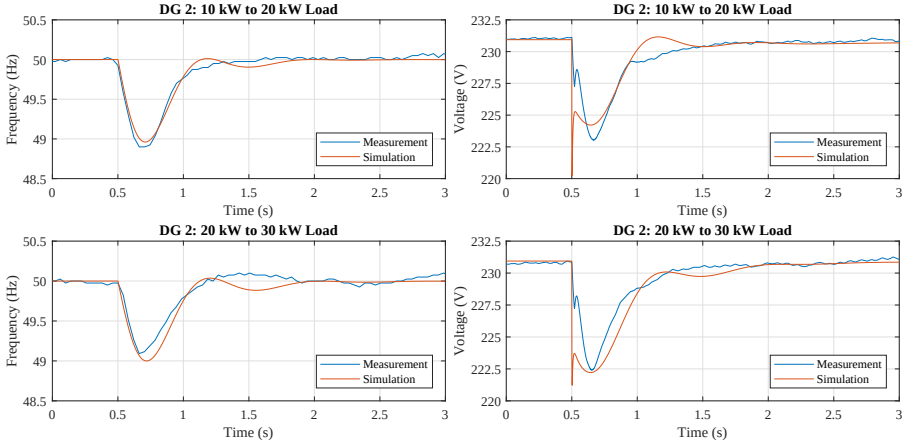

Figure 3.8: Frequency (left) and voltage (right) transients following steps of increasing active load on Diesel Generator 2 with isochronous governor and AVR but no AGC.

As with Diesel Generator 1, the results in Figure 3.8 show a satisfactory match between measurements and simulations both for frequency transients and voltage transients. In general, a slightly higher degree of correlation on the frequency transients than the voltage transients can be observed, which serves to emphasize the complexity of synchronous generators.

The specific model parameters utilized to obtain the simulation results have been determined following the same procedure for Diesel Generators 1 and 2. The total system inertia, J, is found as a combination of values from engine and generator datasheets. The mechanical torque base, $\underline{T}_m$, is found in the engine datasheet, whereas the electrical torque base, $\underline{T}_e$, and the mechanical angular velocity base, $\underline{\omega}_m$, are given by the generator volt-ampere rating, the number of magnetic poles in the rotor, and the nominal electrical angular velocity. The d and q-axis p.u. synchronous inductances, L_d and L_q, and the p.u. armature resistance per phase, R_a, are determined from datasheet values. In general, the parameters describing the rotor cannot be assumed available [Kundur, 1994], since the standards concerning the test procedures relevant for determining datasheet content do not include methods for determining those parameters [IEEE Power Engineering Society, 1983, 2010]. Generator datasheets [Mecc Alte, 2012; Leroy-Somer, 2015] represent typical datasheets with the amount of content that can be assumed available. Consequently, the generator rotor parameters, L_{ffd}, L_{11d}, L_{11q}, L_{f1d}, R_f, R_{1d}, and R_{1q}, are, for both Diesel Generator 1 and 2, determined utilizing the p.u. values in the

'Synchronous Machine Salient Pole (fundamental)' block [MathWorks, 2017] from the Simscape Power Systems toolbox of MATLAB Simulink®, which is based on models described in [Kundur, 1994; Lyshevski, 1999].

Five parameters remain undetermined; namely, the constant term of the engine time constant, τ_m, and the governor and AVR proportional and integral regulator gains, $k_{p\omega}$, $k_{i\omega}$, k_{pv}, and k_{iv}. Exploiting the measurements of increasing active load, those five parameters have been determined rather effortlessly for both Diesel Generator 1 and 2 through simple trial and error hand-tuning. A complete overview of all the utilized model parameters is provided in Table 3.1.

Table 3.1: Complete model parameter sets for DG 1 and DG 2 utilized in model validation.

Parameter	Unit	Diesel Generator 1	Diesel Generator 2
J	kg·m^2	1.8015	2.1654
D	N·m·s/rad	0.1	0.1
$\underline{\omega}_m$	rad/s	50π	50π
$\underline{T}_m$	N·m	390	265
$\underline{T}_e$	N·m	381.97	254.65
τ_m	s	0.1	0.075
σ	-	1	1
$k_{p\omega}$	-	8	13
$k_{i\omega}$	-	15	31
L_d	p.u.	2.83	1.9
L_q	p.u.	1.69	0.98
L_{ad}	p.u.	2.38	1.6
L_{aq}	p.u.	1.24	0.68
L_l	p.u.	0.45	0.3
$\underline{t}$	s	0.0032	0.0032
R_a	p.u.	0.0354	0.0208
L_{ffd}	p.u.	2.6371	1.8571
L_{11d}	p.u.	2.58	1.8
L_{11q}	p.u.	1.4967	0.9367
L_{f1d}	p.u.	2.38	1.6
R_f	p.u.	0.0006	0.0006
R_{1d}	p.u.	0.0354	0.0354
R_{1q}	p.u.	0.0428	0.0428
k_{pv}	-	0.03	0.011
k_{iv}	-	0.06	0.009
τ_v	p.u.	0.0064	0.0064

The restricted availability of generator rotor parameters, has a potentially significant impact on the validity of the presented diesel-driven generator set model. Therefore, formulating a sophisticated parameter identification method, capable of identifying as many parameters as possible, would improve the general applicability of the model. The parameter identification method would need the ability to identify parameters from measurements that are obtainable on any diesel generator. Measurements of controlled load steps, as utilized in this model validation, cannot always be obtained in the field. In [Knudsen et al., 2016b], a linear parameter identification method [Knudsen, 1994] was utilized on measurements of changing internal governor and AVR references with starting conditions given by the hand-tuned parameters; however, applying a linear method to a nonlinear model clearly has significant limitations. As parameter identification has not been within the scope of the present study, no alternative and more suitable methods have been investigated, but would be a clear candidate for subsequent work.

Naturally, diesel-driven generator sets are also subject to decreasing load, that is, the removal of load elements. Figure 3.9 presents measurements and simulations of Diesel Generator 1 for parallel active and reactive load elements simultaneously removed from the load bank.

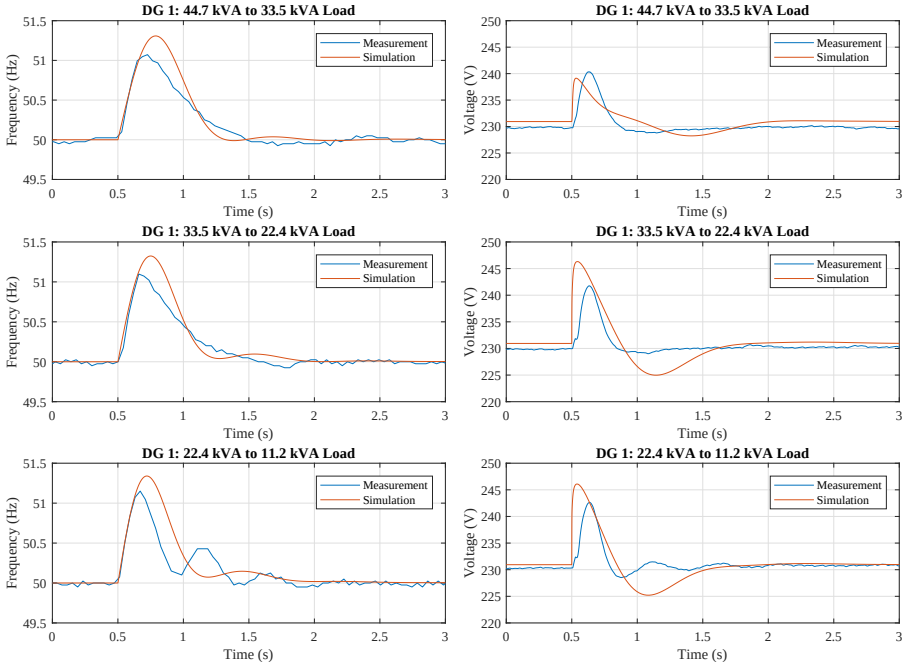

Figure 3.9: Frequency (left) and voltage (right) transients following steps of decreasing active and reactive load on Diesel Generator 1 with isochronous governor and AVR but no AGC.

Please note that the hand-tuned model parameters have been found exclusively considering increasing active load, hence, these results serve as a statement regarding the general validity of the model. As the last results provided, Figure 3.10 presents measurements and simulations of Diesel Generator 2 for steps of decreasing active load elements.

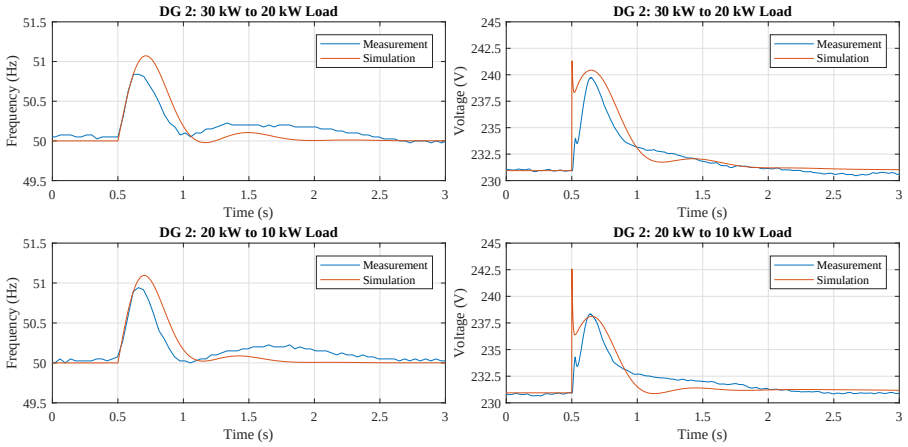

Figure 3.10: Frequency (left) and voltage (right) transients following steps of decreasing active load on Diesel Generator 2 with isochronous governor and AVR but no AGC.

The decreasing load results show, in alignment with the increasing load results, a satisfactory match between measurements and simulations, which at this point concludes the model validation and, thereby, the modeling of a diesel-driven generator set. The presented tenth-order nonlinear per unit model of a turbocharged, four-stroke, four-cylinder diesel engine driving a salient four-pole, three-phase, brushless excited, synchronous generator including governor and AVR PI regulators shows highly satisfactory results in comparison with measurements in a variety of increasing and decreasing active and apparent load step experiments.

4 Automatic Genset Controller Design

This chapter provides the synthesis of an Automatic Genset Controller regulator design for frequency and voltage stabilization during island operation of a single diesel generator, based on the model formulation in the previous chapter. Implementation results are presented in the interest of demonstrating the applicability of the approach.

As introduced in Sections 1.1 and 3.1, an AGC unit sends signals, which act as offsets to the internal governor and AVR references. Seeking an alternative solution that can reduce the regulator parameter tuning complexity during commissioning compared to the current industry-standard PID regulators, a design based on the Linear Quadratic Regulator is proposed. Given the generic nature of the per unit diesel-driven generator model and the LQR method, it is hypothesized that a simple regulator parameter tuning scheme can be formulated for an LQR design as well.

Applying an LQR requires a linear system representation and full state information. Thus, linearization of the nonlinear diesel generator model and formulation of a state estimator to supplement the state feedback regulator are required, since most of the system states are not readily available.

4.1 Model Linearization

Linearization of a nonlinear model is commonly done in a series of operating points to capture the changing dynamics throughout the operating range of the system. Denoted i, the operating points belong to the set $\{1, \ldots, n_{op}\}$ where n_{op} is the number of operating points chosen to capture the changing dynamics. For a diesel-driven generator set the dynamics are significantly impacted by the connected load; with island operation in mind, the effect of any reactive load component is neglected and the per phase p.u. load resistance, R_L, is chosen as the decision variable for operating points. That is, the stator voltages, v_d and v_q, are in the context of linearization and regulator

design determined using only the first terms in Equations (3.13), namely

$$\begin{bmatrix} v_d \\ v_q \end{bmatrix} = R_L \begin{bmatrix} i_d \\ i_q \end{bmatrix} = R_L \begin{bmatrix} \frac{c_{30}}{c_{28}} & 0 & -\frac{c_{31}}{c_{28}} & -\frac{c_{32}}{c_{28}} & 0 \\ 0 & \frac{L_{11q}}{c_{29}} & 0 & 0 & -\frac{L_{aq}}{c_{29}} \end{bmatrix} \begin{bmatrix} \psi_d \\ \psi_q \\ \psi_f \\ \psi_{1d} \\ \psi_{1q} \end{bmatrix}$$

R_L will be referred to as the disturbance, d, in the following. Determination of the disturbance, that is, the per phase p.u. load resistance, is based on three-phase measurements of stator voltages and currents. Assuming a balanced three-phase resistive load, the disturbance is thus considered known at all times, within measurement accuracies.

Using first-order Taylor series expansion as the linearization method, the linear model of the i-th operating point takes the form

$$\dot{x}_i^\delta = \bar{A}_i x_i^\delta + \bar{B}_i u_i^\delta + \bar{B}_{di} d_i^\delta \tag{4.1a}$$
$$y_i^\delta = \bar{C}_i x_i^\delta \tag{4.1b}$$

where $\bar{A}_i \in \mathbb{R}^{10\times10}$, $\bar{B}_i \in \mathbb{R}^{10\times2}$, $\bar{B}_{di} \in \mathbb{R}^{10\times1}$, and $\bar{C}_i \in \mathbb{R}^{2\times10}$ are the linearized system, control input, disturbance input, and output matrices, respectively. Further, x_i^δ, u_i^δ, d_i^δ, and y_i^δ are the small-signal state, input, disturbance, and output vectors around the corresponding i-th operating point, respectively. The large-signal values, x, are given by the small-signal, x_i^δ, and operating point values, $\bar{x}_i$, as

$$x = x_i^\delta + \bar{x}_i$$

exemplified here by the state variables. Recalling that the inputs, u, are offsets to the internal governor and AVR references, ideally $\bar{u}_i = 0$ for all operating points, since both the governor and AVR have integral action included in their internal regulation. Further, the output operating point values are

$$\bar{y}_i = \begin{bmatrix} \underline{\omega}_m & \underline{v}_{rms} \end{bmatrix}^T \qquad \forall i \in \{1, \ldots, n_{op}\}$$

where $\underline{v}_{rms}$ is the nominal three-phase phase-to-neutral p.u. RMS stator voltage. The operating point values of the disturbance, $\bar{d}_i$, should, in general, be chosen such that the linearized models describe the dynamics of the nonlinear system sufficiently well; the exact distribution and number of operating points is rarely obvious though. In this work, the values of the available active load elements in the laboratory facilities were chosen; that is, the per phase p.u. load resistance values for Diesel Generator 1 are

$$\bar{d}_i \in \{6,\ 3,\ 2,\ 1.5,\ 1.2\} \qquad , i \in \{1, \ldots, 5\}$$

corresponding to electrical loads of 10 kW, 20 kW, 30 kW, 40 kW, and 50 kW, respectively, on the 60 kVA diesel-driven generator set with a 400 V phase-to-phase RMS voltage rating. For Diesel Generator 2, the per phase p.u. load resistance values are

$$\bar{d}_i \in \{4,\ 2,\ 4/3\} \qquad ,i \in \{1,\ 2,\ 3\}$$

corresponding to electrical loads of 10 kW, 20 kW, and 30 kW, respectively, on the 40 kVA genset with a 400 V phase-to-phase RMS voltage rating. Finally, the state operating point values, $\bar{x}_i$, can be determined by solving the system equations with $\dot{x} = 0$ for a given disturbance, $\bar{d}_i$.

4.2 Large-Signal State Estimator

Also known as state observers, classical Luenberger state estimators consider small-signal values near the operating point of a linear model [Luenberger, 1964, 1966]. For the linear system model in Equations (4.1) the classical Luenberger small-signal state estimator is

$$\dot{\hat{x}}_i^\delta = \bar{A}_i \hat{x}_i^\delta + \bar{B}_i u_i^\delta + \bar{B}_{di} d_i^\delta + L_i \left(y_i^\delta - \bar{C}_i \hat{x}_i^\delta \right) \tag{4.2}$$

where $\hat{x}_i^\delta$ is the estimated small-signal state vector, $\dot{\hat{x}}_i^\delta$ its time derivative, d_i^δ is the small-signal disturbance, and $L_i \in \mathbb{R}^{10\times 2}$ is the estimator gain matrix; all of the i-th operating point.

Requiring only the small-signal output, y_i^δ, and the system knowledge represented by the linearized model, a Luenberger estimator will estimate the small-signal states of any observable system, such as the linearized models given in Equations (4.1) [Franklin et al., 2010]. Unlike large-signal values, however, small-signal values develop discontinuously during operating point changes, as illustrated by the simple example presented in Figure 4.1, in which the sign difference between two scalar small-signal states, x_1^δ and x_2^δ, at the time of a change in operating point, t_0, is emphasized.

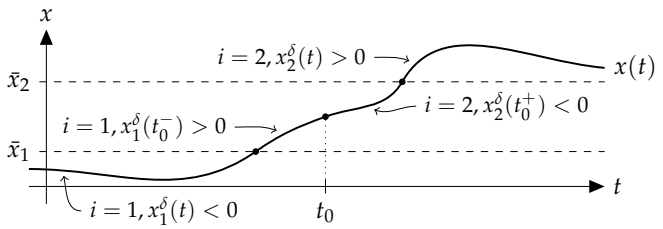

Figure 4.1: Sign difference between the scalar small-signal states, $x_1^\delta(t)$ and $x_2^\delta(t)$, at a change of operating point at time t_0 for the scalar large-signal value, $x(t)$.

In control implementations utilizing estimates for state feedback, such discontinuities must be handled at each change of operating point by resetting the value of the estimated small-signal states to values determined a priori, in order to avoid potential stability issues. The small-signal Luenberger estimator in Equation (4.2) is, therefore, reformulated as a large-signal state estimator for the linearized models of Equations (4.1). Effectively, this reformulation leads to a collection of affine models sharing the same state, thus requiring only a change in constant matrices and inputs. The dynamics of the resulting large-signal estimator are then given by

$$\dot{\hat{x}} = \bar{A}_i(\hat{x} - \bar{x}_i) + \bar{B}_i(u - \bar{u}_i) + \bar{B}_{di}\big(d - \bar{d}_i\big) + L_i(y - \bar{y}_i - \bar{C}_i(\hat{x} - \bar{x}_i))$$

where $\hat{x}$ is the estimated large-signal state vector and $\dot{\hat{x}}$ its time derivative. Since $\bar{u}_i = 0$ and $\bar{y}_i = \bar{C}_i\bar{x}_i$ for all operating points, i, the large-signal state estimator reduces to

$$\dot{\hat{x}} = \bar{A}_i\hat{x} + \bar{B}_i u + \bar{B}_{di}d + L_i(y - \bar{C}_i\hat{x}) - \bar{A}_i\bar{x}_i - \bar{B}_{di}\bar{d}_i \tag{4.3}$$

for which an overview is provided in Figure 4.2.

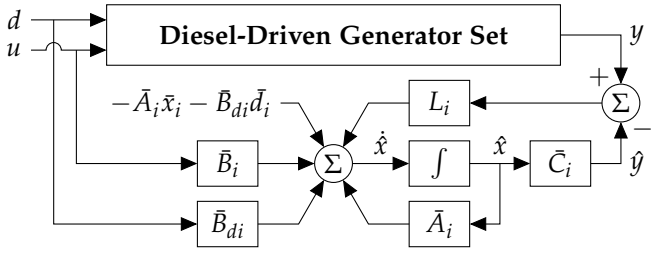

Figure 4.2: Structural diagram of the large-signal state estimator provided in Equation (4.3). Note, all operating point discontinuities have been moved in front of the integration by the reformulation to a large-signal state estimator.

As mentioned in Section 4.1, the operating points have been chosen to match the available active load elements in the laboratory facilities; hence, the system always operates exactly in an operating point or changes directly from one to another in this study. Therefore, the switching of operating point has not been given special attention in this implementation, but is implemented unfiltered. In real-world implementations, where the switching of operating point becomes less predictable, this is very likely to be of greater relevance. A rather simple and often effective approach is to implement a hysteresis on the switching, which guarantee a specific minimum time between switching. An analysis of this issue is presented, for example, in [Hespanha and Morse, 1999], in which the authors guarantee stability of switched systems with requirements for the so-called average dwell-time.

Assuming a correct model is available, the dynamics of the large-signal state estimation error, $e_x = x - \hat{x}$, are given by

$$\begin{aligned}\dot{e}_x &= \bar{A}_i(x - \bar{x}_i) + \bar{B}_i u + \bar{B}_{di}(d - \bar{d}_i) \\ &\quad - \bar{A}_i(\hat{x} - \bar{x}_i) - \bar{B}_i u - \bar{B}_{di}(d - \bar{d}_i) - L_i(y - \bar{C}_i\hat{x}) \\ &= (\bar{A}_i - L_i\bar{C}_i)e_x\end{aligned}$$

Hence, for constant i, the large-signal state estimation error goes to zero, if $\bar{A}_i - L_i\bar{C}_i$ is Hurwitz.

4.3 Linear Quadratic Regulator

In agreement with the research objective to obtain reduced parameter tuning complexity for an AGC regulator, the LQR state feedback theory is applied, due to its generic nature. The LQR theory is well-established and thoroughly described in literature, see for example [Kwakernaak and Sivan, 1972; Anderson and Moore, 1989; Skogestad and Postlethwaite, 1996]; nonetheless, a brief summary is provided in this section.

For each linear system $\dot{x}_i^\delta(t) = \bar{A}_i x_i^\delta(t) + \bar{B}_i u_i^\delta(t)$, where $\bar{A}_i \in \mathbb{R}^{10\times 10}$ and $\bar{B}_i \in \mathbb{R}^{10\times 2}$ are the linearized system and input matrices of the i-th operating point, the optimal state feedback is the small-signal input, $u_i^\delta(t)$, that brings the system to the desired state, $\bar{x}_i$, in an optimal manner. In the LQR problem, the optimal manner is defined as the minimization of

$$J_i(t) = \int_0^\infty x_i^\delta(t)^T Q x_i^\delta(t) + u_i^\delta(t)^T R u_i^\delta(t)\, dt \tag{4.4}$$

where $Q \in \mathbb{R}^{10\times 10}$ and $R \in \mathbb{R}^{2\times 2}$ are positive semi-definite and definite weighting matrices, respectively. For any initial small-signal state, $x_i^\delta(0)$, the minimizing solution to Equation (4.4) can be shown to be

$$u_i^\delta(t) = -K_i x_i^\delta(t)$$

where K_i is the LQR state feedback matrix found as

$$K_i = R^{-1}\bar{B}_i^T P_i$$

where P_i, furthermore, is the unique positive semi-definite solution to the algebraic Riccati equation given by

$$\bar{A}_i^T P_i + P_i\bar{A}_i - P_i\bar{B}_i R^{-1}\bar{B}_i^T P_i + Q = 0$$

Accommodating the large-signal state estimator, formulated in Section 4.2, the large-signal control law becomes

$$u = -K_i\hat{x} + K_i\bar{x}_i \tag{4.5}$$

The performance of the closed-loop system is determined by the design choice of Q and R in Equation (4.4).

4.4 Laboratory Implementation Results

The proposed Automatic Genset Controller design is experimentally investigated through implementation in the Rapid Control Prototyping system introduced in Section 1.2. All measurements presented are obtained with the data collection system similarly introduced in Section 1.2.

Throughout, the control performance achieved by the LQR-based AGC design is compared to the performance of an industry-standard PID regulator solution, tuned by an experienced commissioning engineer, and a so-called open-loop solution. In this context, open-loop is defined as providing no offset to the isochronous governor and AVR, which are operational, and with identical parameters, in every test. Due to communication delays between the Automatic Genset Controller unit and the governor and AVR and various modeling inaccuracies, it is not predetermined that an AGC design will improve the control performance, which is why the open-loop performance is included in this comparison as a baseline.

Linear Quadratic Regulator Tuning

As detailed in Section 3.5, Diesel Generators 1 and 2 in the laboratory facilities are described by individual model parameter sets; provided in Table 3.1.

The generic nature of the per unit diesel-driven generator set model and the LQR method, enables calculation of all the unique LQR feedback gain matrices, K_i, for all operating points, i, of both Diesel Generator 1 and 2, utilizing the same tuning parameter structure. That is, solving the Linear Quadratic Regulator problem, given by Equation (4.4), for all cases by applying the diagonal weighting matrices

$$Q = \begin{bmatrix} 25 & & & & 0 \\ & 1 & & & \\ & & 1 & & \\ & & & \ddots & \\ 0 & & & & 1 \end{bmatrix} \in \mathbb{R}^{10\times 10} \tag{4.6a}$$

$$R = \begin{bmatrix} \rho & 0 \\ 0 & \rho \end{bmatrix} \tag{4.6b}$$

In the LQR problem, the values of the elements in the weighting matrices signify the priority of reducing deviations in the corresponding states and inputs from the equilibrium. The choice of a large value in the $(1,1)$-element of Q in Equation (4.6a) prioritizes deviations in the p.u. angular velocity of the shaft, ω_m, above any other state, as this has a significant impact on stabilizing both the electrical frequency and the voltage. As the voltage affects the engine through the electrical torque, it is common practice to prioritize stabilizing

the frequency. Furthermore, applying weights to the inputs by increasing ρ in Equation (4.6b), generally makes the LQR less aggressive.

The large-signal state estimator gain matrices, L_i, have been computed using identical Q and R for all operating points, i, for both Diesel Generator 1 and 2. The calculations were done using `place()`, MATLAB's implementation of the robust pole assignment algorithm presented in [Kautsky et al., 1985]. The poles of each $\bar{A}_i - L_i\bar{C}_i$ are placed at three times the pole values of the corresponding $\bar{A}_i - \bar{B}_i K_i$, such that the state estimation error, in general, decreases faster than the control error.

Figure 4.3 presents three sets of measurements of Diesel Generator 1 for steps of increasing active load; in open-loop, with the industry-standard PID regulator solution, and with the proposed LQR design. The applied LQR has

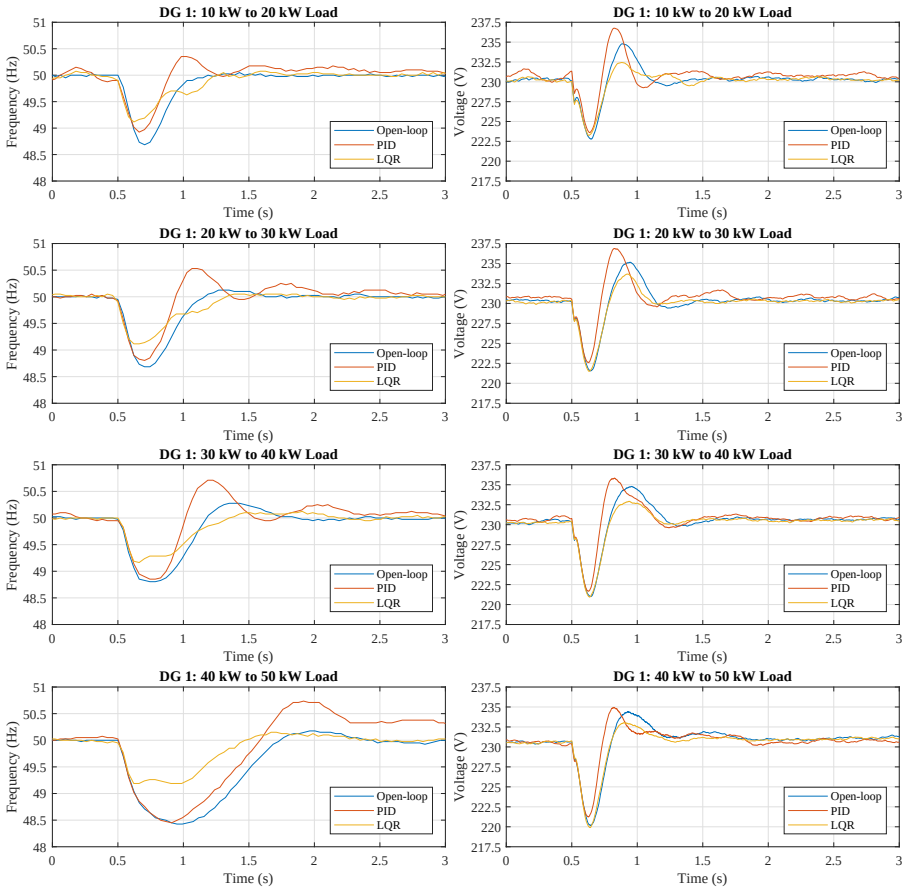

Figure 4.3: Frequency (left) and voltage (right) transients following steps of increasing active load with no supervisory controller, an industry-standard PID regulator, and the proposed LQR on Diesel Generator 1 with isochronous governor and AVR.

been computed with $\rho = 200$ for all five operating points. Similar measurements are presented in Figure 4.4, of Diesel Generator 2 for steps of increasing active load. For Diesel Generator 2, the applied LQR has been computed with $\rho = 300$ for all three operating points.

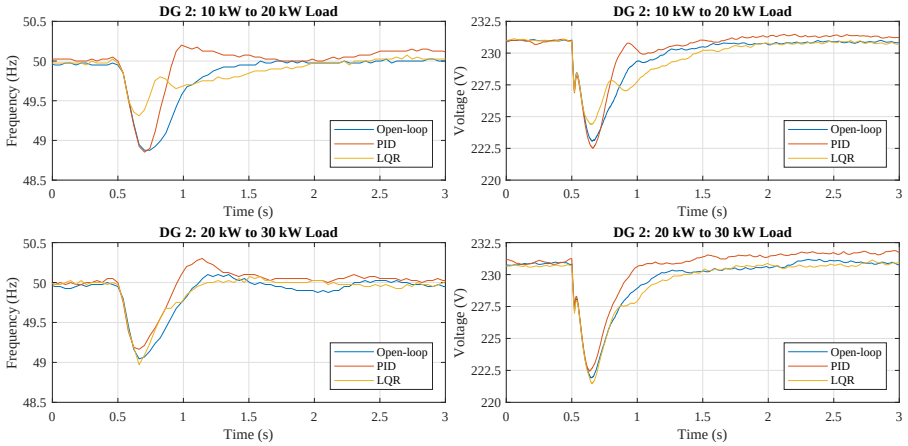

Figure 4.4: Frequency (left) and voltage (right) transients following steps of increasing active load with no supervisory controller, an industry-standard PID regulator, and the proposed LQR on Diesel Generator 2 with isochronous governor and AVR.

In general, the stabilization performance of the LQR-based AGC design is an improvement in both frequency and voltage transients on the open-loop solution for both gensets; except perhaps, the settling time following the step from 10 kW to 20 kW on Diesel Generator 2. In comparison, the PID regulator solution causes excessive overshoot, in most cases. However, it should be noted that the integral action of the PID regulator makes that solution the only one capable of sustaining nominal frequency and voltage in feasible steady-state conditions, which implies that the integral action of the governor and AVR are, in practice, insufficient. Figure 4.5 confirms the observations for a step of decreasing active load of Diesel Generator 1.

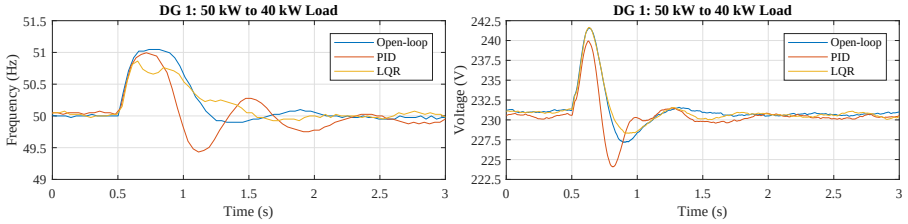

Figure 4.5: Frequency (left) and voltage (right) transients following step of decreasing active load with no supervisory controller, an industry-standard PID regulator, and the proposed LQR on Diesel Generator 1 with isochronous governor and AVR.

The significance of ρ in Equation (4.6b) is presented in Figures 4.6 and 4.7 where measurements of LQR solutions with different ρ-values demonstrate how ρ provides a simple regulator tuning scheme applicable on both gensets.

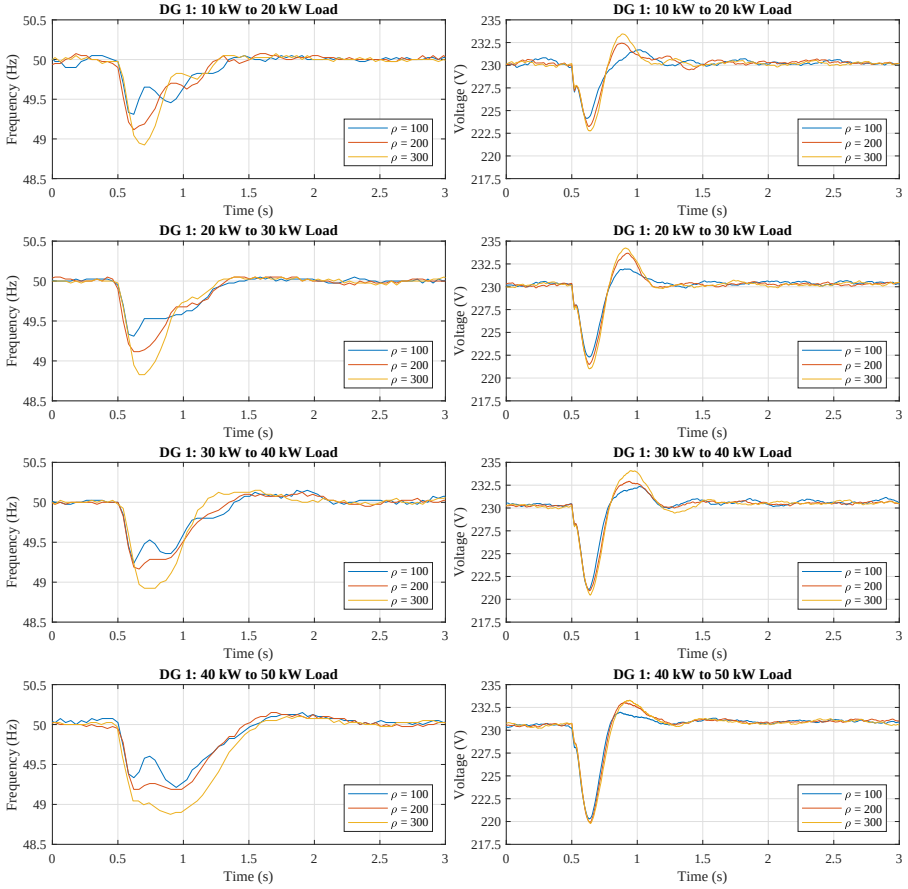

Figure 4.6: Frequency (left) and voltage (right) transients following steps of increasing active load with LQRs of different ρ's on Diesel Generator 1 with isochronous governor and AVR.

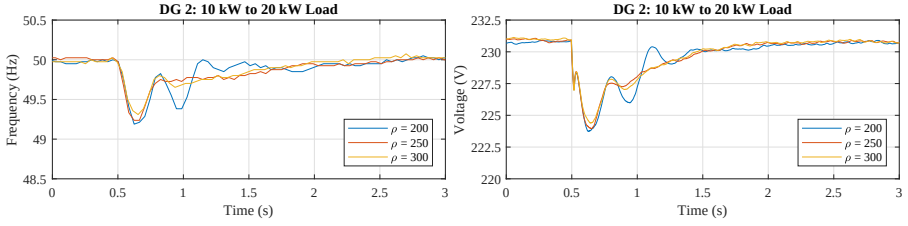

Figure 4.7: Frequency (left) and voltage (right) transients following step of increasing active load with LQRs of different ρ's on Diesel Generator 2 with isochronous governor and AVR.

As part of the linearization approach presented in Section 4.1, effects of any non-resistive load is neglected in the proposed LQR-based AGC design. To investigate the implications of this approach, the inductive elements in the load bank are applied in parallel with resistive elements to expose the diesel-driven generator sets to steps in apparent power. Figure 4.8 presents measurements of Diesel Generator 1 for simultaneous steps of increasing active and reactive load.

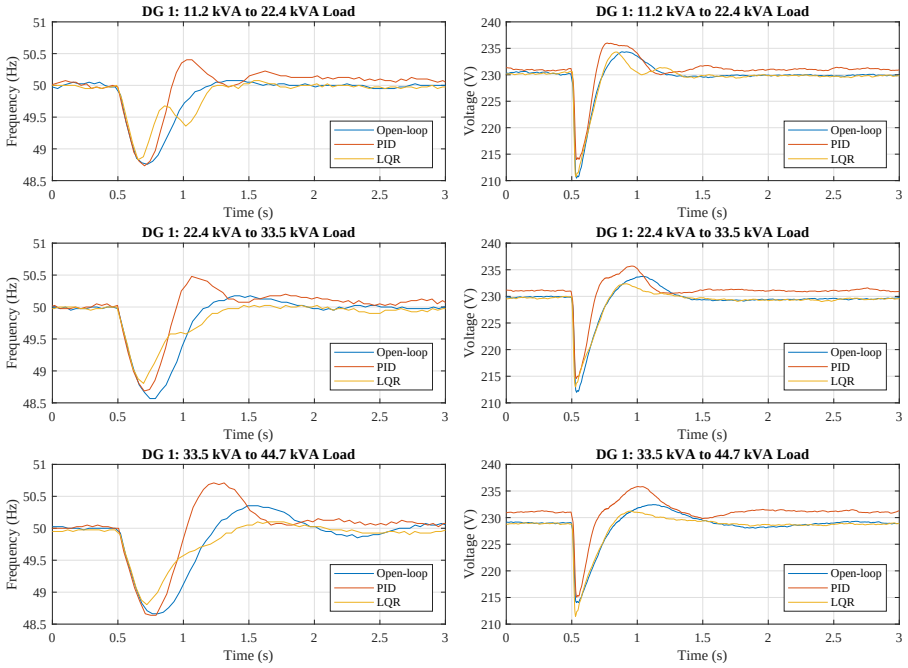

Figure 4.8: Frequency (left) and voltage (right) transients following simultaneous steps of increasing active and reactive load on Diesel Generator 1 with isochronous governor and AVR.

Generally, the LQR solution exhibits stabilization performance improvements in comparison with both the open-loop and the PID regulator solution; even for steps of load not included in the design.

In accordance with earlier observations, the voltage measurements in Figure 4.8 demonstrate the insufficient integral action of the governor and AVR, which is very noticeable when exposed to an apparent power load. The PID regulator solution is the only solution capable of achieving nominal voltage within the measurement period, as the open-loop and LQR solutions suffer from the insufficiency of the governor and AVR integral action in this regard.

Both the stabilization performance and the steady-state observations are confirmed in Figure 4.9, which presents measurements of Diesel Generator 2 for simultaneous steps of increasing active and reactive load.

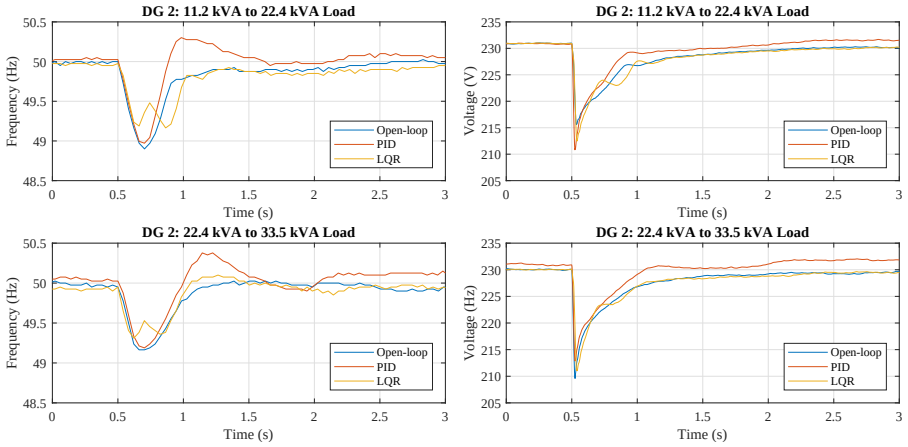

Figure 4.9: Frequency (left) and voltage (right) transients following simultaneous steps of increasing active and reactive load on Diesel Generator 2 with isochronous governor and AVR.

The performance of the LQR solution is additionally confirmed by the measurements of Diesel Generator 2 for simultaneous steps of decreasing active and reactive load presented in Figure 4.10.

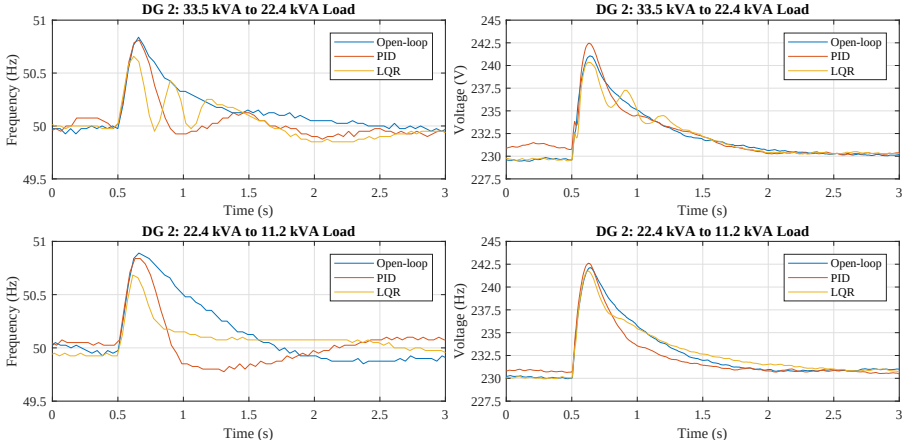

Figure 4.10: Frequency (left) and voltage (right) transients following simultaneous steps of decreasing active and reactive load on Diesel Generator 2 with isochronous governor and AVR.

Furthermore, the simple regulator tuning scheme obtained through ρ in Equation (4.6b) remains valid in the case of parallel resistive and inductive load elements, even though inductive elements are not included in the design. Figure 4.11 presents measurements of Diesel Generator 1 for simultaneous steps of increasing active and reactive load with LQRs of different ρ-values.

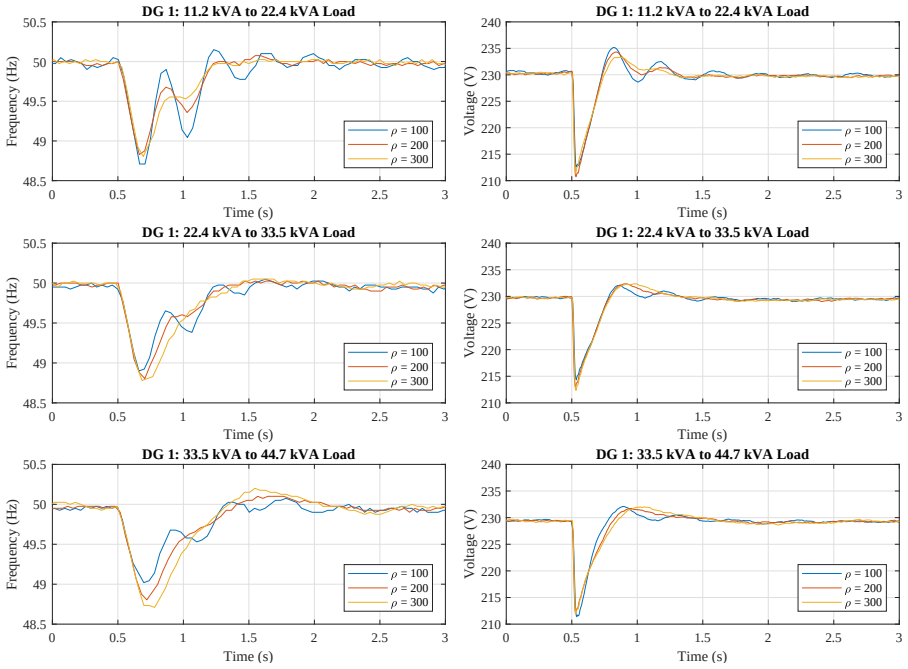

Figure 4.11: Frequency (left) and voltage (right) transients following simultaneous steps of increasing active and reactive load with LQRs of different ρ's on Diesel Generator 1 with isochronous governor and AVR.

These results conclude the experimental investigation of the proposed LQR-based AGC design. A few final remarks concerning the general complexity of diesel-driven generator sets complete this chapter.

The nature of Diesel Generator 2 commands a rather conservative AGC regulator design, whereas Diesel Generator 1 is more lenient towards aggressive AGC regulation. In the field, even the most experienced commissioning engineers cannot know such details a priori. Furthermore, a comparison of the open-loop measurements presented in Figure 3.6 with the open-loop measurements presented in Figure 4.3 reveals a significant discrepancy in the time it takes for Diesel Generator 1 to return to nominal frequency following the step of increasing active load from 40 kW to 50 kW. Probably owing to general wear and tear, such variations in dynamic behavior occur frequently in real-life systems and must be anticipated. Evidently, the proposed LQR-based AGC design approach has a certain robustness against this degree of parameter variation, since no adjustments were made to accommodate it. That is, the parameter identification was completed utilizing the measurements presented in Figure 3.6, whereas the genset exhibits these different dynamics during the control design experiments presented in this section.

5 Fuel Optimization as Plant Management

This chapter provides general considerations regarding fuel efficiency of diesel-driven generator set plants, presents measurements of fuel consumption from a genset operating in different conditions, and proposes a plant fuel optimization method based on Genetic Algorithm theory.

Plant management of diesel-driven generator set plants involves a series of tasks, depending on the purpose and conditions of each plant. In the present study, the plant operational mode commonly denoted Mains Power Export is considered. A genset plant operating in the Mains Power Export mode is connected to a well-established mains and is required to generate a scheduled amount of power. The power schedule is typically specified for hourly intervals and provided one day ahead. When operating in Mains Power Export mode the primary plant management task is to guarantee compliance with the power schedule. Additional plant management tasks include supervision and scheduling of maintenance, supervision of the fuel supply, etc.

Owners of diesel generator plants, generally, attempt to maximize the overall efficiency in planning and operating the plants. Figure 5.1 shows a single-line diagram of a 30 genset plant with one mains connection, applying one specific branch structure across the entire plant; contrary to the previous example in Figure 1.4. Transformers are placed in close physical vicinity of the diesel generators and high capacity cables are utilized in a combined effort to minimize cable losses. Additionally, transformers are typically of the same type, make, and model as this helps minimize maintenance costs. The same is the case for the actual gensets. Altogether, these precautions eliminate any potential efficiency difference due to diesel generator location inside a plant. In other words, only the individual efficiency of the gensets themselves cause considerable differences between them in that regard.

While intelligent planning and regular maintenance are important to the overall efficiency of a plant, various circumstances affect the efficiency of individual diesel generators on a faster timescale than the normal maintenance intervals. Within the area covered by a plant, the ambient air temperature can

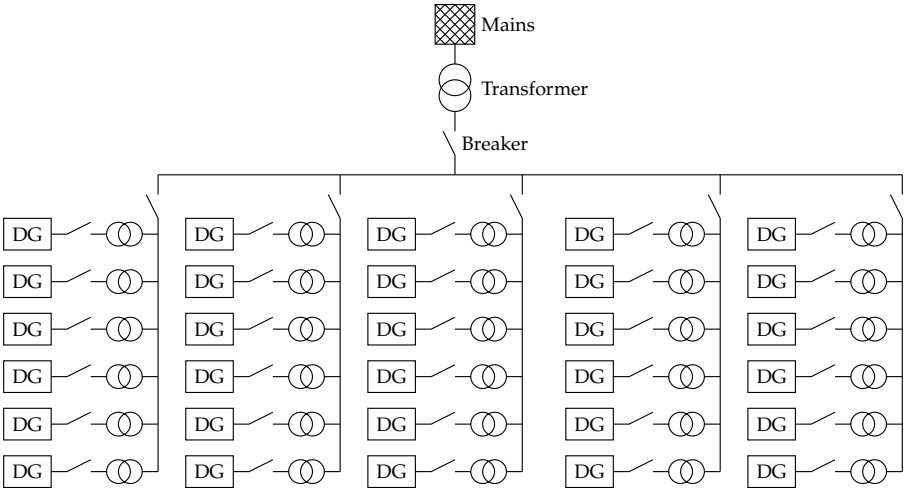

Figure 5.1: Diagram of a 30 genset plant with five branches utilizing identical branch structures.

vary significantly as a result of shade, wind direction, or neighboring gensets. The efficiency of the internal combustion process is affected by the intake air temperature, which is regulated by a cooling system on the diesel engine. Typically for plant gensets, such cooling systems are electrically driven and often consume two to three percent of the rated power of the diesel generator; effectively reducing the overall efficiency of the genset [MTU Onsite Energy, 2017a,b; Kraemer, 2013]. For cooling systems running exclusively at full capacity, optimization of energy use is inherently pointless; however, some cooling systems allow optimization through regulation.

An additional example of circumstances affecting the efficiency of diesel generators, is the state of the air filters. Depending on the pressure difference across the filter with the diesel engine running, air filters are replaced or cleaned during regular maintenance. However, clogging of air filters may happen suddenly, for example, due to wind gusts blowing sand onto diesel generators in an area of a plant. Measurements presented in Section 5.1 verify that clogged air filters cause decreased genset fuel efficiency. Automatically redistributing power demands from diesel generators operating at reduced efficiency, could optimize the plant fuel efficiency until a service engineer is available to identify and, if possible, eliminate the problem.

5.1 Diesel Generator Efficiency

The efficiency of a synchronous generator, typically, lies above 90%, with a variation of only a few percentage points in the power generation range of

20% to 100% [Leroy-Somer, 2015]. For the present study, the efficiency of a synchronous generator is, therefore, considered constant; leaving the diesel engine as the defining component in genset fuel efficiency characterization.

In general, diesel-driven generator set engine datasheets provide sparse information regarding fuel consumption. Typically, fuel consumption at three or four levels of load are provided, for example, at 25%, 50%, 75%, and 100% of rated power. Figure 5.2 presents datasheet information from four differently rated engines [Deutz AG, 2005, 2015; MTU Onsite Energy, 2007, 2017a]. Furthermore, least-square second degree polynomial fits are shown for each set of datasheet values.

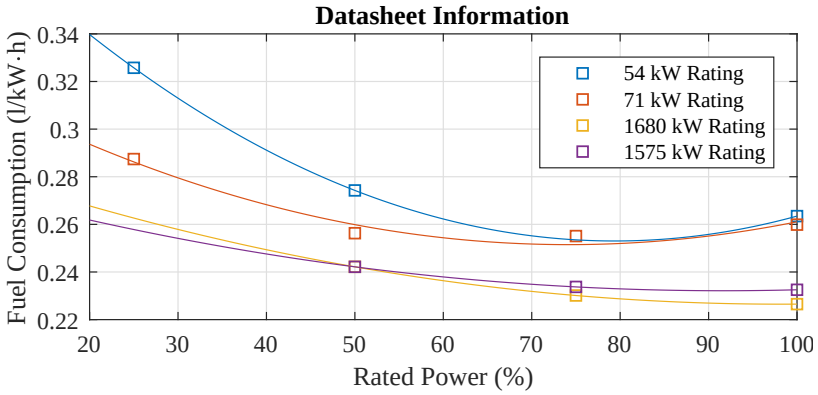

Figure 5.2: Datasheet fuel consumption information for 54 kW [Deutz AG, 2005], 71 kW [Deutz AG, 2015], 1680 kW [MTU Onsite Energy, 2017a], and 1575 kW [MTU Onsite Energy, 2007] rated engines with corresponding second degree polynomial fits.

The least-square second degree polynomial fits are considered sufficient to represent the fuel consumption characteristics of a diesel generator for fuel optimization from a plant management perspective. In an effort to validate this representation further and to demonstrate realistic consumption variations for a diesel-driven generator set, experiments of Diesel Generator 1 with a new and a clogged air filter have been conducted.

To the extent possible with the laboratory facilities, the conditions of the experiments are constant and identical in terms of ambient air temperature and humidity and engine temperature. In one experiment, a brand new air filter is fitted on Diesel Generator 1, whereas the other experiment utilizes a clogged air filter. The clogged air filter is an air filter partly wrapped in duct tape, to emulate a filter that should be replaced. Air filters are replaced when the pressure drop across them reach a specific level, which for the utilized air filter is 50 mbar. After identical warm-up periods, active power load is applied to the genset. The measurements presented in Figure 5.3 are average consumption values over 10-minute steady-state periods.

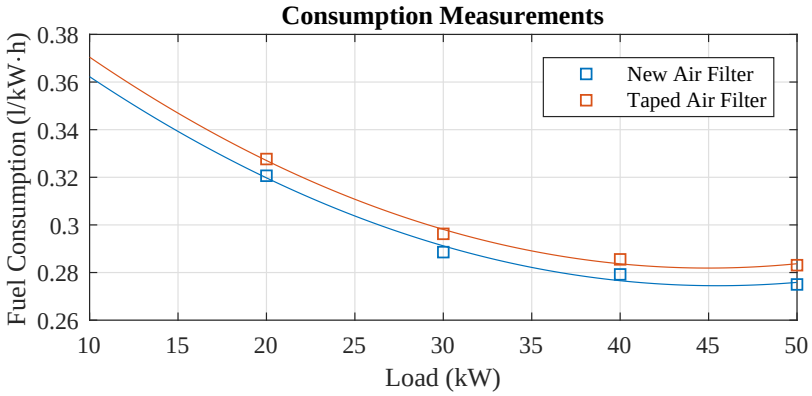

Figure 5.3: Measured fuel consumption with new and taped air filter. Values are 10-minute steady-state averages, while the lines are corresponding second degree polynomial fits.

Figure 5.3 confirms the usage of least-square second degree polynomial fit representations for genset fuel consumption characteristics. Additionally, the measurements show a practically vertical shift of the entire consumption curve of about 2% between the good and bad air filter conditions. Table 5.1 provides the experimental data, shown in Figure 5.3, together with the air filter pressures, measured using a Testo 435 multifunction meter.

Table 5.1: Measurement data from fuel consumption experiment with new and taped air filter and corresponding air filter pressures.

	Fuel Consumption (l/kW·h)		Air Filter Pressure (mbar)	
Load (kW)	New Filter	Taped Filter	New Filter	Taped Filter
20	0.321	0.328	4	33
30	0.289	0.296	5	39
40	0.279	0.286	5	44
50	0.275	0.283	6	51

The reader is urged to analyze the absolute values of this experimental data with caution, due to the simplicity of the experimental setup and the unavoidable measurement tolerances. For one, the Titan/RS Pro OG1-SSS-SSQ-B oval gear flowmeter, which has been used to measure the fuel, has a documented accuracy of $\pm 0.5\%$. However, the key insight to take from these measurement results is the confirmation that the air filter conditions indeed affect the fuel consumption of a diesel-driven generator set. Furthermore, it is interesting to note that the bad air filter conditions cause a practically constant offset to the consumption curve across the entire range. If that effect can be confirmed for alternative conditions affecting the fuel efficiency of

a diesel generator as well, it greatly simplifies the process of acquiring the information needed for a live optimization algorithm based on such curves.

5.2 Fuel Optimization Problem

As discussed in the previous sections of the present chapter, from a plant management perspective, the fuel optimization problem can be expressed by the individual diesel-driven generator set fuel consumption characteristics; approximated by second degree polynomials.

The second degree polynomials provide the fuel consumption in liters per kilowatt hour. However, prior to formulating an optimization problem including many diesel generators, these consumption curves are converted to strictly monotonic increasing third degree polynomials, by the multiplication of kilowatt, providing the consumption in liters per hour. As an example, Figure 5.4 presents the resulting third degree polynomials of Diesel Generator 1 for the second degree polynomials of the new and taped air filter conditions presented in Figure 5.3.

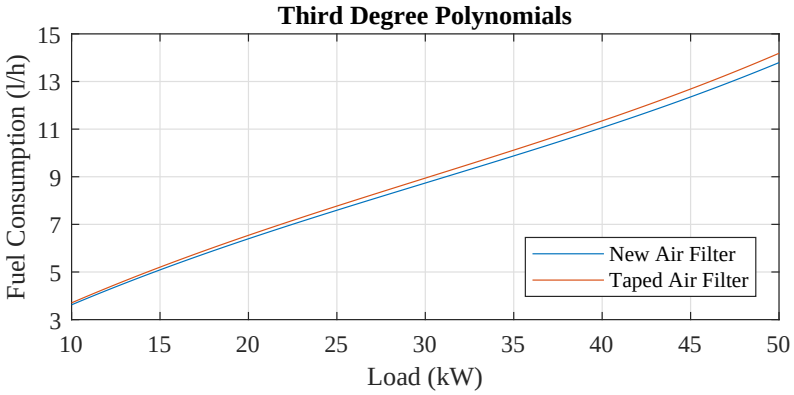

Figure 5.4: Third degree polynomials for fuel consumption in liters per hour of the corresponding new and taped air filter condition second degree polynomials presented in Figure 5.3.

Let $f_i(p_i)$ denote the third degree polynomial of the i-th diesel generator where p_i is the generated power. For a plant consisting of n gensets, the fuel optimization as a plant management problem is given by

$$\min_{p_i} \quad \sum_{i=1}^{n} f_i(p_i) \tag{5.1a}$$

$$\text{s.t.} \quad 0 \leq p_i \leq \bar{p}_i \quad \forall i \tag{5.1b}$$

$$\sum_{i=1}^{n} p_i = r \tag{5.1c}$$

where $\bar{p}_i$ is power generation rating of the i-th diesel generator and r is the plant power reference. All the third degree polynomials, $f_i(p_i)$, are strictly convex for power generation levels above their inflection point, which in the case of diesel generators lie around 50% of the rated power. In other words, $f_i(p_i)$ are strictly convex in the region of highest fuel efficiency. Originally provided in [Knudsen et al., 2017b], Proposition 1 shows that the plant power reference, r, should be distributed equally in a plant consisting of n diesel generators with identical fuel consumption curves, f, operating in the strictly convex power generation region. Figure 5.5 presents an illustration of the proof for the simple case of $n = 2$.

Proposition 1. *For any strictly convex function* $h(p_1, \ldots, p_n) = f(p_1) + \cdots + f(p_n)$*, where the function* $f : \mathbb{R} \to \mathbb{R}$ *is strictly convex, if* dom h *is constrained by* $p_1 + \cdots + p_n = r$*, the minimum of* $h(p_1, \ldots, p_n)$ *is at* $(p_1, \ldots, p_n) = (\frac{r}{n}, \ldots, \frac{r}{n})$.

Proof. By construction, the strictly convex level sets of $h(p_1, \ldots, p_n)$ are symmetric around the n-dimensional line $p_1 = \cdots = p_n$ and the unconstrained (global) minimum is on this n-dimensional line. If dom h is constrained by the surface $p_1 + \cdots + p_n = r$, the function $h(p_1, \ldots, p_n)$ attains a constrained minimum where the surface $p_1 + \cdots + p_n = r$ intersects the n-dimensional line $p_1 = \cdots = p_n$ which is at $(p_1, \ldots, p_n) = (\frac{r}{n}, \ldots, \frac{r}{n})$. ■

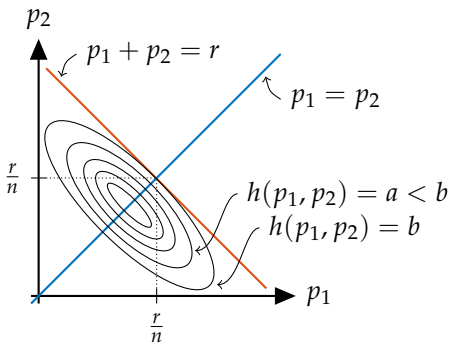

Figure 5.5: Illustration of the constrained minimum for the strictly convex $h(p_1, p_2) = f(p_1) + f(p_2)$ where dom h is constrained by $p_1 + p_2 = r$.

Although of the same type, make, and model, the fuel consumption curves of different diesel generators in a plant can vary significantly, as demonstrated in Section 5.1 for one of various possible reasons. While the optimization problem remains convex as long as the plant power reference allows all the n gensets to operate in the strictly convex power generation region, the equal power distribution is no longer optimal, when the gensets have different fuel consumption curves. Additionally, if the plant power reference is such that not all n diesel generators can operate in the strictly convex

power generation region, the problem is no longer convex. These two issues are addressed in the remaining sections of this chapter.

For the sake of clarity, the diesel-driven generator sets will not have unique fuel consumption characteristics in the case studies of the following sections, rather they will belong to one of five groups; different only in that aspect. Figure 5.6 presents the five group fuel consumption curves, which are utilized in the following analysis.

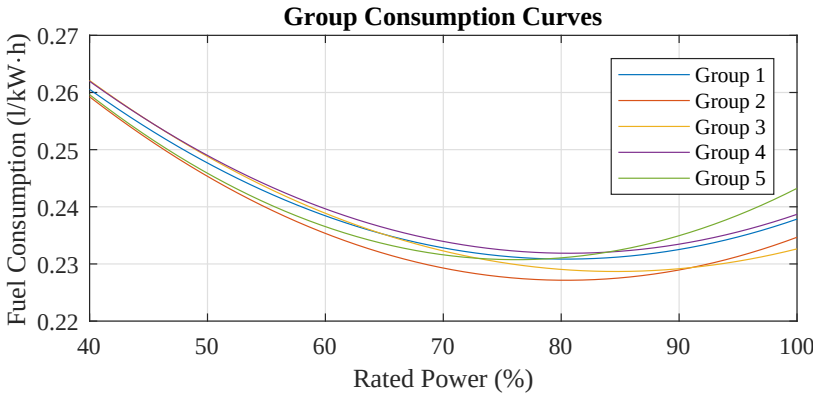

Figure 5.6: Assumed fuel consumption curves of diesel generators in Group 1 to 5, respectively.

5.3 Gradient Search Approach

For the plant presented in Figure 5.1, let each of the 30 diesel generators have a 2 MW rating and let the plant power reference, r, be 55 MW. If, for whatever reason, all 30 diesel generators are required to operate, the industry-standard approach would be to apply an equal distribution of the power among the gensets. Proposition 1 shows, that this approach would be optimal if the fuel consumption characteristics were identical for all 30 diesel generators.

However, if the diesel generators actually have different fuel consumption characteristics the above approach does not provide the optimal solution. Let six diesel generators belong to each of the five groups presented in Figure 5.6 and assume that this information is available through measurements. With the requirement that all 30 diesel generators operate, the fuel optimization problem is convex and a solution can be found utilizing a gradient search approach. Applying the MATLAB toolbox YALMIP [Löfberg, 2004] with the interior-point method of the `fmincon` solver, the solution to this plant fuel optimization problem, on the form provided in Equations (5.1), is found.

Proposition 1 extends, naturally, to diesel generators belonging to the same fuel consumption curve group. That is, each diesel-driven generator

set in a specific group should generate an equal amount of power. The power generation results of this convex fuel optimization problem are presented in Figure 5.7, including an equal distribution solution for comparison.

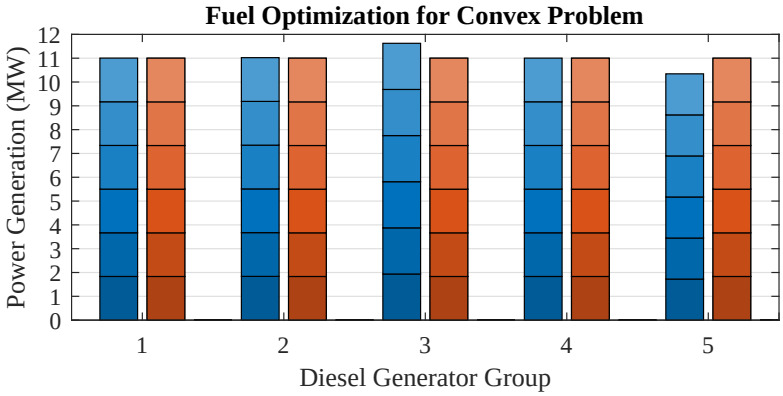

Figure 5.7: Power generation results for the convex fuel optimization problem of gensets in Group 1 to 5, respectively. The blue columns present the gradient search solution, while the red columns present an equal distribution solution; each block in the columns represent one genset.

In Figure 5.7, the blue columns present the solution obtained utilizing the gradient search approach, whereas the red columns present a solution with the industry-standard approach of equal distribution. Each block in the columns represent the power of an individual diesel generator. The key observation to make is the shift of power from diesel generators belonging to Group 5 to diesel generators of Group 3. The results are provided in detail in Table 5.2 together with the corresponding fuel consumptions.

Table 5.2: Power generation and corresponding fuel consumption results for the convex fuel optimization problem utilizing the gradient search approach and the equal distribution approach for a plant consisting of 30 diesel generators with a 2 MW rating.

		Power Generation‡ (MW)		Fuel Consumption‡ (l/h)	
Group	DGs†	Gradient Search	Equal	Gradient Search	Equal
1	6	1.8341	1.8333	428	427
2	6	1.8371	1.8333	422	421
3	6	1.9376	1.8333	448	421
4	6	1.8339	1.8333	429	429
5	6	1.7239	1.8333	402	433
Total	30	55	55	12774	12786

†operational in Group, ‡per DG

The fuel consumption results in Table 5.2 show fuel savings of 12 liters per

hour, which corresponds to approximately 0.1%, utilizing the gradient search approach rather than an equal distribution approach. While these savings might seem insignificant at first, keep in mind that such genset plants most often operate continuously for several months or years. Therefore, every little piece of optimization that can be obtained is desirable, since it could entail significant savings in the long run.

5.4 Genetic Algorithm Approach

If the plant fuel optimization problem is non-convex, a simple gradient search approach will not be able to find the globally optimal solution. The fuel optimization problem could loose its convexity property for various reasons; for example, if the plant power reference does not allow all diesel generators in the plant to operate in the strictly convex power generation region or if the number of diesel generators operating is not predetermined.

Determining the number of diesel generators to operate is an inherent part of plant management, often referred to as Unit Commitment. Industry-standard solutions incorporate a spinning reserve requirement in the process. Spinning reserve is the excess power capacity available from the diesel generators in operation. For example, a 2 MW rated genset generating 1.5 MW leaves a spinning reserve of 0.5 MW. Spinning reserve is a safety precaution, making the plant capable of handling sudden changes, which for a plant in Mains Power Export mode could, for example, be an unexpected shutdown of a diesel generator. For a given plant power reference, the industry-standard approach simply starts up the minimum number of gensets able to achieve the required spinning reserve, based on the genset ratings. That is, for a plant power reference of 9.5 MW and a spinning reserve requirement of 1 MW, six 2 MW diesel-driven generator sets will be in operation according to the industry-standard approach.

As an approach to find the optimal solution of the non-convex fuel optimization problem, which includes Unit Commitment, a Genetic Algorithm (GA) is proposed. Figure 5.8 presents an overview of the elements and the general structure of a GA [Goldberg, 1989; Deb, 2001].

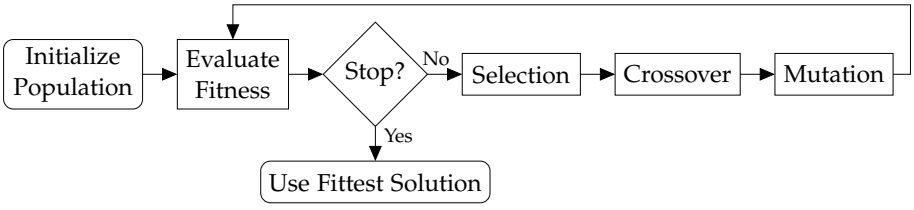

Figure 5.8: General structure of a Genetic Algorithm [Goldberg, 1989; Deb, 2001].

Genetic Algorithms are based on the evolutionary principle of natural selection, often summarized by the phrase "survival of the fittest". Hence, a measure of fitness is a prerequisite for formulating a GA; in fact, it is the only prerequisite. For the particular problem of fuel optimization, the fuel consumption represents a measure of fitness for any potential solution. GAs consider many potential solutions to the problem at the same time, the collection of these solutions are referred to as the population. The exact number of potential solutions in the population is a design parameter, which is denoted the population size. When looking for the optimal solution, each successive iteration of evaluation, selection, crossover, and mutation as shown in Figure 5.8, is denoted a generation. In the following, every element of the proposed GA for the non-convex plant fuel optimization problem is provided.

Initialize Population

Generating an initial population entails producing a collection of potential solutions. For the proposed fuel optimization GA, each potential solution is produced by randomly assigning power to the available diesel generators. Chosen randomly from all of the available gensets, which have not been assigned an amount of power, a genset is assigned power by a uniform selection in the range from the minimum admissible power to the genset rating. The minimum admissible power is defined as the average power required by each of the remaining unassigned diesel generators in every step of producing a potential solution that accommodates the plant power reference.

Once every diesel generator in the plant has been assigned power or the total assigned power becomes higher than the plant power reference, the power assigning process stops. If the total assigned power exceeds the reference, that excess power is removed from the last assigned diesel generator. If any gensets have not been assigned an amount of power at this stage, they are part of that potential solution as diesel generators, which are not operating. The entire process is repeated until the initial population contains a number of potential solutions matching the specified population size.

Evaluate Fitness

Utilizing the third degree polynomial fuel consumption curves, the fitness of each potential solution in the population is evaluated by determining the total plant fuel consumption for that specific distribution of the power.

Stop?

The criterion for stopping a Genetic Algorithm depends highly on the nature of the particular problem. In problems where the region of the optimal fitness

value is unknown a priori, the stopping criterion is often specified as a limit on the number of generations evaluated. For other problems, obtaining a certain level of fitness or a certain level of change in fitness between successive generations can be the stopping condition [Goldberg, 1989; Deb, 2001]. The proposed GA utilizes a stopping criterion based on a specified number of generations to be evaluated. When the stopping criterion is fulfilled, the most fit solution in the population will be used; however, there exists no formal guarantee that the solution is in fact optimal.

Selection

In the selection process, a new population is produced based on the potential solutions in the existing population. Utilizing the so-called tournament selection with replacement, two solutions from the existing population are chosen at random and the solution with the best fitness, that is, the lowest total plant fuel consumption, of those two is put in the new population. The procedure is repeated, always using the entire existing population to choose from, until the new population reaches the specified population size.

By the principle of elitism, a specified number of the most fit potential solutions in the existing population are put directly in the new population, which guarantees the survival of the fittest. Without elitism there is no guarantee that the most fit solution would be chosen and, thereby, survive in a tournament selection with replacement [Goldberg, 1989; Deb, 2001].

Crossover

The crossover process, which is often referred to as mating, entails combining potential solutions in the population as a method of producing new, and hopefully more fit, solutions. The so-called single-point crossover has been the inspiration for the crossover process design in the proposed plant fuel optimization Genetic Algorithm [Goldberg, 1989; Deb, 2001].

Two random potential solutions, α and β, are chosen from the population. Both α and β contain assigned power for the n diesel generators in the plant accommodating the plant power reference. A random number, γ, between 1 and $n-1$ is chosen uniformly. By a fifty-fifty chance, it is decided whether to manipulate the 1 to γ or the $\gamma+1$ to n gensets; the set of gensets to be manipulated is denoted m. Should the total assigned power of the m diesel generators in either α or β equal zero, a new random γ is chosen. An example where m is the set from 1 to γ and the total assigned power in m is non-zero for both α and β is provided in Equations (5.2).

$$\alpha = \big[\underbrace{p_{\alpha 1} \quad \cdots \quad p_{\alpha\gamma}}_{m_\alpha} \quad \cdots \quad p_{\alpha n}\big] \quad , \sum_{k=1}^{\gamma} p_{\alpha k} = p_{\alpha m} \neq 0 \tag{5.2a}$$

$$\beta = [\underbrace{p_{\beta 1} \quad \cdots \quad p_{\beta \gamma}}_{m_\beta} \quad \cdots \quad p_{\beta n}] \quad , \sum_{k=1}^{\gamma} p_{\beta k} = p_{\beta m} \neq 0 \tag{5.2b}$$

The distribution of assigned power in m_α and m_β are found. Then, the power distribution of m_α is applied to the diesel generators in m_β while maintaining the total assigned power, $p_{\beta m}$, and vice versa.

This produces two new potential solutions, which both accommodate the plant power reference; however, at this point, some diesel generators in the new solutions possibly exceed their power rating due to the utilization of a different assigned power distribution. Any excess assigned power is removed from the particular diesel generator and added randomly to a different diesel generator in m, such that no gensets exceed their power rating in the end.

The probability that the chosen pair of potential solutions, α and β, will be manipulated as detailed in the above is a specified design parameter of the GA; alternatively, the chosen α and β are put directly into a new population without any manipulation. The crossover process is repeated until the new population is of the specified population size. Similar to the selection process, the principle of elitism guarantees that a specified number of the most fit solutions are put directly into the new population.

Mutation

The purpose of the mutation process is to increase the population diversity [Goldberg, 1989; Deb, 2001]. With a specified probability, every potential solution in the population is subject to mutation. The mutation process of the proposed GA entails assigning zero power to a diesel generator, which is chosen randomly from all the n diesel generators in the solution. The amount of assigned power removed by the mutation is assigned to a different randomly chosen genset of the solution. In the case that this causes the genset to exceed its power rating, the excess power is assigned randomly to another diesel generator, until no gensets exceed their power rating.

Case Study

For the plant presented in Figure 5.1, suppose each branch consists of 10 diesel generators; providing a total of 50 diesel generators in the plant. Similar to the case investigated in Section 5.3, let each diesel generator have a 2 MW rating and let the plant power reference, r, be 55 MW. Let ten gensets belong to each of the five groups presented in Figure 5.6 and assume that this information is available through measurements.

With a typical spinning reserve requirement corresponding to the rating of one genset, the industry-standard approach would operate 29 diesel generators to accommodate that specific reference, without knowledge about fuel

consumption characteristics. The proposed GA is utilized with a population size of 1000, a stopping criterion of 7500 generations, a crossover probability of 0.75, a mutation probability of 0.9, and putting 10 solutions directly into the new population according to the elitism principle.

The power generation results for this non-convex plant fuel optimization problem is presented in Figure 5.9, including two solutions of the industry-standard approach for comparison.

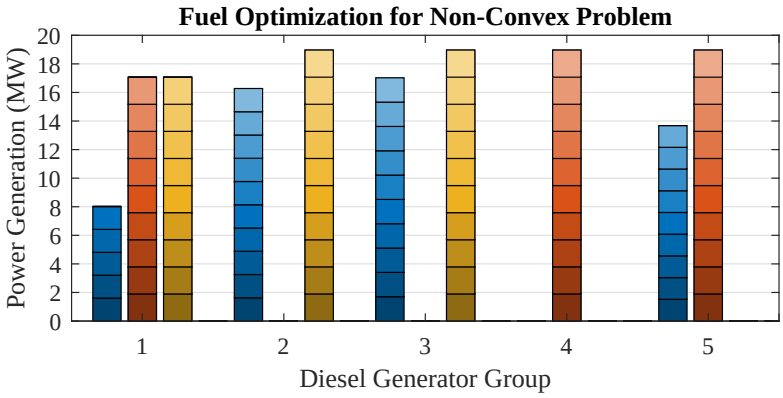

Figure 5.9: Power generation results for the non-convex fuel optimization problem of gensets in Group 1 to 5, respectively. The blue columns present the Genetic Algorithm solution, while the red and yellow columns present two industry-standard approach solutions; each block in the columns represent one genset.

The red and yellow columns in Figure 5.9, are provided to demonstrate the potential difference in the industry-standard approach solution. The red solution represents a solution in which the industry-standard approach has been unfortunate enough to operate the 29 diesel generators providing the worst fuel consumption results possible. On the other hand, the yellow solution represents a solution where the industry-standard approach has been fortunate enough to operate the 29 gensets providing the best possible fuel consumption result. As described, the industry-standard approach does not utilize fuel consumption information; therefore, any solution in the range from the red to the yellow is equally plausible.

The blue columns represent the GA approach solution, which operates 34 diesel generators, all at a lower power generation than the diesel generators in the industry-standard approach solutions.

Table 5.3 provides the power generation results in detail together with the corresponding fuel consumptions of all three solutions. To present all the results in one clear-cut table, the solution of the red columns is denoted the industry-standard worst (ISW) solution, while the solution of the yellow columns is denoted the industry-standard best (ISB) solution.

Table 5.3: Power generation and corresponding fuel consumption results for the non-convex fuel optimization problem utilizing the Genetic Algorithm approach and two industry-standard approach solutions for a plant consisting of 50 diesel generators with a 2 MW rating.

	DGs†			Power Generation‡ (MW)			Fuel Consumption‡ (l/h)		
Group	GA	ISW	ISB	GA	ISW	ISB	GA	ISW	ISB
1	5	9	9	1.6035	1.8966	1.8966	370	445	445
2	10	-	10	1.6277	-	1.8966	370	-	439
3	10	-	10	1.7026	-	1.8966	389	-	437
4	-	10	-	-	1.8966	-	-	447	-
5	9	10	-	1.5200	1.8966	-	351	452	-
Total	34	29	29	55	55	55	12599	12995	12765

†operational in Group, ‡per DG

The GA approach achieves fuel savings of 396 and 166 liters per hour (3.1% and 1.3%) in comparison with the ISW and ISB solutions, respectively. Five additional diesel generators are in operation to obtain these savings.

These results conclude the investigation of fuel optimization as plant management for diesel generator plants in Mains Power Export mode. In general, the industry-standard approach employs an equal power distribution among the diesel generators in a plant. In terms of fuel consumption, this approach is optimal if all the gensets have the exact same fuel consumption characteristics, but not in the likely event of fuel characteristic differences. A significant potential for fuel savings has been found based on obtaining and utilizing information about the fuel consumption characteristics of each diesel-driven generator set in the plant, assuming differences in fuel characteristics. Both a gradient search approach and a Genetic Algorithm approach have demonstrated significant fuel savings in specific case studies; the choice of approach depends on the flexibility in the selection of diesel generators to operate for a provided plant power reference.

6 Concluding Remarks

This chapter summarizes the work of the present thesis by concluding on the research objectives. Finally, reflections on the perspectives of the study are provided as future work considerations.

The motivation behind this Industrial Ph.D. study has been to investigate potential improvements to the market-leading, industry-standard solutions regarding control of diesel generators; individually and in plants.

The first research objective concerned formulation of a simulation model, which based on physical principles of a diesel-driven generator set is suitable for applying supervisory control algorithms in an AGC unit. This objective has been addressed in Chapter 3 and by the contributions of Paper A and Paper C. In this work, attention has been focused on one of the fundamental operating modes of a diesel generator, namely, frequency and voltage stabilization in island operation. A tenth-order nonlinear state-space model has been formulated, utilizing a mean value approach to model the diesel engine in combination with a first principles approach for the synchronous generator and including isochronous governor and AVR as PI regulators. The formulated model has been satisfactorily validated in the laboratory facilities for steps of increasing and decreasing active and apparent power loads.

The second and third research objectives targeted proposing and testing an adaptive supervisory control algorithm capable of reducing parameter tuning complexity for AGC units during commissioning of diesel generators. Chapter 4 and the contributions of Paper B and Paper C has addressed these objectives. Despite not being adaptive, an LQR-based AGC regulator design, which facilitates self-tuning, has been proposed and implemented in the laboratory facilities utilizing a RCP system. The successful laboratory implementation results have demonstrated general improvements in control performance in comparison with the so-called open-loop performance of the isochronous governor and AVR and an industry-standard PID-based AGC regulator solution. Furthermore, the results demonstrated the capabilities of the reduced parameter tuning complexity scheme.

The fourth and final research objective concerned proposing an algorithm for fuel optimization in plant management of diesel generator plants utilizing

available fuel consumption information. This last research objective has been addressed in Chapter 5 and by the contributions of Paper D. For plants operating in Mains Power Export mode, the industry-standard approach has been proven optimal if and only if the fuel consumption characteristics of every genset in the plant are identical. Measurements demonstrated the likelihood of significant differences in fuel characteristics by the example of variations in air filter conditions. A gradient search approach and a Genetic Algorithm has been proposed, showing significant fuel saving potential in specific case studies in which the fuel characteristics vary between diesel generators. The gradient search approach is capable of optimizing the fuel consumption for a predetermined selection of diesel generators, while the Genetic Algorithm has the additional ability of finding the optimal selection of diesel generators to operate for fuel optimization in a plant in Mains Power Export mode.

Future Perspectives

Distinguishing between short-term and long-term, reflections on the future perspectives of the work presented in this thesis are provided in the remainder of this chapter. The following short-term perspectives concern a potential direct continuation of this study.

In modeling and control of diesel-driven generator sets, the lacking information in relation to, especially, generator rotor parameters would be a natural issue to address. The applied utilization of a generic set of p.u. rotor parameters and a number of parameters found by hand-tuning has been sufficient to prove the general validity of the formulated model; however, hand-tuning of model parameters is hardly a practical solution for a real-life, industrial implementation. A higher degree of genset specific parameters would not only be likely to improve the validity of the proposed model, it would also enable self-tuning regulator designs, which is in complete alignment with the industrial ambition to reduce, and ultimately remove, the time spent on regulator tuning during commissioning.

To achieve a suitable and applicable parameter identification approach, two immediate challenges come to mind. In the context of AGC regulator design, the modeled diesel generator system is a closed-loop system, which inherently complicates parameter identification considerably in comparison with open-loop systems. Additionally, the measurements required for a successful parameter identification must be obtainable in any genset application for which the AGC regulator design is to be implemented. Hence, relying on controlled load step measurements limits the applicability of the approach to those genset applications where that is actually possible.

The proposed LQR-based AGC regulator design utilizes a set of linearized diesel generator models. This set is defined by the chosen operating points,

which in the available laboratory facilities has been a rather straightforward choice, due to the available load elements. The implications of that choice has, therefore, not been investigated, but the possible issues in relation to the determination and switching of operating point in real-life implementations, in which the load is most often less predictable, should be addressed. Alternatively, a nonlinear control approach could preempt these issues by completely avoiding the use of operating points.

While the proposed GA for fuel optimization as plant management, is perfectly capable of identifying the optimal selection of gensets to operate for a specific plant power reference, finding the exact optimal power distribution is rather time inefficient. Redefining the GA to exclusively deal with determination of the optimal diesel generator selection, based on individual fuel consumption characteristics, and solving the remaining problem of the exact optimal power distribution by a gradient search approach is likely to increase the computational efficiency considerably. Furthermore, such a combined approach would probably be more suited for solving fuel optimization problems where every genset in the plant has unique fuel characteristics than the present GA approach.

The above perspectives relate to an immediate continuation of the work presented in this thesis; whereas, for a slightly larger time horizon, the following long-term perspectives are provided.

Besides the complexity of the diesel-driven generator set itself, one of the most extensive challenges in model-based control of gensets is the great complexity and often unpredictability of the connected system. Whether that entails only electrical loads, additional diesel generators, renewable energy resources, or an entire mains connection, a complete modeling framework has been beyond the scope of this study. Precise load models, as the ones utilized in the modeling of this study, are practically impossible to obtain for most real-life load conditions [Kundur, 1994]. Consequently, a suitable interface simplification for each of the scenarios should be identified to enable real-life, industrial implementations.

The fundamental conditions for the proposed fuel optimization algorithm is the availability of individual diesel-driven generator set fuel consumption characteristics and the differences in such characteristics throughout a plant. While measurements have demonstrated a specific possible difference, due to the likely event of a bad air filter, a more comprehensive analysis of actual variations in a plant along with the possibility for obtaining these detailed characteristics should be conducted before further developments towards a real-life implementation are made.

References

E. S. Abdin, A. M. Oshelba, and M. M. Khater, "Modeling and optimal controllers design for a stand-alone photovoltaic-diesel generating unit," *IEEE Transactions on Energy Conversion*, vol. 14, no. 3, pp. 560–563, 1999.

A. M. Ameen, J. Pasupuleti, and T. Khatib, "Simplified performance models of photovoltaic/diesel generator/battery system considering typical control strategies," *Energy Conversion and Management*, vol. 99, pp. 313–325, 2015.

B. D. O. Anderson and J. B. Moore, *Optimal Control: Linear Quadratic Methods*. Prentice-Hall, Inc., 1989.

APR Energy, *Case Study: Peru | Peak Shaving*, 2017.

——, *Case Study: Argentina | Distributed Generation*, 2017.

M. Ashari, C. Nayar, and W. Keerthipala, "Optimum operation strategy and economic analysis of a photovoltaic-diesel-battery-mains hybrid uninterruptible power supply," *Renewable Energy*, vol. 22, no. 1-3, pp. 247–254, 2001.

A. Askarzadeh, "Distribution generation by photovoltaic and diesel generator systems: Energy management and size optimization by a new approach for a stand-alone application," *Energy*, vol. 122, pp. 542–551, 2017.

S. Benhamed, H. Ibrahim, K. Belmokhtar, H. Hosni, A. Ilinca, D. Rousse, A. Chandra, and D. Ramdenee, "Dynamic modeling of diesel generator based on electrical and mechanical aspects," in *IEEE Electrical Power and Energy Conference (EPEC)*, 2016, p. 6.

R. J. Best, D. J. Morrow, D. J. McGowan, and P. A. Crossley, "Synchronous islanded operation of a diesel generator," *IEEE Transactions on Power Systems*, vol. 22, no. 4, pp. 2170–2176, 2007.

B. Bokabo and K. Kusakana, "Optimized scheduling of diesel - renewable systems with pumped hydro storage," in *Conference on the Industrial and Commerical Use of Energy (ICUE)*, 2016, pp. 286–291.

T. Broomhead, C. Manzie, P. Hield, R. Shekhar, and M. Brear, "Economic model predictive control and applications for diesel generators," *IEEE Transactions on Control Systems Technology*, vol. 25, no. 2, pp. 388–400, 2017.

J. Carpentier, "'To be or not to be modern' that is the question for automatic generation control (point of view of a utility engineer)," *International Journal of Electrical Power and Energy Systems*, vol. 7, no. 2, pp. 81–91, 1985.

M. Carrion and J. Arroyo, "A computationally efficient mixed-integer linear formulation for the thermal unit commitment problem," *IEEE Transactions on Power Systems*, vol. 21, no. 3, pp. 1371–1378, 2006.

B. Challen and R. Baranescu, *Diesel Engine Reference Book*, 2nd ed. Butterworth-Heinemann Ltd, 1999.

A. Chen, "Speed regulator of diesel-generator based on model free adaptive control," in *WRI Global Congress on Intelligent Systems (GCIS)*, vol. 3, no. 3, 2010, pp. 193–196.

K. L. Cheong, P. Y. Li, and J. Xia, "Control oriented modeling and system identification of a diesel generator set (genset)," in *American Control Conference (ACC)*, 2010, pp. 950–955.

A. R. Cooper, D. J. Morrow, and K. D. R. Chambers, "A turbocharged diesel generator set model," in *International Universities Power Engineering Conference (UPEC)*, 2009, p. 5.

A. Cooper, D. McGowan, D. Morrow, and K. Chambers, "Temperature-dependant voltage regulator operation for optimal load acceptance of a diesel generator," *IET Electric Power Applications*, vol. 6, no. 8, pp. 553–560, 2012.

K. Deb, *Multi-Objective Optimization using Evolutionary Algorithms*. John Wiley & Sons, Inc., 2001.

DEIF, "Power efficiency | DEIF- Power efficiency | DEIF," 2017. [Online]. Available: www.deif.com

——, *Power & Control Technology: Independent Power Producers*, 2017.

——, *Land Power Application Guide*, 2016.

——, *Marine & Offshore Application Guide*, 2016.

Deutz AG, *2012 The Genset Engine*, 2005.

——, *Genset Manual BF4M2012C*, 2015.

ENTSO-E, "Frequency Stability Evaluation Criteria for the Synchronous Zone of Continental Europe," Tech. Rep., 2016.

M. Eremia and M. Shahidehpour, Eds., *Handbook of Electrical Power System Dynamics*. John Wiley & Sons, Inc., 2013.

G. F. Franklin, J. D. Powell, and A. Emami-Naeini, *Feedback Control of Dynamic Systems*, 6th ed. Upper Saddle River, New Jersey: Pearson Education, Inc., 2010.

A. Gasparjan, A. Terebkov, and A. Zhiravetska, "Monitoring of Electromechanical System "Diesel - Synchronous Generator"," in *IEEE International Conference on Power Engineering, Energy and Electrical Drives (POWERENG)*, 2015, pp. 103–108.

C. Ghenai, T. Salameh, A. Merabet, and A. K. Hamid, "Modeling and optimization of hybrid solar-diesel-battery power system," in *International Conference on Modeling, Simulation, and Applied Optimization (ICMSAO)*, 2017, p. 5.

C. E. Goering, M. L. Stone, D. W. Smith, and P. K. Turnquist, *Off-Road Vehicle Engineering Principles*. American Society of Agricultural Engineers, 2003.

K. B. Goh, S. K. Spurgeon, and N. Barrie Jones, "Higher-order sliding mode control of a diesel generator set," *Institution of Mechanical Engineers. Part I: Journal of Systems and Control Engineering*, vol. 217, no. 3, pp. 229–241, 2003.

D. E. Goldberg, *Genetic Algorithms in Search, Optimization and Machine Learning*, 1st ed. Addison-Wesley, 1989.

M. Guermouche, S. Ali, and N. Langlois, "Sliding Mode Control for Diesel Generator via Disturbance Observer," in *Mediterranean Conference on Control and Automation (MED)*, 2015, pp. 487–494.

L. Guo, X. Fu, X. Li, and C. Wang, "Coordinated control of battery storage system and diesel generators in AC island microgrid," in *International Power Electronics and Motion Control Conference*, vol. 1, no. 1, 2012, pp. 112–117.

L. Guzzella and A. Amstutz, "Control of diesel engines," *IEEE Control Systems Magazine*, vol. 18, no. 5, pp. 53–71, 1998.

I. Hassan, R. Weronick, R. Bucci, and W. Busch, "Evaluating the transient performance of standby diesel-generator units by simulation," *IEEE Transactions on Energy Conversion*, vol. 7, no. 3, pp. 470–477, 1992.

J. Hespanha and A. Morse, "Stability of Switched Systems with Average Dwell-Time," in *IEEE Conference on Decision and Control*, vol. 3, 1999, pp. 2655–2660.

J. B. Heywood, *Internal Combustion Engine Fundementals*. McGraw-Hill, Inc., 1988.

H. Hilal, M. Oktaufik, A. Prastawa, B. Prasetyo, and R. Hutahaean, "Smart diesel generator to compensate on-grid PV fluctuation: A case study in Sumba Island Indonesia," in *Conference on Power Engineering and Renewable Energy (ICPERE)*, 2016, pp. 33–37.

R. Huang, E. Farantatos, G. J. Cokkinides, and A. P. Meliopoulos, "Physical parameters identification of synchronous generators by a dynamic state estimator," in *IEEE Power & Energy Society General Meeting*, 2013, p. 5.

IEEE Power Engineering Society, "IEEE Guide: Test Procedures for Synchronous Machines," *IEEE Std 115-1983 (Revision of IEEE Std 115-1965)*, p. 87, 1983.

——, "IEEE Guide for Test Procedures for Synchronous Machines," *IEEE Std 115-2009 (Revision of IEEE Std 115-1995)*, p. 207, 2010.

J. D. Irwin and R. M. Nelms, *Basic Engineering Circuit Analysis*, 9th ed. John Wiley & Sons, Inc., 2008.

C. Jiang, X. Wang, S. Zheng, and M. Yu, "On Hardware-In-The-Loop simulation system of diesel generator set," in *Chinese Control Conference (CCC)*, 2014, pp. 6229–6234.

G. Johnson, *Generator Sets Report*. Market Analysis, IHS Technology, 2014.

——, "Short-term headwinds, long-term growth for generator sets market," 2016. [Online]. Available: https://technology.ihs.com/582961/short-term-headwinds-long-term-growth-for-generator-sets-market

J. Karlsson and J. Fredriksson, "Cylinder-by-cylinder engine models vs mean value engine models for use in powertrain control applications." SAE Technical Paper 1999-01-0906, 1999.

M. Karrari and O. Malik, "Identification of physical parameters of a synchronous generator from online measurements," *IEEE Transactions on Energy Conversion*, vol. 19, no. 2, pp. 407–415, 2004.

A. M. Kassem and A. M. Yousef, "Robust control of an isolated hybrid wind-diesel power system using Linear Quadratic Gaussian approach," *International Journal of Electrical Power and Energy Systems*, vol. 33, pp. 1092–1100, 2011.

J. Kautsky, N. K. Nichols, and P. Van Dooren, "Robust Pole Assignment in Linear State Feedback," *International Journal of Control*, vol. 41, no. 5, pp. 1129–1155, 1985.

S. Kazarlis, A. Bakirtzis, and V. Petridis, "A genetic algorithm solution to the unit commitment problem," *IEEE Transactions on Power Systems*, vol. 11, no. 1, pp. 83–92, 1996.

S. Keerti, V. M. Balijepalli, Y. Shicong, A. Ukil, N. Karthikeyan, and A. K. Gupta, "Modeling diesel generators for weak and strong grid conditions: Emphasis on LVRT compliance," in *IEEE Region 10 Conference (TENCON)*, 2016, pp. 1724–1727.

U. Kiencke and L. Nielsen, *Automotive Control Systems: For Engine, Driveline, and Vehicle*, 2nd ed. Springer, 2005.

J. Knudsen, J. Bendtsen, P. Andersen, and K. Madsen, "Self-tuning linear quadratic supervisory regulation of a diesel generator using large-signal state estimation," in *Australian Control Conference*, 2016, pp. 32–37.

J. Knudsen, J. Bendtsen, P. Andersen, K. Madsen, and C. Sterregaard, "Control-oriented first principles-based model of a diesel generator," in *European Control Conference*, 2016, pp. 321–327.

——, "Supervisory control implementation on diesel-driven generator sets," *Submitted for IEEE Transactions on Industrial Electronics*, 2017.

J. Knudsen, J. Bendtsen, P. Andersen, K. Madsen, C. Sterregaard, and A. Rossiter, "Fuel optimization in multiple diesel driven generator power plants," in *IEEE Conference on Control Technology and Applications (CCTA)*, 2017, pp. 493–498.

M. Knudsen, "A Sensitivity Approach for Estimation of Physical Parameters," in *IFAC Symposium on System Identification*, vol. 2, 1994, pp. 231–236.

B. Kraemer, *Understanding Generator Set Ratings For Maximum Performance and Reliability*. Technical Article, MTU Onsite Energy, 2013.

P. Krause, O. Wasynczuk, S. Sudhoff, and S. Pekarek, Eds., *Analysis of Electric Machinery and Drive Systems*. John Wiley & Sons, Inc., 2013.

P. Kundur, *Power System Stability and Control*. McGraw-Hill, Inc., 1994.

K. Kusakana, "Optimal operation of parallel-connected diesel generators for remote electrification through energy management approach," in *IEEE PES PowerAfrica*, 2017, pp. 380–384.

H. Kwakernaak and R. Sivan, *Linear Optimal Control Systems*. Wiley & Sons, Inc., 1972.

Leroy-Somer, *Low Voltage Alternators - 4 pole*. Datasheet, 2015.

T.-C. Lin, Y.-H. Huang, M.-Y. Jhan, and L.-R. Chen, "Grid-connected digital controller of diesel-engined generator for a hybrid power system," in *International Symposium on Computer, Consumer and Control (IS3C)*, 2016, pp. 1085–1088.

J. Löfberg, "YALMIP: A toolbox for modeling and optimization in MATLAB," in *IEEE International Conference on Computer Aided Control Systems Design*, 2004, pp. 284–289.

D. G. Luenberger, "Observers for Multivariable Systems," *IEEE Transactions on Automatic Control*, vol. 11, no. 2, pp. 190–197, 1966.

——, "Observing the State of a Linear System," *IEEE Transactions on Military Electronics*, vol. 8, no. 2, pp. 74–80, 1964.

S. E. Lyshevski, *Electromechanical Systems, Electric Machines, and Applied Mechatronics*. CRC Press, 1999.

——, "Analysis of auxiliary power systems with conventional synchronous generators," *Energy Conversion and Management*, vol. 41, pp. 1379–1387, 2000.

J. Machowski, J. W. Bialek, and J. R. Bumby, *Power System Dynamics: Stability and Control*, 2nd ed. John Wiley & Sons, Inc., 2008.

J. Mamboundou and N. Langlois, "Application of indirect adaptive model predictive control supervised by fuzzy logic to a diesel generator," in *IEEE International Conference on Control and Automation (ICCA)*, 2011, pp. 1037–1043.

MAN Diesel & Turbo, *Power Solutions Independent Power Producers*, 2017.

MathWorks, "Simscape Power Systems," 2017. [Online]. Available: https://se.mathworks.com/products/simpower.html

D. McGowan, D. Morrow, and M. McArdle, "A digital PID speed controller for a diesel generating set," in *IEEE Power Engineering Society General Meeting*, vol. 3, 2003, pp. 1472–1477.

D. McGowan, D. Morrow, and B. Fox, "Integrated governor control for a diesel-generating set," *IEEE Transactions on Energy Conversion*, vol. 21, no. 2, pp. 476–483, 2006.

——, "Multiple input governor control for a diesel generating set," *IEEE Transactions on Energy Conversion*, vol. 23, no. 3, pp. 851–859, 2008.

Mecc Alte, *Generator Type ECO 32-3S/4*. Datasheet, 2012.

M. Mirosevic and Z. Maljkovic, "The Dynamics of Diesel Generator Units with Different Voltage Controller Parameters," in *Electrical Systems for Aircraft, Railway and Ship Propulsion*, 2012, p. 5.

Mordor Intelligence, *Global Diesel Generator Market - Analysis by Deployment Location - Growth Trends and Forecasts (2016 - 2021)*. Market Analysis, 2016.

MTU Onsite Energy, *Technical Engine Data 12V4000G23*. Datasheet, 2007.

——, *Diesel Generator Set MTU 16V4000 DS2250*. Datasheet, 2017.

——, *Diesel Generator Set MTU 16V4000 DS2500*. Datasheet, 2017.

N. Padhy, "Unit Commitment—A Bibliographical Survey," *IEEE Transactions on Power Systems*, vol. 19, no. 2, pp. 1196–1205, 2004.

K. Pandiaraj, B. Fox, D. Morrow, S. Persaud, and J. Martin, "Centralised control of diesel gen-sets for peak shaving and system support," *IEE Proceedings - Generation, Transmission and Distribution*, vol. 149, no. 2, pp. 126–132, 2002.

R. H. Park, "Two-Reaction Theory of Synchronous Machines - Generalized Method of Analysis - Part I," *Journal of the American Institute of Electrical Engineers*, vol. 48, no. 3, pp. 716–727, 1929.

S. D. Pekarek, O. Wasynczuk, and H. J. Hegner, "An efficient and accurate model for the simulation and analysis of synchronous machine/converter systems," *IEEE Transactions on Energy Conversion*, vol. 13, no. 1, pp. 42–48, 1998.

J. Perahia and C. V. Nayar, "Model and simulation of a stand alone power system comprising a diesel engine driven synchronous generator and a power conditioner," *International Journal of Electrical Engineering Education*, vol. 35, no. 3, pp. 245–270, 1998.

C. D. Rakopoulos and E. G. Giakoumis, *Diesel Engine Transient Operation*. Springer London, 2009.

K. S. Rao, P. J. Chauhan, S. K. Panda, G. Wilson, X. Liu, and A. K. Gupta, "Optimal scheduling of diesel generators in offshore support vessels to minimize fuel consumption," in *Annual Conference of the IEEE Industrial Electronics Society (IECON)*, 2015, pp. 4726–4731.

S. Roy, O. Malik, and G. Hope, "An adaptive control scheme for speed control of diesel driven power-plants," *IEEE Transactions on Energy Conversion*, vol. 6, no. 4, pp. 605–611, 1991.

O. Sakamoto, "A Diesel Generator Model with Fluctuating Engine Torque Including Magnetic Saturation for Transient Analysis using XTAP," *Journal of Electrical Engineering and Technology*, vol. 10, no. 3, pp. 1298–1303, 2015.

T. Senjyu, K. Shimabukuro, K. Uezato, and T. Funabashi, "A fast technique for unit commitment problem by extended priority list," *IEEE Transactions on Power Systems*, vol. 18, no. 2, pp. 882–888, 2003.

G. B. Sheblé and T. T. Maifeld, "Unit commitment by genetic algorithm and expert system," *Electric Power Systems Research*, vol. 30, no. 2, pp. 115–121, 1994.

R. Shi, X. Zhang, L. Fang, H. Xu, C. Hu, Y. Yu, and H. Ni, "Research on Power Compensation Strategy for Diesel Generator System Based on Virtual Synchronous Generator," in *International Power Electronics and Motion Control Conference (IPEMC-ECCE Asia)*, 2016, pp. 939–943.

W. Shi, J. Yang, and T. Tang, "RBF NN based marine diesel engine generator modeling," in *American Control Conference*, 2005, pp. 2745–2749.

A. Singh and B. Singh, "Design, Modeling and Simulation of Intelligent Controller for Small Isolated Diesel Generator System," in *International Conference on Industrial and Information Systems (ICIIS)*, 2010, pp. 638–643.

B. Singh and J. Solanki, "Load compensation for diesel generator-based isolated generation system employing DSTATCOM," *IEEE Transactions on Industry Applications*, vol. 47, no. 1, pp. 238–244, 2011.

B. Singh, J. Solanki, and A. Chandra, "Adaline based control of battery energy storage system for diesel generator set," in *IEEE Power India Conference*, 2005, pp. 411–415.

M. Sivertsson and L. Eriksson, "Optimal Transient Control Trajectories in Diesel–Electric Systems—Part I: Modeling, Problem Formulation, and Engine Properties," *Journal of Engineering for Gas Turbines and Power*, vol. 137, no. 2, p. 11, 2015.

S. Skogestad and I. Postlethwaite, *Multivariable Feedback Control*. John Wiley & Sons, Inc., 1996.

T. Theubou, R. Wamkeue, and I. Kamwa, "Dynamic Model of Diesel Generator Set for Hybrid Wind-Diesel Small Grids Applications," in *IEEE Canadian Conference on Electrical and Computer Engineering (CCECE)*, 2012, p. 4.

S. Tong, S. Shahidehpour, and Z. Ouyang, "A heuristic short-term unit commitment," *IEEE Transactions on Power Systems*, vol. 6, no. 3, pp. 1210–1216, 1991.

M. Torres and L. A. Lopes, "Inverter-Based Virtual Diesel Generator for Laboratory-Scale Applications," in *Annual Conference on IEEE Industrial Electronics Society (IECON)*, 2010, pp. 532–537.

M. Tuffaha and J. T. Gravdahl, "Control-Oriented Model of a Generating Set Comprising a Diesel Engine and a Synchronous Generator," *Modeling, Identification and Control*, vol. 36, no. 4, pp. 199–214, 2015.

——, "Modeling and Control of a Marine Diesel Engine driving a Synchronous machine and a Propeller," in *IEEE Conference on Control Applications (CCA)*, 2014, pp. 897–904.

——, "Discrete state-space model to solve the unit commitment and economic dispatch problems," *Energy Systems*, vol. 8, no. 3, pp. 525–547, 2017.

A. N. Voroshilov, A. I. Khristolyubova, A. A. Khristolyubov, and S. V. Kuchak, "Diesel-generator set working in parallel with electrical energy storage system," in *International Conference on Micro/Nanotechnologies and Electron Devices*, 2013, pp. 288–292.

R. Wamkeue, F. Baetscher, and I. Kamwa, "Hybrid-state-model-based time-domain identification of synchronous machine parameters from saturated load rejection test records," *IEEE Transactions on Energy Conversion*, vol. 23, no. 1, pp. 68–77, 2008.

L. Wang, J. Jatskevich, V. Dinavahi, H. W. Dommel, J. A. Martinez, K. Strunz, M. Rioual, G. W. Chang, and R. Iravani, "Methods of interfacing rotating machine models in transient simulation programs," *IEEE Transactions on Power Delivery*, vol. 25, no. 2, pp. 891–903, 2010.

A. J. Wood, B. F. Wollenberg, and G. B. Sheblé, *Power Generation, Operation, and Control*, 3rd ed. Hoboken, New Jersey: John Wiley & Sons, Inc., 2014.

L. Wu, M. Shahidehpour, and T. Li, "Stochastic security-constrained unit commitment," *IEEE Transactions on Power Systems*, vol. 22, no. 2, pp. 800–811, 2007.

H. Yasin, A. EI-Zeftawy, M. Serag, and A. Gado, "Design of a controller for operating diesel generator to supply isolated loads," in *International Middle East Power Systems Conference (MEPCON)*, vol. 2, 2006, pp. 487–491.

G. Zhang, "Speed-Frequency Controller Design Based on Sliding Mode for Marine Diesel-Generator," in *WRI Global Congress on Intelligent Systems (GCIS)*, 2010, pp. 31–34.

——, "Marine diesel-generator excitation controller based on adaptive on-line GA tuning PID," in *Chinese Control Conference*, 2011, pp. 3868–3871.

Part II

Papers

Paper A

Control-Oriented First Principles-Based Model of a Diesel Generator

Jesper Knudsen, Jan Bendtsen, Palle Andersen, Kjeld Madsen, and Claes Sterregaard

The paper has been published in the
Proceedings of the European Control Conference, pp. 321–327, 2016.

The layout has been revised.

Abstract

This paper presents the development of a control-oriented tenth-order nonlinear model of a diesel driven generator set, using first principles modeling. The model provides physical system insight, while keeping the complexity at a level where it can be a tool for future design of improved automatic generation control (AGC), by including important nonlinearities of the machine. The nonlinearities are, as would be expected for a generator, primarily of bilinear nature. Validation of the model is done with measurements on a 60 kVA/48 kW diesel driven generator set in island operation during steps of active electrical load.

1 Introduction

Steadily developing regions around the world bring increasing demands for electrical power in highly diverse infrastructural settings. In many developing rural and remote areas around the world renewable energy resource (RER) solutions remain out of economical reach, leaving a single or a few conventional energy resource units as the sole suppliers of electricity in so called island operation. Further, recent decades with increased adoption of intermittent and volatile RERs, such as wind and solar power, has in many microgrid situations increased the dependency on the reliability of conventional energy resources in providing a stable electricity grid. Such situations include, but are not limited to, rural and remote areas in which the benefits of RER solutions are desirable but no established strong electricity grid is available to provide backup supply.

Currently, diesel driven generator sets (DGs) dominate the world market for generator sets (gensets) in the range from a few kW to a few MW, and are expected to remain dominant in the foreseeable future [1]. Naturally, all these DGs are part of electrical power installations of great diversity all around the world. Adding in the inherent variability of electrical power usage over the course of days, months, and years, it is obvious that DGs in general are utilized across their entire operating range.

Control of electrical power generation from a DG, although highly dependent on the situation, basically consists of two control tasks; fuel injection control and excitation control. For further intelligence (e.g. synchronization, active and reactive power control), an automatic generation control (AGC) unit is often added on top, providing references for the two first-level controllers depending on the situation. A conceptual diagram of DG control including an AGC unit is provided in Fig. 1.

The global market leaders of AGC units for DGs all implement fundamentally similar classical proportional-integral-derivative (PID) control algorithms and have done so for many years. In industrial applications, the

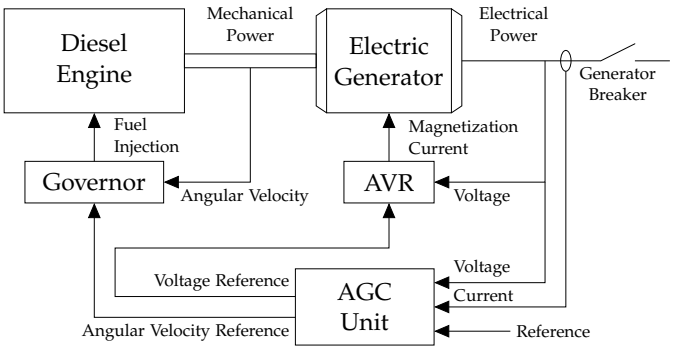

Fig. 1: Conceptual diagram of control on a diesel driven generator set. The fuel injection regulating governor and the magnetization current regulating automatic voltage regulator (AVR) act on references provided by the automatic generation control (AGC) unit.

simplicity and reliability of the PID controller are valuable qualities which should not be overlooked. However, if an adequately detailed model was available, more sophisticated control algorithms could provide advantages, such as increased efficiency and reduced commissioning costs, through e.g., the possibility of compensating for nonlinearities of a genset throughout its operating range. Although inherently robust towards these nonlinearities, PID control will need to be conservatively tuned and will exhibit unwanted changes in response characteristics depending on the prevailing operating point, motivating further development.

In survey papers [2]-[6] a large amount of work on AGC is reported, covering several areas of control theory e.g., predictive control, adaptive control, optimal control, robust control, and neural network control. To a large extent, modeling of DGs in the surveyed work is cast as a highly complicated problem overcome by common linear approximations, often as combinations of first and second order dynamics. Depending on the control application in focus, these simplifications might be justified, but when the focus is on the performance of individual DGs a higher degree of detail in the model would be advantageous.

In this paper, a control-oriented nonlinear model of a DG based on first principles modeling is developed and then validated on measurements from a 60 kVA/48 kW DG. The developed model provides physical insight, due to the first principles modeling approach, while keeping the complexity low enough for control design.

The remainder of this paper is organized as follows. Section 2 introduces the system through a physical description. In Section 3, the development of the nonlinear DG model is presented. Comparison of the developed model with experimental data is conducted in Section 4. Finally, Section 5 provides concluding remarks and future work considerations.

2 Physical System Description

This section provides an introduction to the physical background of a diesel driven generator set.

2.1 Diesel Engine

The most common type of diesel engine is the four stroke cycle diesel engine [7]. A stroke is the full movement of the piston, upwards or downwards, inside the cylinder. Through a connecting rod, the piston is connected to the crankshaft effectively converting the linear motion into rotational movement. All pistons connect to the crankshaft, combining the total engine torque at one shaft. In a single-cylinder engine the torque is delivered in periodic peaks, whereas multiple-cylinder engines deliver a less peaky torque, most often, further smoothened through a flywheel [8]. For control purposes, it suffices to model a four stroke diesel engine by a mean torque value model.

2.2 Synchronous Generator

Synchronous generators are the dominant source of electric power [9]. In Fig. 2, a cross section schematic of a salient pole, one field pole pair, three-phase synchronous generator is shown. The machine essentially consists of two parts; the rotor and the stator. The field winding f on the rotor carries a direct current from the excitation system, generating a rotating magnetic field that induces alternating voltages in the stator windings. The three-phase windings of the stator a, b, and c are located 120 degrees apart in space, generating voltages of 120 degrees separation in time phase during uniform rotation of the magnetic field. Electrical circuits of the stator and rotor are shown in Fig. 3. To produce a steady torque, the stator and rotor fields must rotate at the same speed, i.e., the rotor must rotate at synchronous speed. When the rotor has more than one pair of field poles, the electrical rotational velocity of the rotor ω_e is related to the mechanical rotational velocity of the crankshaft ω_m by the number of field poles in the generator p_f as[1] [9]

$$\omega_e = \omega_m \frac{p_f}{2}$$

For a common two pole-pair rotor, i.e., $p_f = 4$, the engine rotates at 1500 rpm to generate a 50 Hz supply.

In modeling of synchronous generators, a change of coordinates is often used. The employed transformation has multiple advantages, the most obviously significant being that it turns the alternating quantities of the stator

[1] For convenience, we suppress explicit time dependence (t) throughout.

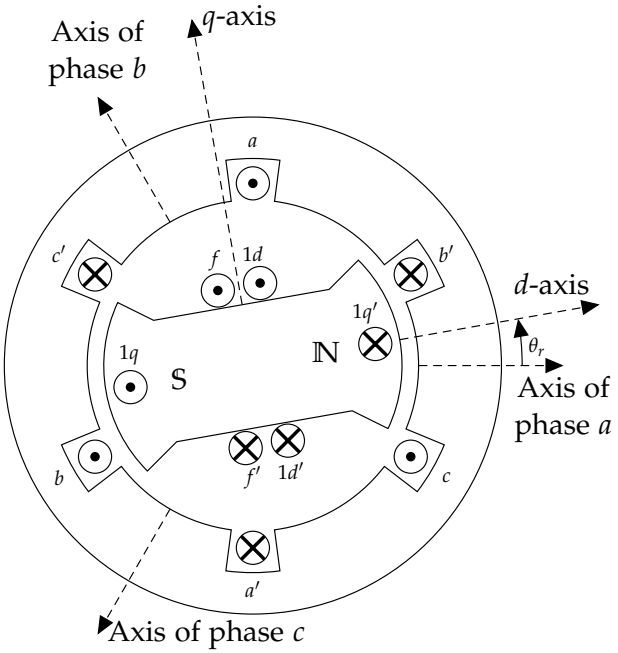

Fig. 2: Cross section schematic of a three-phase synchronous machine [9].

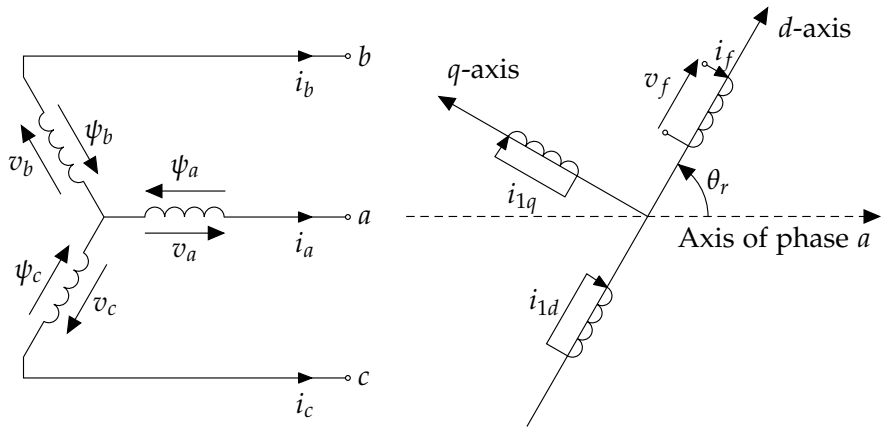

Fig. 3: Electrical stator (left) and rotor (right) circuits [9].

into constants during synchronous operation while having only slow variations when used for stability studies [9]. The transformation is known as the *direct*, *quadrature* and *zero* (*dq0*) transformation.

Initially provided by [10], the transformation of stator *abc* quantities into new variables in terms of a rotational *dq*0 reference frame, as shown in Fig.

2, is given by

$$\begin{bmatrix} i_d \\ i_q \\ i_0 \end{bmatrix} = \begin{bmatrix} k_d \cos\theta & k_d \cos\left(\theta - \frac{2\pi}{3}\right) & k_d \cos\left(\theta + \frac{2\pi}{3}\right) \\ -k_q \sin\theta & -k_q \sin\left(\theta - \frac{2\pi}{3}\right) & -k_q \sin\left(\theta + \frac{2\pi}{3}\right) \\ \frac{1}{3} & \frac{1}{3} & \frac{1}{3} \end{bmatrix} \begin{bmatrix} i_a \\ i_b \\ i_c \end{bmatrix}$$

where i_a, i_b, and i_c are the alternating currents of phase a, b, and c, respectively, and θ is the angle between the direct axis and the magnetic axis of the phase a winding in the stator, as indicated in Fig. 2. The transformation given for currents here, is equally valid for voltages and stator flux linkages. Since the 0 quantity equals zero in balanced systems it will be omitted in the development of the model. Having the transformation coefficients $k_d = k_q = \frac{2}{3}$, as used in the present work, yields equal peak values of the abc and $dq0$ quantities. The transformation coefficients are arbitrary and can be chosen to provide alternative properties of the transformation if desirable e.g., power invariance. Traditionally, in a salient pole generator, one damper winding in each axis, denoted $1d$ and $1q$, respectively, is included on the rotor offering short-circuited paths for eddy currents to dampen oscillations.

2.3 Governor and Automatic Voltage Regulator

In general, the first level of fuel injection control is handled by a governor, while the first level of excitation control is handled by an automatic voltage regulator (AVR). The governor uses measurements of the rotational velocity of the crankshaft to adjust the fuel injection for the engine and the AVR uses measurements of the stator voltages to adjust the magnetization current in the excitation system, thereby adjusting the rotating magnetic field and the induced voltages in the stator windings. In most installations, the governor and AVR employ one of two simple control schemes based on PID control algorithms. One scheme called isochronous, where the aim is to keep the frequency or voltage constant independent of the load on the DG. Another scheme called droop, where the frequency or voltage is adjusted linearly according to the load.

2.4 Electrical Load

Generally, characterization of electrical load is a highly complex task. Many loads are dynamic in nature (e.g., flourescent lighting, induction motors) and the combination of multiple loads can be close to impossible to determine [9]. In a greatly simplified manner, we can describe electrical load by two categories; active load and reactive load. When connected to a larger grid with several generating units, a grid impedance connecting the generator to an ideal source will be relevant. As a first step, the developed model will deal

only with active loads, as this is also the type available in the experimental setup utilized in Section 4.

3 Diesel Generator Model

With this section, we present the development of the nonlinear model of a diesel generator set.

The basic equation, known as the swing equation, describing the motion behavior of a synchronous machine with total system inertia J and total system damping D is

$$J\dot{\omega}_m = T_m - T_e - D\omega_m$$

where T_m and T_e are the mechanical and electrical torques.

3.1 Diesel Engine

The mechanical torque of a four stroke cycle diesel engine, under the assumption of constant thermodynamic efficiency η, can be expressed as [7]

$$T_m = \frac{1}{2} m_f n_{cyl} c_f \eta$$

where m_f is the mass of injected fuel per cylinder per combustion cycle, n_{cyl} is the number of cylinders, c_f is the lower calorific value of the fuel, and the factor $\frac{1}{2}$ is due to the two engine revolutions in a combustion cycle of a four stroke cycle diesel engine. In practice, the mass of injected fuel is handled by a fuel injection system with non-negligible dynamics. We ignore any such nonlinear effects and model these dynamics as a first-order low-pass filter with time constant τ_f, providing

$$\dot{m}'_f = \frac{1}{\tau_f} m_f - \frac{1}{\tau_f} m'_f$$

where τ_f must be expected to depend on the make and model of the fuel injection system.

3.2 Synchronous Generator

Developing in a per unit system and under the assumptions that (i) the stator windings are sinusoidally distributed along the air-gap as far as the mutual effects with the rotor are concerned, (ii) the stator slots cause no appreciable variation of the rotor inductances with rotor position, (iii) magnetic hysteresis is negligible, and (iv) magnetic saturation effects are negligible [9], the actual

electrical torque of a salient pole, synchronous generator, as used above, using $dq0$ components is given by [9]

$$T_e = T_{base}\left(\psi_d i_q - \psi_q i_d\right)$$

where T_{base} is the torque base [9] and ψ_d, ψ_q, i_d, and i_q are the per unit stator flux linkages and per unit stator currents in the direct and quadrature axis, respectively. The per unit stator flux linkages and their associated per unit time-derivatives are given by [9]

$$\begin{aligned} \psi_d &= -L_d i_d + L_{ad} i_f + L_{ad} i_{1d}, & \dot{\psi}_d &= v_d + \psi_q \omega_e + R_a i_d \\ \psi_q &= -L_q i_q + L_{aq} i_{1q}, & \dot{\psi}_q &= v_q - \psi_d \omega_e + R_a i_q \end{aligned}$$

where i_f, i_{1d}, and i_{1q} are the per unit field, direct axis damper, and quadrature axis damper currents, respectively. L_d and L_q are the per unit direct and quadrature axis synchronous inductances. R_a is the per unit armature resistance per phase. For resistive loads, the per unit direct and quadrature stator voltages v_d and v_q are given by $v_d = R_L i_d$ and $v_q = R_L i_q$ where R_L is the per unit per phase resistance of the load. L_{ad} and L_{aq} are the per unit mutual inductances given by the subtraction of the direct and quadrature axis synchronous inductance by the leakage inductance L_l as $L_{ad} = L_d - L_l$ and $L_{aq} = L_q - L_l$. Finally, ω_e is the per unit electrical rotational velocity of the rotor given by [9]

$$\omega_e = \frac{\omega_m}{\omega_{mbase}}$$

where ω_m is the mechanical rotational velocity of the crankshaft, as in Section 3.1, and ω_{mbase} is the mechanical rotational velocity base. The per unit rotor flux linkages ψ_f, ψ_{1d}, and ψ_{1q} and their associated per unit time-derivatives are given by [9]

$$\begin{aligned} \psi_f &= L_{ff} i_f + L_{f1d} i_{1d} - L_{ad} i_d, & \dot{\psi}_f &= v_f - R_f i_f \\ \psi_{1d} &= L_{11d} i_{1d} + L_{f1d} i_f - L_{ad} i_d, & \dot{\psi}_{1d} &= -R_{1d} i_{1d} \\ \psi_{1q} &= L_{11q} i_{1q} - L_{aq} i_q, & \dot{\psi}_{1q} &= -R_{1q} i_{1q} \end{aligned}$$

where L_{ff}, L_{11d}, and L_{11q} are the per unit field, direct axis damper, and quadrature axis damper self-inductances, respectively, L_{f1d} is the per unit field and direct axis damper mutual inductance, R_f, R_{1d}, and R_{1q} are the per unit field, direct axis damper, and quadrature damper resistances, respectively, and v_f is the per unit field voltage.

3.3 Governor and Automatic Voltage Regulator

Obviously, the governor and AVR have great impact on the dynamics of the DG and are as a consequence assumed present and included in the model

in isochronous regulation mode as classical PI-regulators. In our model, the governor adjusts the fuel mass m_f while the AVR adjusts the per unit field voltage v_f according to

$$\begin{bmatrix} m_f \\ v_f \end{bmatrix} = \begin{bmatrix} k_{p\omega} & 0 \\ 0 & k_{pv} \end{bmatrix} \begin{bmatrix} e_\omega \\ e_v \end{bmatrix} + \begin{bmatrix} k_{i\omega} & 0 \\ 0 & k_{iv} \end{bmatrix} \begin{bmatrix} e'_\omega \\ e'_v \end{bmatrix}$$

where $k_{p\omega}$, k_{pv}, $k_{i\omega}$, and k_{iv} are the proportional and integral governor and AVR constants, respectively, the integral error states e'_ω and e'_v are updated as $\dot{e}'_\omega = e_\omega$ and $\dot{e}'_v = e_v$, respectively, and e_ω and e_v are the errors given by

$$\begin{bmatrix} e_\omega \\ e_v \end{bmatrix} = \begin{bmatrix} r_\omega \\ r_v \end{bmatrix} - \begin{bmatrix} \omega_e \omega_{base} \\ v'_{rms} \end{bmatrix}$$

where r_ω is the electrical rotational velocity reference, r_v is the voltage reference, ω_{base} is the electrical rotational velocity base [9] and v'_{rms} is the filtered three-phase RMS value of the stator voltages. In practice, RMS values are generally calculated with measurements from the last period of the ac signals effectively causing a filtering of the instantaneous RMS value v_{rms} to the value used for regulation. The filtering of this measurement is approximated as

$$\dot{v}'_{rms} = \frac{1}{\tau_v} v_{rms} - \frac{1}{\tau_v} v'_{rms}$$

where τ_v is twice the per unit time period of the nominal frequency and v_{rms} is given by

$$v_{rms} = v_{sbase} R_L \sqrt{\frac{1}{2}\left(i_d^2 + i_q^2\right)}$$

where v_{sbase} is the stator voltage base [9].

3.4 Electrical Load

In this work, the load is modeled as purely resistive. In an application, this load will of course be replaced by a relevant model. Modeling the electrical load as purely resistive, the per unit per phase load resistance, in terms of the total active power P delivered to the load, is given by

$$R_L = \frac{1}{Z_{sbase}} \frac{V^2}{P}$$

where V is the phase-to-phase RMS voltage and Z_{sbase} is the stator impedance base [9]. For the loads available in the experimental setup, i.e., 10 kW, 20 kW, 30 kW, 40 kW, and 50 kW, the actual per phase load resistance is 16 Ω, 8 Ω, 5.33 Ω, 4 Ω, and 3.2 Ω, respectively, with $V = 400$ V.

3.5 Combined Model

Gathering all of the above, we have a tenth-order nonlinear model, shown in Fig. 4, on the form

$$\dot{x} = Ax + x_1F_1x + x_3F_3x + x_4F_4x + dG_1x + dG_2\sqrt{\frac{1}{2}\left(x_3^2 + x_4^2\right)} + Bu \quad \text{(1a)}$$

$$y = Cx \quad \text{(1b)}$$

where the matrices $A \in \mathbb{R}^{n\times n}$ ($n = 10$), $F_1 \in \mathbb{R}^{n\times n}$, $F_3 \in \mathbb{R}^{n\times n}$, $F_4 \in \mathbb{R}^{n\times n}$, $G_1 \in \mathbb{R}^{n\times n}$, $G_2 \in \mathbb{R}^{n\times 1}$, $B \in \mathbb{R}^{n\times m}$ ($m = 2$), and $C \in \mathbb{R}^{m\times n}$ are as defined in the Appendix, d is the scalar disturbance, and $x \in \mathbb{R}^n$, $u \in \mathbb{R}^m$, and $y \in \mathbb{R}^m$ are the state, input and output vector, respectively, given by

$$x = \begin{bmatrix} \omega_m & m_f' & i_d & i_q & i_f & i_{1d} & i_{1q} & v_{rms}' & e_\omega' & e_v' \end{bmatrix}^T$$

$$u = \begin{bmatrix} r_\omega & r_v \end{bmatrix}^T$$

$$y = \begin{bmatrix} \omega_e\omega_{base} & v_{rms}' \end{bmatrix}^T$$

The states are the mechanical rotational velocity of the engine ω_m, the filtered mass of injected fuel per cylinder per combustion cycle m_f', the per unit current in the direct axis i_d, the per unit current in the quadrature axis i_q, the per unit field current i_f, the per unit direct axis damper current i_{1d}, the per unit quadrature axis damper current i_{1q}, the filtered three-phase RMS stator voltage v_{rms}', the integral governor error state e_ω', and the integral AVR error state e_v', respectively. The two inputs are the references for the governor r_ω and the AVR r_v, respectively. The scalar disturbance is the per unit per phase load R_L. Finally, the two outputs are the actual electrical rotational velocity of the rotor $\omega_e\omega_{base}$ and the filtered three-phase RMS stator voltage v_{rms}', respectively.

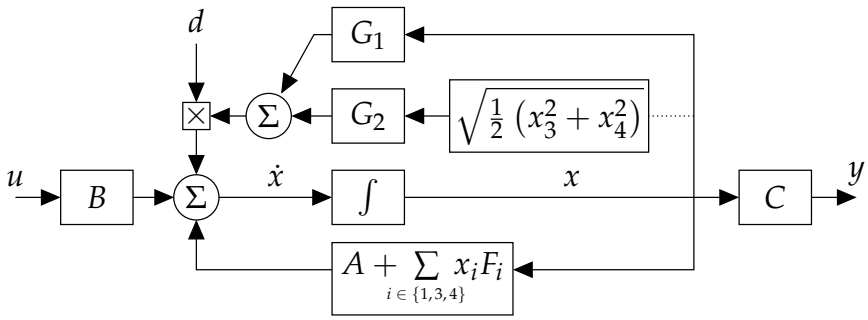

Fig. 4: Structural diagram of the nonlinear DG model provided in (1).

3.6 Bode Plot Analysis

Linearizing the model given in (1) in the operating points used in Section 4, i.e., electrical load of 10 kW, 20 kW, 30 kW, 40 kW, and 50 kW, we can demonstrate nonlinear behavior through the differences in the linearized models using e.g. Bode plots. The parameter values used for linearizing can be found in the Appendix. In Figs. 5 and 6, Bode plots from input, i.e., reference, to corresponding output are shown. It is evident that the governor-related transfer function exhibits the smallest differences across the operating range, but differences are present. Figures 7 and 8 show Bode plots from disturbance, i.e., electrical load, to the outputs. Both plots demonstrate the large effect the electrical load has on the dynamics of a DG. As an example, we see as much as 30 to 40 dB differences in magnitude from the disturbance to the outputs at low frequencies.

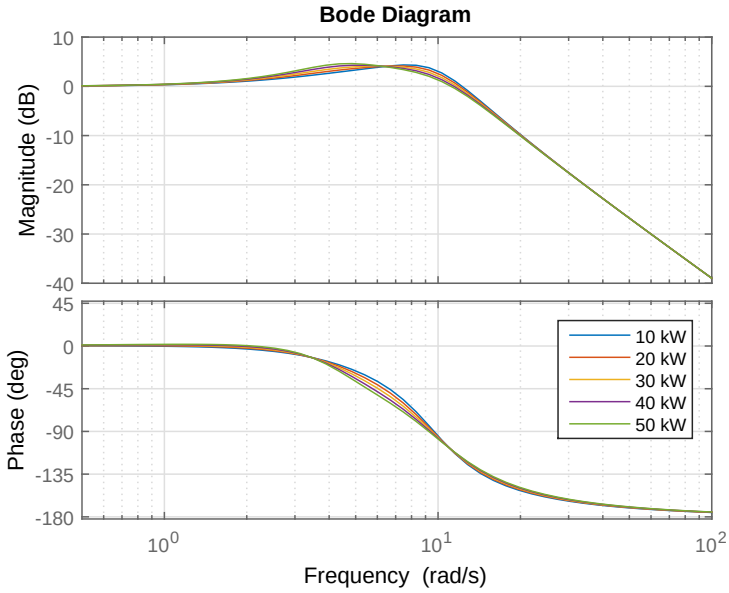

Fig. 5: Bode plots from r_ω to $\omega_e\omega_{base}$ of the linearized combined model transfer function in the five operating points available in experimental data.

4 Comparison With Experimental Data

In this section, simulation of the developed tenth-order nonlinear model (1) is compared with experimental data when subject to steps in electrical load. The simulations are performed using MATLAB Simulink®. For parameter values used in the simulation, see the Appendix.

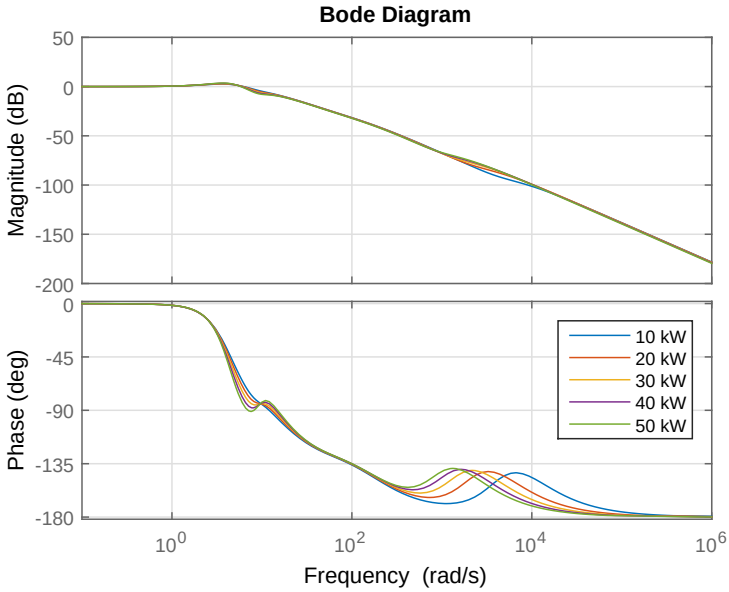

Fig. 6: Bode plots from r_v to v'_{rms} of the linearized combined model transfer function in the five operating points available in experimental data.

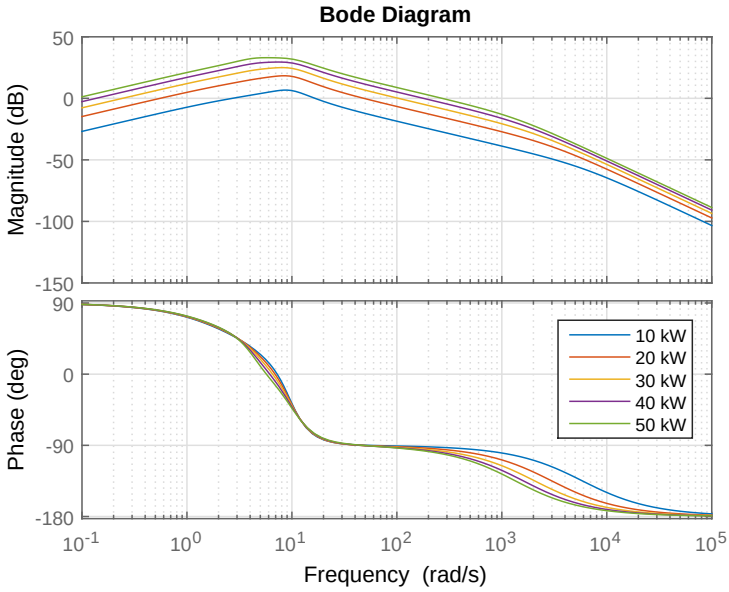

Fig. 7: Bode plots from d to $\omega_e\omega_{base}$ of the linearized combined model transfer function in the five operating points available in experimental data.

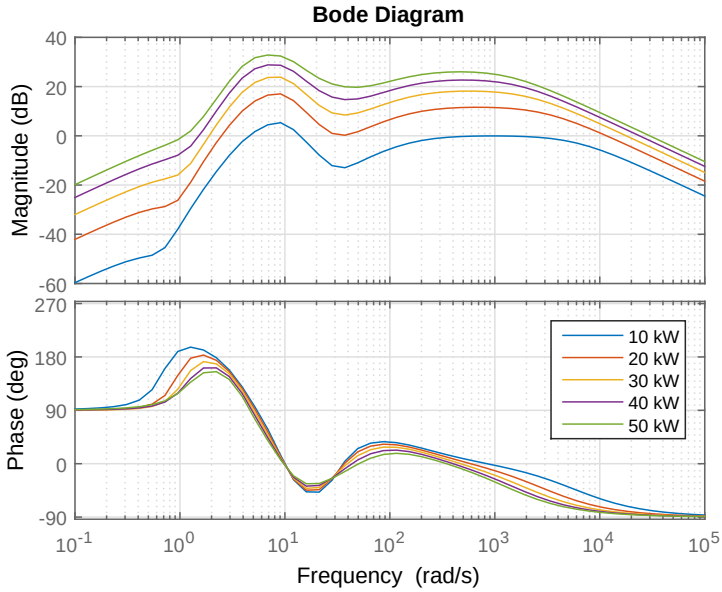

Fig. 8: Bode plots from d to v'_{rms} of the linearized combined model transfer function in the five operating points available in experimental data.

4.1 Experimental Setup

The measurements have been obtained by controlled load stepping on a DG in island operation, i.e., DG and load not connected to the grid, with governor and AVR following the isochronous control scheme. The diesel engine is a 94 HP Deutz BF 4M 2012 and the synchronous generator is a Leroy Somer LSA 42.3 L9 C6/4 60 kVA/48 kW alternator. The applied electrical load is controlled in steps of 10 kW.

The data has been collected at a sampling rate of 50 kHz with measurements of the three-phase stator voltages and currents and a 129-tooth tachometer on the engine shaft.

4.2 Electrical Load Step Responses

Usually, most of the model parameters can be deduced from datasheets. In the experimental setup, as will be the case in most future real-life implementations, the parameters of the existing governor and AVR could not easily be extracted. In total, the following parameters have been hand tuned to achieve step responses comparable to responses seen on the real DG; D, L_l, τ_f, $k_{p\omega}$, $k_{i\omega}$, k_{pv}, and k_{iv}. In Fig. 9, the frequency responses of the measured and simulated DG are shown for steps in electrical load from 10 to 20 kW, 20 to 30 kW, 30 to 40 kW, and 40 to 50 kW. Figure 10 shows the corresponding sta-

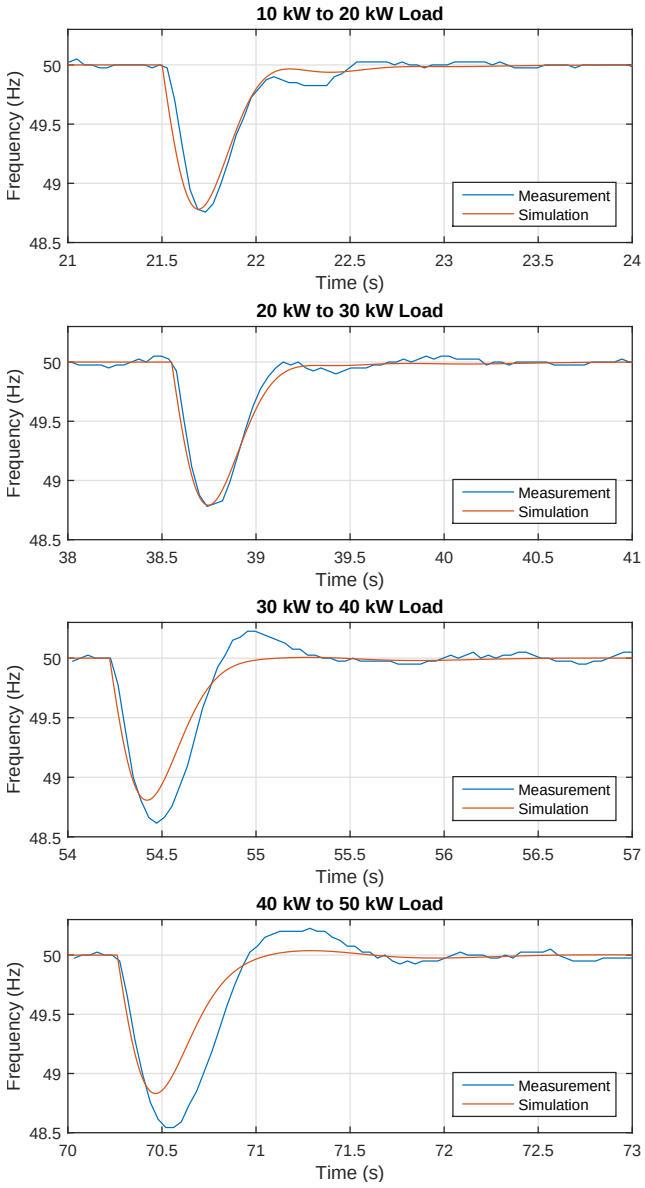

Fig. 9: Measured and simulated frequency response with steps in electrical load from 10 to 20 kW, 20 to 30 kW, 30 to 40 kW, and 40 to 50 kW.

tor RMS voltage responses. The comparisons show that the model describes the dominant characteristics of the measured DG responses. Regarding the frequency responses in Fig. 9, the increasing drop and overshoot at higher

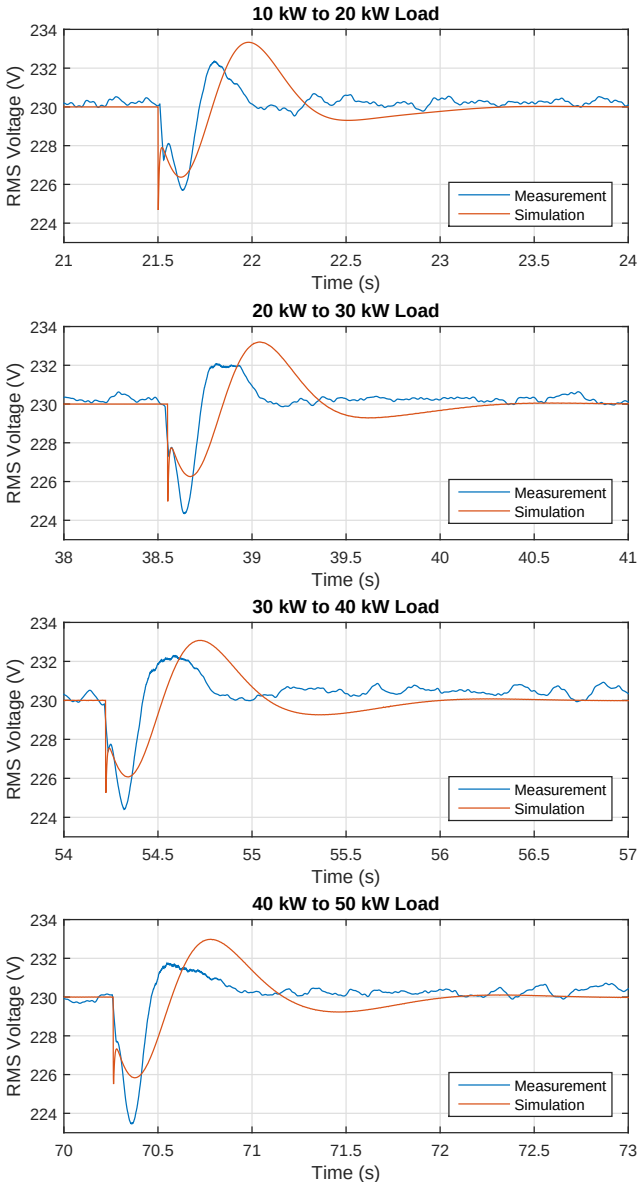

Fig. 10: Measured and simulated voltage response with steps in electrical load from 10 to 20 kW, 20 to 30 kW, 30 to 40 kW, and 40 to 50 kW.

loading conditions develop more aggressively in the measurements than the simulations, however, the development is present in the simulations. The voltage responses in Fig. 10 show discrepancies in both the time and magni-

tudes; however, the main characteristics are evidently present. It should be noted that the frequency and voltage responses are strongly coupled.

5 Conclusions

In this paper, a first principles tenth-order nonlinear model of a diesel driven generator set has been presented. The model has a degree of detail which allows for physical insight, while keeping the complexity at a level that can be used for control design purposes. The nonlinearities exhibited across the operating range, with governor and AVR included, indicate that simple PI-controllers are not sufficient to maintain the same transient response across the entire operating range. The model has been validated against measurements from a real DG.

Further development of the model would naturally include a load-dependent variable efficiency of the diesel engine to increase the validity of the model further. The hope is that a control design, which can ease commissioning, can be based on parameters extracted from engine and generator datasheets, possibly supplemented by simple parameter identification to employ adaptive, self-tuning, or gain-scheduling control schemes.

Appendix

The matrices $A \in \mathbb{R}^{n\times n}$, $F_1 \in \mathbb{R}^{n\times n}$, $F_3 \in \mathbb{R}^{n\times n}$, $F_4 \in \mathbb{R}^{n\times n}$, $G_1 \in \mathbb{R}^{n\times n}$, $G_2 \in \mathbb{R}^{n\times 1}$, $B \in \mathbb{R}^{n\times m}$, and $C \in \mathbb{R}^{m\times n}$ for the model on the form in (1) are given by

$$A = \begin{bmatrix} -c_{10} & c_{11} & 0 & 0 & 0 & 0 & 0 & 0 & 0 & 0 \\ -c_{12} & -c_{13} & 0 & 0 & 0 & 0 & 0 & 0 & c_{14} & 0 \\ 0 & 0 & c_{15} & 0 & c_{16} & -c_{17} & 0 & c_{18} & 0 & -c_{19} \\ 0 & 0 & 0 & -c_{20} & 0 & 0 & -c_{21} & 0 & 0 & 0 \\ 0 & 0 & c_{22} & 0 & c_{23} & -c_{24} & 0 & c_{25} & 0 & -c_{26} \\ 0 & 0 & -c_{27} & 0 & c_{28} & -c_{29} & 0 & c_{30} & 0 & -c_{31} \\ 0 & 0 & 0 & -c_{32} & 0 & 0 & -c_{33} & 0 & 0 & 0 \\ 0 & 0 & 0 & 0 & 0 & 0 & 0 & -c_{34} & 0 & 0 \\ -c_{35} & 0 & 0 & 0 & 0 & 0 & 0 & 0 & 0 & 0 \\ 0 & 0 & 0 & 0 & 0 & 0 & 0 & -1 & 0 & 0 \end{bmatrix} \tag{2a}$$

$$F_1 = \begin{bmatrix} 0 & 0 & 0 & 0 & 0 & 0 & 0 & 0 & 0 & 0 \\ 0 & 0 & 0 & 0 & 0 & 0 & 0 & 0 & 0 & 0 \\ 0 & 0 & 0 & -c_{36} & 0 & 0 & c_{37} & 0 & 0 & 0 \\ 0 & 0 & -c_{38} & 0 & c_{39} & c_{39} & 0 & 0 & 0 & 0 \\ 0 & 0 & 0 & -c_{40} & 0 & 0 & c_{41} & 0 & 0 & 0 \\ 0 & 0 & 0 & c_{42} & 0 & 0 & -c_{43} & 0 & 0 & 0 \\ 0 & 0 & -c_{44} & 0 & c_{45} & c_{45} & 0 & 0 & 0 & 0 \\ 0 & 0 & 0 & 0 & 0 & 0 & 0 & 0 & 0 & 0 \\ 0 & 0 & 0 & 0 & 0 & 0 & 0 & 0 & 0 & 0 \\ 0 & 0 & 0 & 0 & 0 & 0 & 0 & 0 & 0 & 0 \end{bmatrix} \tag{2b}$$

$$F_3 = \begin{bmatrix} 0 & 0 & 0 & 0 & 0 & 0 & c_{46} & 0 & 0 & 0 \\ 0 & & & & \cdots & & & & & 0 \\ \vdots & & & & \ddots & & & & & \vdots \\ 0 & & & & \cdots & & & & & 0 \end{bmatrix} \tag{2c}$$

$$F_4 = \begin{bmatrix} 0 & 0 & c_{47} & 0 & -c_{48} & -c_{48} & 0 & 0 & 0 & 0 \\ 0 & & & & \cdots & & & & & 0 \\ \vdots & & & & \ddots & & & & & \vdots \\ 0 & & & & \cdots & & & & & 0 \end{bmatrix} \tag{2d}$$

$$G_1 = \begin{bmatrix} 0 & 0 & 0 & 0 & 0 & 0 & 0 & 0 & 0 & 0 \\ 0 & 0 & 0 & 0 & 0 & 0 & 0 & 0 & 0 & 0 \\ 0 & 0 & c_{49} & 0 & 0 & 0 & 0 & 0 & 0 & 0 \\ 0 & 0 & 0 & -c_{50} & 0 & 0 & 0 & 0 & 0 & 0 \\ 0 & 0 & c_{51} & 0 & 0 & 0 & 0 & 0 & 0 & 0 \\ 0 & 0 & -c_{52} & 0 & 0 & 0 & 0 & 0 & 0 & 0 \\ 0 & 0 & 0 & -c_{53} & 0 & 0 & 0 & 0 & 0 & 0 \\ 0 & 0 & 0 & 0 & 0 & 0 & 0 & 0 & 0 & 0 \\ 0 & 0 & 0 & 0 & 0 & 0 & 0 & 0 & 0 & 0 \\ 0 & 0 & 0 & 0 & 0 & 0 & 0 & 0 & 0 & 0 \end{bmatrix} \tag{2e}$$

$$G_2 = \begin{bmatrix} 0 & 0 & 0 & 0 & 0 & 0 & 0 & c_{54} & 0 & 0 \end{bmatrix}^T \tag{2f}$$

$$B = \begin{bmatrix} 0 & c_{55} & 0 & 0 & 0 & 0 & 0 & 0 & 1 & 0 \\ 0 & 0 & -c_{18} & 0 & -c_{25} & -c_{30} & 0 & 0 & 0 & 1 \end{bmatrix}^T \tag{2g}$$

$$C = \begin{bmatrix} c_{35} & 0 & 0 & 0 & 0 & 0 & 0 & 0 & 0 & 0 \\ 0 & 0 & 0 & 0 & 0 & 0 & 0 & 1 & 0 & 0 \end{bmatrix} \tag{2h}$$

The constants used in (2) are defined as

$$\begin{aligned} c_1 &= \left(L_d L_{f1d}^2 + L_{ad}^2 L_{ff} + L_{11d} L_{ad}^2 - L_d L_{11d} L_{ff} \right) t_{base} \\ &\quad -2 L_{ad}^2 L_{f1d} t_{base}, \quad c_2 = \left(L_q L_{11q} - L_{aq}^2 \right) t_{base}, \\ c_3 &= \left(L_{ff} L_{11d} - L_{f1d}^2 \right), \quad c_4 = \left(L_{11d} - L_{f1d} \right) L_{ad}, \\ c_5 &= \left(L_{f1d} - L_{ff} \right) L_{ad}, \quad c_6 = \left(L_d L_{11d} - L_{ad}^2 \right), \end{aligned}$$

$$c_7 = \left(L_d L_{f1d} - L_{ad}^2\right), \quad c_8 = \left(L_{ad}^2 - L_d L_{ff}\right),$$
$$c_9 = \left(L_{ad}^2 - L_d L_{f1d}\right), \quad c_{10} = \frac{D}{J}, \quad c_{11} = \frac{nc_f\eta}{2J},$$
$$c_{12} = \frac{k_{p\omega} p_f}{2\tau_f}, \quad c_{13} = \frac{1}{\tau_f}, \quad c_{14} = \frac{k_{i\omega}}{\tau_f}, \quad c_{15} = \frac{c_3 R_a}{c_1},$$
$$c_{16} = \frac{c_4 R_{fd}}{c_1}, \quad c_{17} = \frac{c_5 R_{1d}}{c_1}, \quad c_{18} = \frac{c_4 k_{pv}}{c_1}, \quad c_{19} = \frac{c_4 k_{iv}}{c_1},$$
$$c_{20} = \frac{L_{11q} R_a}{c_2}, \quad c_{21} = \frac{L_{aq} R_{1q}}{c_2}, \quad c_{22} = \frac{c_4 R_a}{c_1},$$
$$c_{23} = \frac{c_6 R_{fd}}{c_1}, \quad c_{24} = \frac{c_7 R_{1d}}{c_1}, \quad c_{25} = \frac{c_6 k_{pv}}{c_1}, \quad c_{26} = \frac{c_6 k_{iv}}{c_1},$$
$$c_{27} = \frac{c_5 R_a}{c_1}, \quad c_{28} = \frac{c_9 R_{fd}}{c_1}, \quad c_{29} = \frac{c_8 R_{1d}}{c_1}, \quad c_{30} = \frac{c_9 k_{pv}}{c_1},$$

$$c_{31} = \frac{c_9 k_{iv}}{c_1}, \quad c_{32} = \frac{L_{aq} R_a}{c_2}, \quad c_{33} = \frac{L_q R_{1q}}{c_2}, \quad c_{34} = \frac{1}{\tau_v},$$
$$c_{35} = \frac{p_f}{2}, \quad c_{36} = \frac{c_3 L_q}{c_1 \omega_{mbase}}, \quad c_{37} = \frac{c_3 L_{aq}}{c_1 \omega_{mbase}},$$
$$c_{38} = \frac{L_d L_{11q}}{c_2 \omega_{mbase}}, \quad c_{39} = \frac{L_{ad} L_{11q}}{c_2 \omega_{mbase}}, \quad c_{40} = \frac{c_4 L_q}{c_1 \omega_{mbase}},$$
$$c_{41} = \frac{c_4 L_{aq}}{c_1 \omega_{mbase}}, \quad c_{42} = \frac{c_5 L_q}{c_1 \omega_{mbase}}, \quad c_{43} = \frac{c_5 L_{aq}}{c_1 \omega_{mbase}},$$
$$c_{44} = \frac{L_d L_{aq}}{c_2 \omega_{mbase}}, \quad c_{45} = \frac{L_{ad} L_{aq}}{c_2 \omega_{mbase}}, \quad c_{46} = \frac{T_{base} L_{aq}}{J},$$
$$c_{47} = \frac{T_{base}\left(L_d - L_q\right)}{J}, \quad c_{48} = \frac{T_{base} L_{ad}}{J}, \quad c_{49} = \frac{c_3}{c_1},$$
$$c_{50} = \frac{L_{11q}}{c_2}, \quad c_{51} = \frac{c_4}{c_1}, \quad c_{52} = \frac{c_5}{c_1}, \quad c_{53} = \frac{L_{aq}}{c_2},$$
$$c_{54} = \frac{v_{sbase}}{\tau_v}, \quad c_{55} = \frac{k_{p\omega}}{\tau_f}$$

where t_{base} is the time base [9] and the remaining parameters therein, used for simulations, are

$$D = 0.1 \text{ Nms}, \quad J = 1.8015 \text{ kgm}^2, \quad n_{cyl} = 4, \quad \eta = 0.4,$$
$$c_f = 43.4 \frac{\text{MJ}}{\text{kg}}, \quad p_f = 4, \quad \tau_f = 0.1 \text{ s}, \quad \tau_v = 0.0064 \text{ pu},$$
$$k_{p\omega} = 0.29, \quad k_{i\omega} = 0.67, \quad k_{pv} = 0.0001, \quad k_{iv} = 0.0003,$$
$$R_a = 0.011 \text{ pu}, \quad R_f = 0.0006 \text{ pu}, \quad R_{1d} = 0.0354 \text{ pu},$$
$$R_{1q} = 0.0428 \text{ pu}, \quad L_d = 1.05 \text{ pu}, \quad L_q = 0.7 \text{ pu},$$

$$L_l = 0.15 \text{ pu}, \quad L_{ad} = 0.9 \text{ pu}, \quad L_{aq} = 0.55 \text{ pu},$$
$$L_f = 0.2571 \text{ pu}, \quad L_{ff} = 1.1571 \text{ pu}, \quad L_{f1d} = 0.9 \text{ pu},$$
$$L_{1d} = 0.2 \text{ pu}, \quad L_{11d} = 1.1 \text{ pu}, \quad L_{1q} = 0.2567 \text{ pu},$$
$$L_{11q} = 0.8067 \text{ pu}$$

References

[1] G. Johnson, *Generator Sets Report*. Market Analysis, IHS Technology, 2014.

[2] I. Ibraheem, P. Kumar, and D. P. Kothari, "Recent Philosophies of Automatic Generation Control Strategies in Power Systems," *IEEE Transactions on Power Systems*, vol. 20, no. 1, pp. 346–357, 2005.

[3] H. Shayeghi, H. A. Shayanfar, and A. Jalili, "Load Frequency Control Strategies: A State-of-the-Art Survey for the Researcher," *Energy Conversion and Management*, vol. 50, no. 2, pp. 344–353, 2009.

[4] S. K. Pandey, S. R. Mohanty, and N. Kishor, "A literature survey on load-frequency control for conventional and distribution generation power systems," *Renewable and Sustainable Energy Reviews*, vol. 25, pp. 318–334, 2013.

[5] O. Singh, P. Tiwari, Ibraheem, and A. K. Singh, "A Survey of Recent Automatic Generation Control Strategies in Power Systems," *International Journal of Emerging Trends in Electrical and Electronics*, vol. 7, no. 2, pp. 1–14, 2013.

[6] E. E. Ejegi, J. A. Rossiter, and P. Trodden, "A Survey of Techniques and Opportunities in Power System Automatic Generation Control," in *UKACC International Conference on Control*, 2014, pp. 537–542.

[7] U. Kiencke and L. Nielsen, *Automotive Control Systems: For Engine, Driveline, and Vehicle*, 2nd ed. Springer, 2005.

[8] C. E. Goering, M. L. Stone, D. W. Smith, and P. K. Turnquist, *Off-Road Vehicle Engineering Principles*. American Society of Agricultural Engineers, 2003.

[9] P. Kundur, *Power System Stability and Control*. McGraw-Hill, Inc., 1994.

[10] R. H. Park, "Two-Reaction Theory of Synchronous Machines - Generalized Method of Analysis - Part I," *Journal of the American Institute of Electrical Engineers*, vol. 48, no. 3, pp. 716–727, 1929.

Paper B

Self-Tuning Linear Quadratic Supervisory Regulation of a Diesel Generator using Large-Signal State Estimation

Jesper Knudsen, Jan Bendtsen, Palle Andersen,
and Kjeld Madsen

The paper has been published in the
Proceedings of the Australian Control Conference, pp. 32–37, 2016.

The layout has been revised.

Abstract

In this paper, a self-tuning linear quadratic supervisory regulator using a large-signal state estimator for a diesel driven generator set is proposed. The regulator improves operational efficiency, in comparison to current implementations, by (i) automating the initial tuning process and (ii) enabling automated retuning capabilities. Utilizing a first principles-based nonlinear model detailed in [1], the procedure is demonstrated through simulations after real system measurements have been used for parameter identification. The regulator is able to suppress load-induced variations successfully throughout the operating range of the diesel generator.

1 Introduction

Reliability, sustainability and efficiency are common requirements for essentially all electricity supplies around the world; large or small, complex or simple, strong or weak. With the increased utilization of intermittent and volatile renewable energy resources (RERs) in recent decades, these requirements have become increasingly complicated to fulfill. Besides improved control of RERs, much research is aimed at integrating intelligent consumption of electric energy as a part of the solution to this issue, known as the so-called Smart Grid, see for example [2], [3] and references therein.

However, for many developing rural areas the solutions of a Smart Grid, in the sense described above, are not currently appropriate, and perhaps never will be. One reason could be that the initial investment of RERs such as wind turbines or photovoltaic panels might simply be too big in those areas. Another factor is the amount of controllable consumption, which might be too small to be of any use in guaranteeing a reliable electricity supply. Instead, in many situations around the world, not only rural areas, reliability is achieved through the choice of supply sources. These situations include backup supply at, e.g., hospitals, laboratories, and data centers, and temporary supply at, e.g., musical festivals and sport events.

Used in great numbers around the world [4], the diesel driven generator set (DG) is one source capable of providing highly reliable electricity. Sustainability and efficiency are properties that come naturally to mind in relation to RERs, but less so in the case of diesel driven generator sets. Nonetheless, sustainability and efficiency is of great interest to DG owners and manufacturers. From the fuel itself to the production, transportation, and operation of DGs, many aspects influence the sustainability and efficiency. Although application dependent, when a DG is generating electrical power the control fundamentally consists of two tasks; fuel injection and generator excitation. In industrial solutions additional capabilities, such as synchronization and power regulation, are most often realized by adding a supervisory control

layer in a so-called automatic generation control (AGC) unit, as shown conceptually in Fig. 1. The AGC units for DGs provided by market leading manufacturers all implement fundamentally similar classical proportional-integral-derivative (PID) control algorithms. In terms of operational efficiency, however, classical PID control has one potentially costly drawback: The performance of PID controlled DGs depends on the chosen regulation parameters during commissioning. Manually determined by a commissioning engineer, these parameters will most often be chosen conservatively according to the individual engineer's preferences. In addition to the obvious likelihood of non-optimal performance, this procedure is time-consuming and thus operationally inefficient.

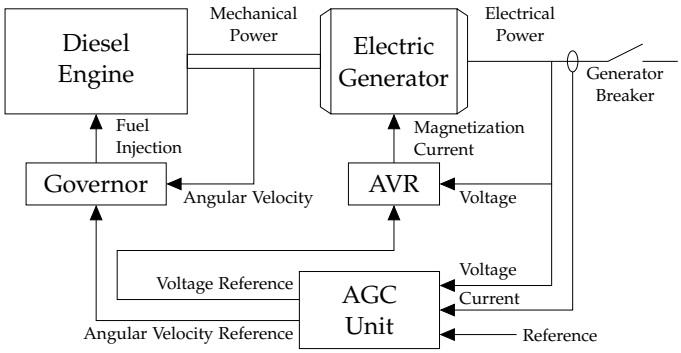

Fig. 1: Control diagram of a diesel driven generator set. The automatic generation control (AGC) unit provides references for the governor and the automatic voltage regulator (AVR) which regulates the fuel injection and the magnetization current.

In this paper, we propose a model-based self-tuning supervisory regulator that can improve the operational efficiency. The lower layer controllers (see examples [5], [6]) and the higher supervisory control layer (see examples [7]-[9]) have been subjects of significant research in the past. However, implementation of self-tuning regulation algorithms could help improve the operational efficiency of DGs in both of the above mentioned regards, as previously examined in [10]. The work in [10] uses a DG model based on polynomial approximations, whereas the present work is formulated using a first principles-based model, initially detailed in [1]. The term self-tuning regulator (STR) was used for the first time in [11], and is now a well-understood and proven field, properties that are of high value in the industry. The same is true for the theory concerning the linear quadratic regulator (LQR) [12], [13], which we apply as the regulator design method in the present work.

This paper is organized as follows. In Section 2, we present the system description and the model, initially derived in [1]. Section 3 establishes the design of a STR, which performs as demonstrated in Section 4. Finally, Sec-

tion 5 provides discussions and concluding remarks.

2 Diesel Generator Model

This section provides an introductory description of the diesel driven generator set system and the used model thereof. For a detailed derivation, see [1].

2.1 Introductory System Description

As illustrated in Fig. 1, a diesel driven generator set is the combination of a diesel engine and an electric generator. Most often [14] and in particular in this case, the generator is a three-phase synchronous generator.

Having supervisory control in mind, it is appropriate to model the diesel engine by a mean torque value model controlled by a fuel injection-regulating governor [1]. As an additional degree of model detail, the dynamics of the fueling system is included as a first-order low-pass filter.

Commonly denoted, a, b, and c, the three stator phases of a three-phase synchronous generator are mechanically distributed 120° apart, as shown in a simplifying manner in Fig. 2. The voltage of each stator phase, distributed electrically 120° apart under balanced conditions, depends on the rotating magnetic field of the rotor, the size of which is controlled by the excitation field current i_f. In modeling three-phase synchronous generators, a transformation of the abc quantities from the stator reference frame to a rotating reference frame is usually applied. This rotating reference frame is defined by the direct, quadrature, and zero ($dq0$) axes and the transformation, introduced in [15] and since referred to as the Park transformation, is given by[1]

$$\begin{bmatrix} i_d \\ i_q \\ i_0 \end{bmatrix} = \begin{bmatrix} k_d \cos\theta & k_d \cos\left(\theta - \frac{2\pi}{3}\right) & k_d \cos\left(\theta + \frac{2\pi}{3}\right) \\ -k_q \sin\theta & -k_q \sin\left(\theta - \frac{2\pi}{3}\right) & -k_q \sin\left(\theta + \frac{2\pi}{3}\right) \\ \frac{1}{3} & \frac{1}{3} & \frac{1}{3} \end{bmatrix} \begin{bmatrix} i_a \\ i_b \\ i_c \end{bmatrix}$$

where k_d and k_q are transformation constants and θ is the angle between the magnetic axes of the direct and the phase a winding in the stator, as indicated in Fig. 2. Provided only for currents here, the transformation is equally valid for voltages and stator flux linkages. As the 0 quantity equals zero in balanced systems, it has been omitted in the development of the model. So-called rotor damper windings are traditionally included in the direct and quadrature axis, denoted $1d$ and $1q$, as depicted along with the excitation field current i_f and voltage v_f in Fig. 3. Included in the model is control of

[1] For convenience, the explicit time dependence (t) is suppressed throughout the paper when context allows.

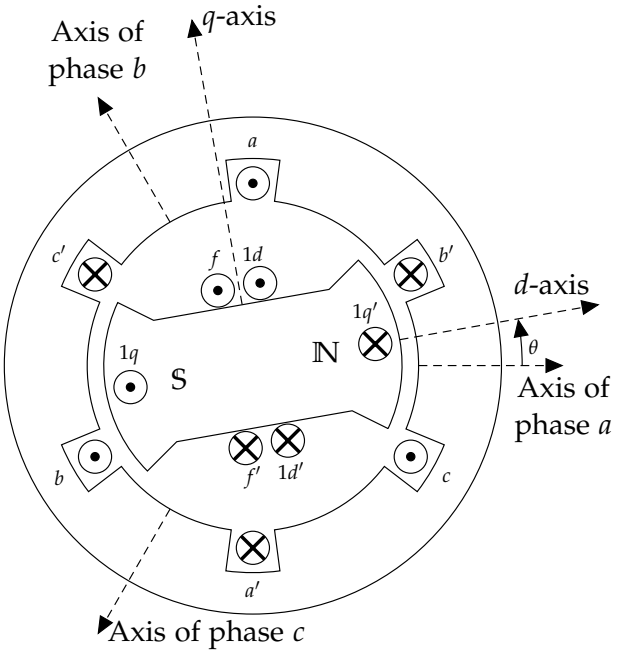

Fig. 2: Three-phase synchronous generator cross section schematic [14].

the excitation field current, or interchangeably voltage, done by an automatic voltage regulator (AVR). Usually, the reference for control of excitation is an RMS voltage value. Calculating an RMS quantity requires the values from an entire period of the alternating signal, effectively causing a damping of sudden signal changes. This damping is modeled as a first-order low-pass filter.

Considering the test facilities available in [1], the electrical load is modeled as a purely resistive load.

2.2 State-Space Model

Shown in Fig. 4 on block diagram form, the complete tenth-order ($n = 10$), two input ($m = 2$), two output, nonlinear model can be written on the compact form

$$\dot{x} = Ax + x_1F_1x + x_3F_3x + x_4F_4x + dG_1x + dG_2\sqrt{\frac{1}{2}\left(x_3^2 + x_4^2\right)} + Bu \quad \text{(1a)}$$

$$y = Cx \quad \text{(1b)}$$

where the matrices $A \in \mathbb{R}^{n\times n}$, $F_1 \in \mathbb{R}^{n\times n}$, $F_3 \in \mathbb{R}^{n\times n}$, $F_4 \in \mathbb{R}^{n\times n}$, $G_1 \in \mathbb{R}^{n\times n}$, $G_2 \in \mathbb{R}^{n\times 1}$, $B \in \mathbb{R}^{n\times m}$, and $C \in \mathbb{R}^{m\times n}$ are defined in [1], d is the scalar

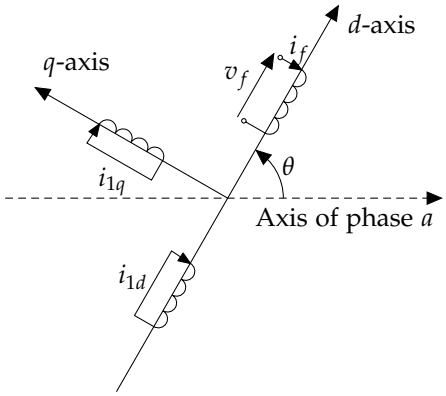

Fig. 3: Electrical circuit diagram of a salient pole rotor [14].

disturbance, and $x \in \mathbb{R}^n$, $u \in \mathbb{R}^m$, and $y \in \mathbb{R}^m$ are the state, input and output vector, respectively, given by

$$x = \begin{bmatrix} \omega_m & m_f & i_d & i_q & i_f & i_{1d} & i_{1q} & v_{rms} & e_\omega & e_v \end{bmatrix}^T$$
$$u = \begin{bmatrix} r_\omega & r_v \end{bmatrix}^T$$
$$y = \begin{bmatrix} \omega_e & v_{rms} \end{bmatrix}^T$$

The ten states are the mechanical rotational velocity of the diesel engine ω_m, the filtered mass of injected fuel per cylinder per combustion cycle m_f, the per unit current in the d-axis i_d, the per unit current in the q-axis i_q, the per unit field current i_f, the per unit d-axis damper current i_{1d}, the per unit q-axis damper current i_{1q}, the filtered phase-to-neutral RMS stator voltage v_{rms}, the governor integral error state e_ω, and the AVR integral error state e_v, respectively. The two inputs are the electrical rotational velocity reference r_ω and the phase-to-neutral RMS stator voltage reference r_v. The two outputs

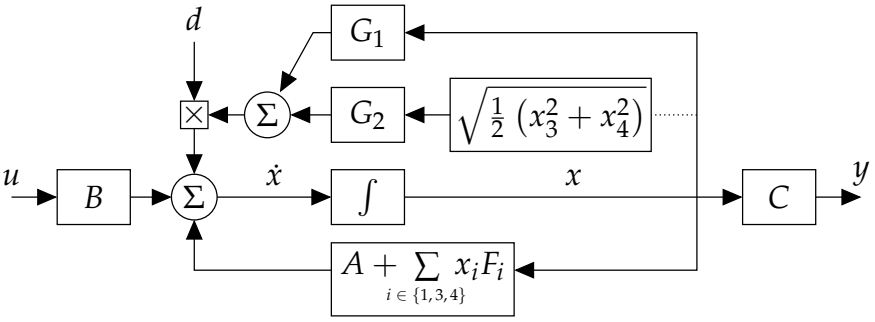

Fig. 4: Block diagram of the DG model provided in (1) [1].

are the electrical rotational velocity of the rotor ω_e and the filtered phase-to-neutral RMS stator voltage v_{rms}. Finally, the scalar disturbance d is the per unit per phase resistive load R_L, which has significant impact on the dynamics of the DG and, hence, determines the operating point for linearization of (1) when applying a linear control technique, such as LQR.

3 Self-Tuning Regulator Design

In general, the STR involves two separate tasks; parameter identification and regulator design [16]. These tasks can be split further into (i) the formulation of a suitable mathematical system model, (ii) the identification of model parameters, provided a set of test measurements from the real system, (iii) the specification of regulation requirements, (iv) the choice of a regulator design method, and (v) the regulator synthesis.

Section 2 covered the formulation of a suitable mathematical system model, with the introduction of (1). The remaining tasks are detailed in the following.

3.1 Parameter Identification

Naturally, the test on the real system must be such that the measurements reveal information about the parameters to be identified. Reflecting the test possibilities on any DG at a real site, our test involves running the DG disconnected from the grid under fixed load conditions, e.g., no load. Then, transients following a change of frequency and voltage references are analyzed to obtain the desired information. Specifically, our test, on the same DG as used for validation in [1], i.e., a 94 HP Deutz BF 4M 2012 diesel engine with a Leroy Somer LSA 42.3 L9 C6/4 60 kVA/48 kW generator, ran with a fixed load of 10 kW and steps in frequency and voltage references as shown in Figs. 5 and 6, along with the resulting measurement transients.

The model parameters to be identified are the proportional and integral gains of the governor and AVR, i.e., $k_{p\omega}$, $k_{i\omega}$, k_{pv}, and k_{iv}, respectively, and the time constant τ_f describing the fuel system dynamics. These parameters are chosen based on experience (from the modeling process in [1]), since they provide a suitable degree of leeway for model fitting. Furthermore, these parameters are unlikely to be available in a real setup, whereas the remaining parameters can be found in engine and generator datasheets.

Generally, parameter identification involves minimizing a performance function measuring the size of the model error

$$\varepsilon(t) = y(t) - y_m(t)$$

where $y(t)$ is the model output and $y_m(t)$ is the measured output. Any suitable grey-box identification method may be chosen; here, we apply the

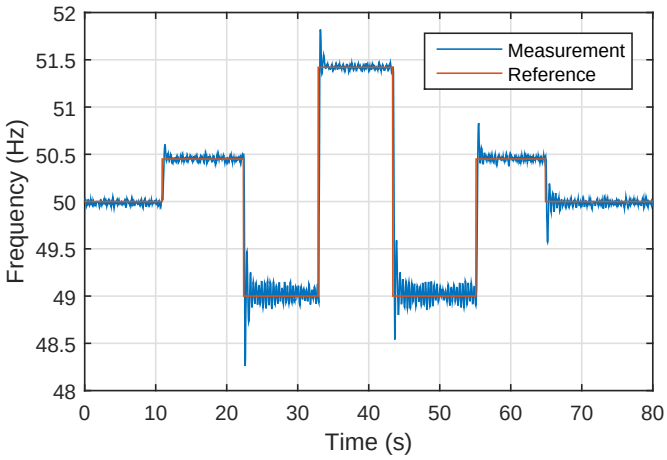

Fig. 5: Frequency measurements of parameter identification test on DG.

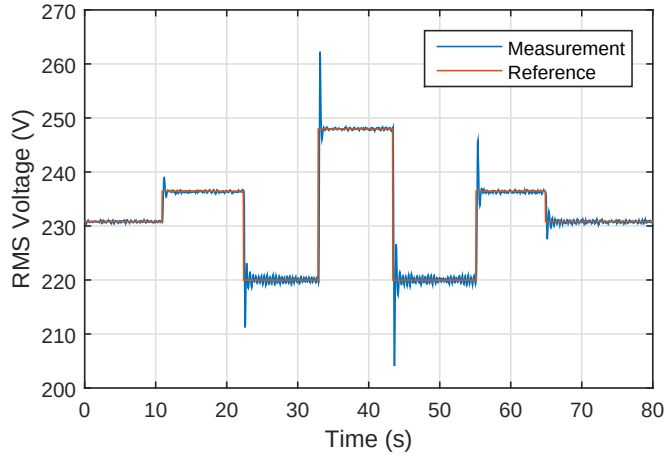

Fig. 6: Voltage measurements of parameter identification test on DG.

method presented in [17], which implements a Newton-based numerical gradient search algorithm. Given an initial parameter estimate of the provided parameters in [1], which were determined by hand-tuning, the parameter identification yields the parameters

$$k_{p\omega} = 0.3193 \tag{2a}$$
$$k_{i\omega} = 0.6499 \tag{2b}$$
$$k_{pv} = 1.2812 \cdot 10^{-4} \tag{2c}$$
$$k_{iv} = 2.6413 \cdot 10^{-4} \tag{2d}$$

$$\tau_f = 0.0795 \text{ s} \tag{2e}$$

which will be used in the following design.

3.2 Regulator Design

In the assumed setup, i.e., disconnected from a grid, the regulation requirements for an AGC are to suppress load-induced frequency and voltage variations throughout the operating range of the DG. In fact, these requirements are shared with the underlying governor and AVR. That is, if no AGC unit is installed and the governor and AVR are given constant references, they will suppress load-induced frequency and voltage variations. As introduced in Section 1, AGC units are installed to add additional capabilities, e.g., synchronization and power regulation, each of which pose different regulation requirements than the requirements dealt with in the present work.

We apply state feedback using the LQR design method, which is described briefly in the following. The LQR theory has been thoroughly presented in many books, see examples in [12] and [13]. The LQR state feedback $u^\delta(t) = -Kx^\delta(t)$ is found, for any initial state $x^\delta(0)$, as the solution to

$$\min_{u^\delta(t)} J(t) = \int_0^\infty x^\delta(t)^T Q x^\delta(t) + u^\delta(t)^T R u^\delta(t)\, dt$$

where Q is a positive semi-definite weighting matrix and R is a positive definite weighting matrix. The unique solution P to the algebraic Riccati equation

$$A^T P + PA - PBR^{-1}B^T P + Q = 0$$

where $P = P^T \geq 0$ provides the solution $K = R^{-1}B^T P$ as the LQR state feedback matrix for a given linear system $\dot{x}^\delta(t) = Ax^\delta(t) + Bu^\delta(t)$ where A and B are the system and input matrices of appropriate dimensions. The design choice of weighting matrices Q and R determines the performance of the closed-loop system $\dot{x}^\delta(t) = (A - BK)x^\delta(t)$.

As clarified in the conclusion of Section 2.2, the dynamics of a DG are significantly impacted by the applied load. To achieve adequate model precision throughout the operating range, when utilizing the linear regulator theory of LQR, the model is linearized in multiple operating points. Choosing the same operating points as in [1], which were determined based on the available test facilities, we linearize the model (1) around five operating points corresponding to 10, 20, 30, 40, and 50 kW load on the 48 kW DG. The appropriate number of operating points is application specific and would have to be investigated before commissioning on a real system. Let a δ superscript denote small-signal values, e.g., the small-signal state variable x^δ and its operating point value $\bar{x}$, such that

$$x = x^\delta + \bar{x} \tag{3}$$

The five linearized models, approximating the DG dynamics around the operating points, take the form

$$\dot{x}^{\delta} = \bar{A}_i x^{\delta} + \bar{B}_i u^{\delta} + \bar{B}_{di} d^{\delta} \tag{4a}$$
$$y^{\delta} = \bar{C}_i x^{\delta} \tag{4b}$$

where $\bar{A}_i \in \mathbb{R}^{n\times n}$, $\bar{B}_i \in \mathbb{R}^{n\times m}$, $\bar{B}_{di} \in \mathbb{R}^{n\times 1}$, and $\bar{C}_i \in \mathbb{R}^{m\times n}$ are the linearized system matrices of the i-th operating point. Linearization requires the operating point values $\bar{x}_i$, $\bar{u}_i$, $\bar{d}_i$, and $\bar{y}_i$. The input and output operating point values of this system are constant for all operating points, that is

$$\bar{u}_i = \bar{y}_i = \begin{bmatrix} 2\pi 50 \frac{\text{rad}}{\text{s}} & \frac{400}{\sqrt{3}}\ \text{V} \end{bmatrix}^T \qquad \forall i$$

Following the selection of $\bar{d}_i$ values, determination of the corresponding $\bar{x}_i$ values is possible by solving for x in (1) with $\dot{x} = 0$. The LQR feedback matrix $K_i \in \mathbb{R}^{m\times n}$ is determined for each operating point.

3.3 Large-Signal State Estimator

Applying LQR state feedback requires access to the internal states x of the system. However, only the outputs y are readily available, calling for the design of a state estimator. Initially proposed and developed in [18] and further developed in [19], often referred to as observers, classical estimators of state variables deal with small-signal variables near operating points of linear models. The classical Luenberger estimator for (4) is given by

$$\dot{\hat{x}}^{\delta} = \bar{A}_i \hat{x}^{\delta} + \bar{B}_i u^{\delta} + \bar{B}_{di} \hat{d}^{\delta} + L_i \left(y^{\delta} - \bar{C}_i \hat{x}^{\delta} \right) \tag{5}$$

where $\hat{x}^{\delta}$ and $\hat{d}^{\delta}$ are the estimated small-signal states and disturbance and $L_i \in \mathbb{R}^{n\times m}$ is the estimator gain matrix of the i-th operating point.

In general, large-signal values will be developing continuously over time. At a change of operating point, however, it follows from the simple example in Fig. 7 that the small-signal values in general will be discontinuous. To avoid this discontinuity, using (3) we reformulate the classical small-signal Luenberger state estimator (5) to a large-signal state estimator given for our linearized models (4) as

$$\dot{\hat{x}} = \dot{\hat{x}}^{\delta} = \bar{A}_i(\hat{x} - \bar{x}_i) + \bar{B}_i(u - \bar{u}_i) + \bar{B}_{di}\left(\hat{d} - \bar{d}_i\right) + L_i(y - \bar{y}_i - \bar{C}_i(\hat{x} - \bar{x}_i))$$

where $\hat{x}$ and $\hat{d}$ are the estimated large-signal states and disturbance. Since the output matrix C in (1b) is constant, we have $\bar{y}_i = \bar{C}_i \bar{x}_i$ for all i, which reduces the large-signal state estimator to

$$\dot{\hat{x}} = \bar{A}_i \hat{x} + \bar{B}_i u + \bar{B}_{di} \hat{d} + L_i(y - \bar{C}_i \hat{x}) - \bar{A}_i \bar{x}_i - \bar{B}_i \bar{u}_i - \bar{B}_{di} \bar{d}_i$$

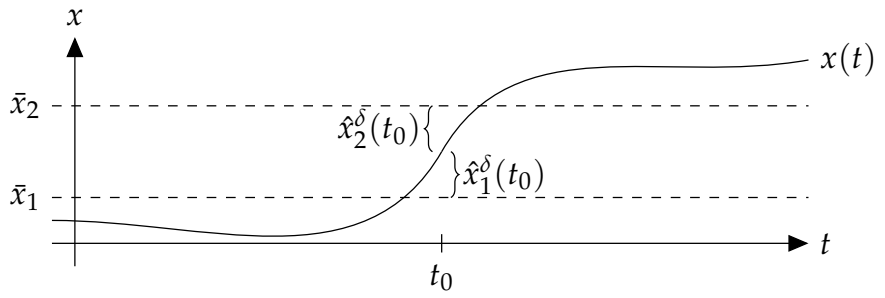

Fig. 7: Visualization of the relation between the large-signal value $x(t)$, the small-signal state estimates $\hat{x}_1^\delta(t)$ and $\hat{x}_2^\delta(t)$, and the operating point values $\bar{x}_1$ and $\bar{x}_2$ at a change of operating point at time t_0.

Let $e = x - \hat{x}$ denote the large-signal state estimation error with the dynamics given by

$$\begin{aligned}\dot{e} = \dot{x} - \dot{\hat{x}} &= \bar{A}_i(x - \bar{x}_i) + \bar{B}_i(u - \bar{u}_i) + \bar{B}_{di}\big(d - \bar{d}_i\big) \\ &\quad - \bar{A}_i(\hat{x} - \bar{x}_i) - \bar{B}_i(u - \bar{u}_i) - \bar{B}_{di}\Big(\hat{d} - \bar{d}_i\Big) - L_i(y - \bar{C}_i\hat{x}) \\ &= (\bar{A}_i - L_i\bar{C}_i)e + \bar{B}_{di}e_d \end{aligned} \tag{6}$$

which goes to zero, for constant i, if $\bar{A}_i - L_i\bar{C}_i$ is Hurwitz and the disturbance estimate error $e_d = d - \hat{d}$ goes to zero. The estimated disturbance $\hat{d}$, i.e., the estimated applied resistive load, is found from voltage and current measurements, which within measurement accuracy will equal the true value at all times, under the system and load assumptions made in [1], i.e., balanced system and purely resistive load. Hence, the disturbance estimate error will ideally equal zero at all times as well. From (6) it is clear that the estimator gains L_i govern the state estimation performance.

Subsequent to feedback design, one estimator gain L_i is determined for each of the five operating points. We design each L_i using the pole placement function $place()$ implemented in MATLAB, which is based on the algorithm in [20]. We choose the poles of $\bar{A}_i - L_i\bar{C}_i$ as five times the poles of the corresponding $\bar{A}_i - \bar{B}_iK_i$.

Using the large-signal state estimate for LQR state feedback, the large-signal control signal u is given by

$$u = -K_i\hat{x} + K_i\bar{x}_i + \bar{u}_i$$

4 Simulations

The method presented in Section 3, is evaluated using simulation in MATLAB Simulink®.

Using the identified parameters (2) for linearization, an LQR feedback K_i for each of the five operating points is found, as presented in Section 3.2, applying the diagonal weighting matrices

$$Q = \mathrm{diag}\big(\begin{bmatrix}10 & 1 & 1 & 1 & 1 & 1 & 1 & 6 & 1 & 1\end{bmatrix}\big)$$
$$R = \mathrm{diag}\big(\begin{bmatrix}10 & 10\end{bmatrix}\big)$$

which prioritize deviations in the states ω_m and v_{rms} and the control signals r_ω and r_v above all other signals.

The simulation is run as a series of load steps in increments of 10 kW from 10 to 50 kW, corresponding exactly to the operating points. For comparison, the simulation is also run without any supervisory regulator, i.e., with constant reference to the governor and AVR, and with a PID supervisory regulator, i.e., one PID regulator for the governor reference and one PID regulator for the AVR reference, hand-tuned to achieve comparable transient performance. We use the default continuous PID regulator block [21] of MATLAB Simulink® with parameters $P = 1$, $I = 0.01$, $D = 0.01$, and $N = 10$ for the governor supervision and $P = 0.5$, $I = 1$, $D = 0.01$, and $N = 10$ for the AVR supervision. In Figs. 8 and 9, the transients are shown, along with the respective references to the governor and AVR. The results demonstrate that the presented model-based approach can achieve highly acceptable transients throughout the operating range.

5 Conclusions

This paper presents a procedure for developing a self-tuning linear quadratic supervisory regulator using a large-signal state estimator for a diesel driven generator set utilizing a first principles-based nonlinear model detailed in [1]. The fundamentals of parameter identification and regulator design based on the LQR design method are described before reformulation of the classical small-signal Luenberger estimator to a large-signal estimator is presented.

The procedure is demonstrated using measurements from a real system for parameter identification. Simulation of the response to incremental load steps of the closed-loop system shows the usability of the presented procedure.

The choice of LQR as the regulator design method is not critical to the presented procedure. Any desirable regulation method can, after appropriate modifications, be applied. However, one advantage of the LQR design method demonstrated in the present work, for this particular system, is that we achieve highly acceptable transients throughout the operating range specifying only one set of Q and R weighting matrices, significantly reducing the time needed for regulator tuning during commissioning.

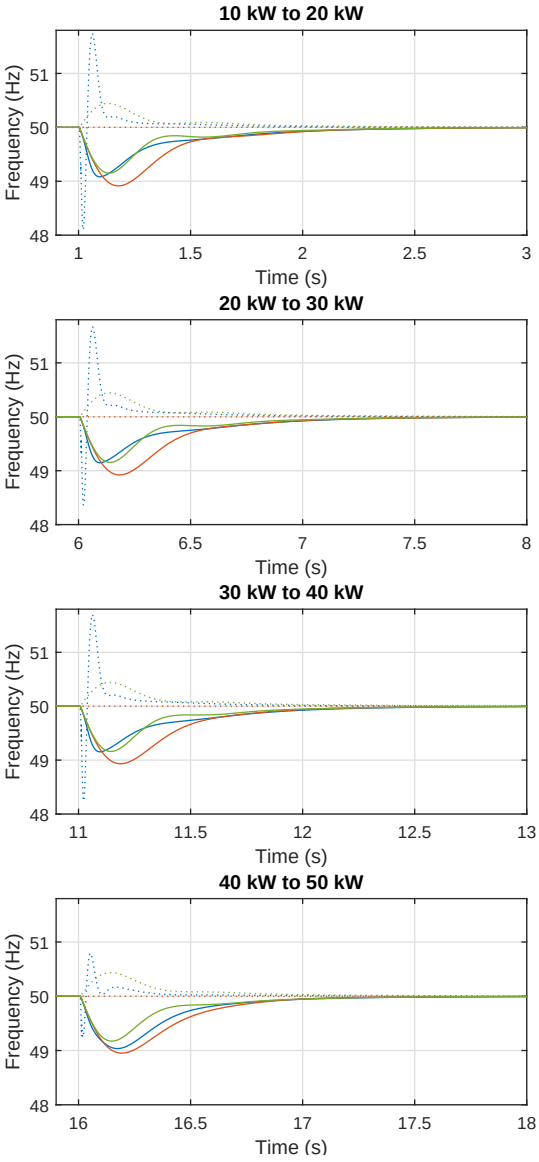

Fig. 8: Frequency transients following load-steps with the LQR (solid blue), the PID (solid green), and no (solid red) supervisory regulator and the corresponding applied references for the governor (dotted).

Future work on the presented procedure could include, e.g., (i) an analysis of the stability properties of the developed regulator, (ii) consideration of alternative, possibly nonlinear, large-signal estimator design methods, and (iii)

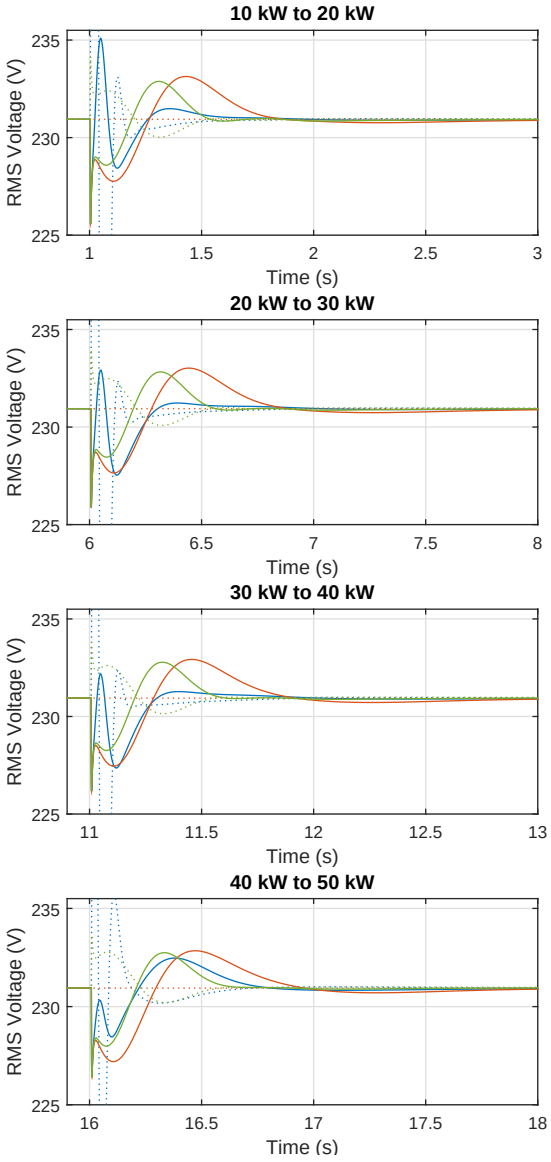

Fig. 9: Voltage transients following load-steps with the LQR (solid blue), the PID (solid green), and no (solid red) supervisory regulator and the corresponding applied references for the AVR (dotted).

implementation on a real system to validate the procedure and in extension, of course, the model.

References

[1] J. Knudsen, J. Bendtsen, P. Andersen, K. Madsen, and C. Sterregaard, "Control-oriented first principles-based model of a diesel generator," in *European Control Conference*, 2016, pp. 321–327.

[2] A. M. Annaswamy (Project Lead), "Vision for Smart Grid: 2030 and Beyond," M. Amin, C. DeMarco, and T. Samad, Eds. IEEE Standards Publication, 2013.

[3] T. Samad and S. Kiliccote, "Smart grid technologies and applications for the industrial sector," *Computers and Chemical Engineering*, vol. 47, pp. 76–84, 2012.

[4] G. Johnson, *Generator Sets Report*. Market Analysis, IHS Technology, 2014.

[5] J. Jiang, "Optimal Gain Scheduling Controller for a Diesel Engine," *IEEE Control Systems*, vol. 14, no. 4, pp. 42–48, 1994.

[6] M. Tuffaha and J. T. Gravdahl, "Modeling and Control of a Marine Diesel Engine driving a Synchronous machine and a Propeller," in *IEEE Conference on Control Applications (CCA)*, 2014, pp. 897–904.

[7] E. E. Ejegi, J. A. Rossiter, and P. Trodden, "A Survey of Techniques and Opportunities in Power System Automatic Generation Control," in *UKACC International Conference on Control*, 2014, pp. 537–542.

[8] H. Shayeghi, H. A. Shayanfar, and A. Jalili, "Load Frequency Control Strategies: A State-of-the-Art Survey for the Researcher," *Energy Conversion and Management*, vol. 50, no. 2, pp. 344–353, 2009.

[9] I. Ibraheem, P. Kumar, and D. P. Kothari, "Recent Philosophies of Automatic Generation Control Strategies in Power Systems," *IEEE Transactions on Power Systems*, vol. 20, no. 1, pp. 346–357, 2005.

[10] H. Rasmussen and J. Aagaard, "Distributed and Self-Tuning Control System for Diesel Generators," *IFAC Symposium on Low Cost Automation (LCA)*, pp. 223–228, 1992.

[11] K. Åström and B. Wittenmark, "On Self Tuning Regulators," *Automatica*, vol. 9, no. 2, pp. 185–199, 1973.

[12] H. Kwakernaak and R. Sivan, *Linear Optimal Control Systems*. Wiley & Sons, Inc., 1972.

[13] B. D. O. Anderson and J. B. Moore, *Optimal Control: Linear Quadratic Methods*. Prentice-Hall, Inc., 1989.

[14] P. Kundur, *Power System Stability and Control*. McGraw-Hill, Inc., 1994.

[15] R. H. Park, "Two-Reaction Theory of Synchronous Machines - Generalized Method of Analysis - Part I," *Journal of the American Institute of Electrical Engineers*, vol. 48, no. 3, pp. 716–727, 1929.

[16] K. Åström and B. Wittenmark, *Adaptive Control*. Addison-Wesley, 1989.

[17] M. Knudsen, "A Sensitivity Approach for Estimation of Physical Parameters," in *IFAC Symposium on System Identification*, vol. 2, 1994, pp. 231–236.

[18] D. G. Luenberger, "Observing the State of a Linear System," *IEEE Transactions on Military Electronics*, vol. 8, no. 2, pp. 74–80, 1964.

[19] ——, "Observers for Multivariable Systems," *IEEE Transactions on Automatic Control*, vol. 11, no. 2, pp. 190–197, 1966.

[20] J. Kautsky, N. K. Nichols, and P. Van Dooren, "Robust Pole Assignment in Linear State Feedback," *International Journal of Control*, vol. 41, no. 5, pp. 1129–1155, 1985.

[21] MathWorks, "PID Controller," 2016. [Online]. Available: http://se.mathworks.com/help/simulink/slref/pidcontroller.html

Paper C

Supervisory Control Implementation on Diesel-Driven Generator Sets

Jesper Knudsen, Jan Bendtsen, Palle Andersen, Kjeld Madsen, and Claes Sterregaard

The paper has been submitted for publication in the *IEEE Transactions on Industrial Electronics,* 2017.

Abstract

Diesel-driven generator sets (DGs) are widely utilized in distributed electrical power generation, due to their high reliability. This paper presents a tenth-order nonlinear state-space DG model, for which a supervisory Linear Quadratic Regulator is designed. The proposed model-based design reduces the time-consuming task of regulator tuning in comparison with current industry-standard solutions while demonstrating improved transient frequency and voltage performance, when subject to electrical load steps. These improvements are shown experimentally on two differently rated DGs.

1 Introduction

In distributed electrical power generation, diesel-driven generator sets (DGs) are important components in a large range of applications, an importance only expected to increase in the coming years [1]-[3]. One vital quality of DGs is their high reliability. Typical DG applications vary from single DG solutions up to hundred-plus DG plants. Single DGs often provide, e.g., backup power at hospitals, television and radio broadcast stations, data centers, and process control facilities, whereas DG plants provide, e.g., temporary power at sporting events, musical festivals, or in remote areas [4, 5].

DG manufacturers continuously work to improve operating efficiency, including maintenance costs; however, during commissioning, that responsibility lies with the commissioning engineers and the control units they are to make use of. Unfortunately, human involvement may often lead to suboptimal and/or inconsistent tuning and performance.

In many applications, DGs are equipped with a supervisory control unit, denoted the Automatic Genset Controller (AGC), adding capabilities such as synchronization, active and reactive power control, and automatic mains failure response. As shown in Fig. 1, two primary controllers are always present; the governor for engine control and the Automatic Voltage Regulator (AVR) for generator control [6]. The global market-leading manufacturers of AGC units all implement fundamentally equivalent regulation algorithms, based on classical proportional-integral-derivative (PID) regulators. Through many years of industrial use the PID regulator has proven its worth in terms of simplicity and reliability. A PID regulator is simple to implement, as it requires limited system information, and simple to adjust due to the straightforward interpretation of the regulation parameters. However simple, regulation parameter adjustments must be performed for each DG; a time-consuming task, which is critical to the performance.

Implementing a regulator that can reduce, or possibly remove, the need for time-consuming manual adjustments while keeping the commissioning

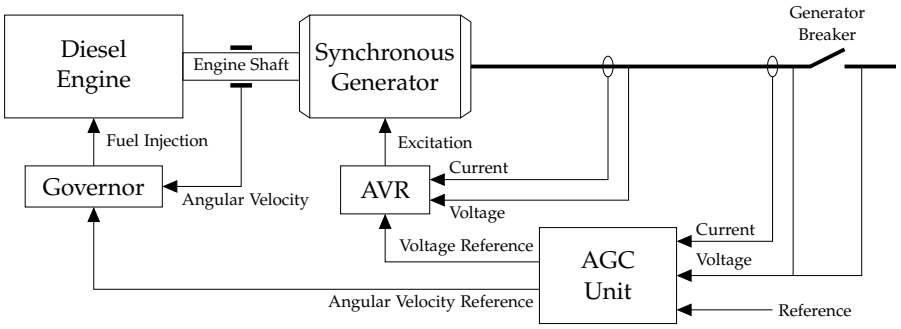

Fig. 1: DG control system with the fuel injection regulating governor, the excitation regulating AVR, and the supervisory AGC unit.

engineering interface simple, could aid in improving DG efficiency in terms of commissioning costs and possibly operational efficiency through automated adjustment procedures.

Control of diesel-driven generator sets, in various applications, has been presented in works such as [7]-[21]. However, the vast majority concerns control design for governor and/or AVR, individually or in combination. To the best of the authors' knowledge, only [20] presents work that relates directly to AGC design. However, applying constant-gain PI regulation as [20] on complex and highly nonlinear systems, such as DGs, will in many cases yield suboptimal performance.

In the present work, AGC regulator design for frequency and voltage stabilization of an islanded DG exposed to load changes is considered. Demonstrating implementation results of an AGC design on two differently rated DGs, this paper extends and enhances the work in [22, 23]. The implemented AGC design utilizes Linear Quadratic Regulator (LQR) feedback of estimated system states for a tenth-order nonlinear control-oriented first principles-based state-space DG model. Certain model parameter values can be derived directly from engine and generator datasheets, whereas others must be identified from measurement data. The model complexity is sufficient to describe the dynamical behavior of actual DGs, while remaining suitable for control design; as demonstrated by experimental results. The structure of LQRs enables incorporation of well-known cross dependencies between frequency and voltage, and generally exploiting system knowledge, in the control design, which is not common practice in PID implementations. Additionally, designing the control system for a set of operating points improves the ability to handle varying system dynamics throughout the operating range.

The remainder of the paper is organized as follows. Section 2 presents the DG model while Section 3 provides the AGC regulator design, which builds on the design presented in [23]. Section 4 introduces the utilized experimen-

tal setup while Section 5 presents the experimental results. Finally, Section 6 provides concluding remarks.

2 Diesel-Driven Generator Set Model

The explicit time dependency of variables is suppressed throughout the paper. Note that all variables, constants, etc., are assumed scalar and real unless stated otherwise.

2.1 Diesel Engine and Governor

In preparation for a generic LQR control design, the diesel engine model utilizes per unit values, in agreement with the synchronous generator model, such that all states of the model evolve within the same range. This entails utilizing a per unit swing equation to describe the rotary behavior of the synchronous machine given by

$$J\underline{\omega}_m\dot{\omega}_m = \underline{T}_m T_m - \underline{T}_e T_e - D\underline{\omega}_m\omega_m$$

where ω_m is the per unit angular velocity of the shaft, T_m and T_e are the per unit mechanical and electrical torques applied to the shaft, J and D are the total system inertia and damping, and $\underline{\omega}_m$, $\underline{T}_m$ and $\underline{T}_e$ are the mechanical angular velocity base, mechanical torque base, and electrical torque base, respectively. For clarity, these base values denote the nominal angular velocity of the crankshaft, the rated engine torque at rated angular velocity, and the rated electrical torque at rated voltage and frequency, respectively. Additionally, the dynamics of the per unit mechanical torque T_m delivered to the shaft by the diesel engine are given by

$$\dot{T}_m = \frac{1}{\tau_m(1+T_m)}(\mu - T_m)$$

where τ_m is the constant term of the engine time constant and μ is the per unit fuel injection requested by the governor. This first-order differential equation with a varying time constant is introduced to accommodate observations of increased retarding from the time between load impact to torque changes at increased torque levels.

A governor is included in the DG model as a PI regulator attempting to maintain nominal per unit angular velocity of the shaft ω_m; a control scheme referred to as isochronous mode. The governor control law is given by

$$\begin{aligned}\dot{e}_{i\omega} &= r_\omega + u_\omega - \omega_m \\ \mu &= k_{p\omega}(r_\omega + u_\omega - \omega_m) + k_{i\omega}e_{i\omega}\end{aligned}$$

where $e_{i\omega}$ is the governor integral error state, r_ω is the per unit angular velocity internal governor reference, which in isochronous mode remains at nominal value, u_ω is the per unit angular velocity reference offset, which is one control variable of the supervisory AGC, and $k_{p\omega}$ and $k_{i\omega}$ are the proportional and integral governor regulator gains.

2.2 Synchronous Generator and AVR

The synchronous generator model is expressed in per unit dq-components [24], with subscripts indicating the specific dq-component. The per unit flux linkages ψ and their associated per unit time derivatives $\dot{\psi}$ are given by [6]

$$\begin{aligned}
\psi_d &= -L_d i_d + L_{ad} i_f + L_{ad} i_{1d}, & \dot{\psi}_d &= v_d + \psi_q \omega_e + R_a i_d \\
\psi_q &= -L_q i_q + L_{aq} i_{1q}, & \dot{\psi}_q &= v_q - \psi_d \omega_e + R_a i_q \\
\psi_f &= L_{ff} i_f + L_{f1d} i_{1d} - L_{ad} i_d, & \dot{\psi}_f &= v_f - R_f i_f \\
\psi_{1d} &= L_{11d} i_{1d} + L_{f1d} i_f - L_{ad} i_d, & \dot{\psi}_{1d} &= -R_{1d} i_{1d} \\
\psi_{1q} &= L_{11q} i_{1q} - L_{aq} i_q, & \dot{\psi}_{1q} &= -R_{1q} i_{1q}
\end{aligned}$$

where i's are per unit generator currents, L's are per unit self and mutual inductances, R's are per unit resistances, ω_e is the per unit electrical angular velocity, which is assumed equal to ω_m, v_d and v_q are per unit terminal voltages, and v_f is the per unit field excitation voltage set by the AVR. The control law of the included AVR, modeled as a PI regulator, attempting to maintain nominal per unit three-phase phase-to-neutral RMS voltage v_{rms} is given by

$$\begin{aligned}
\dot{e}_{iv} &= r_v + u_v - v_{rms} \\
v_f &= k_{pv}(r_v + u_v - v_{rms}) + k_{iv} e_{iv}
\end{aligned}$$

where e_{iv} is the AVR integral error state, r_v is the per unit three-phase phase-to-neutral RMS internal AVR voltage reference, which in isochronous mode remains at nominal value, u_v is the per unit three-phase phase-to-neutral RMS voltage offset, which is the second control variable of the supervisory AGC, and k_{pv} and k_{iv} are the proportional and integral AVR regulator gains. Calculating RMS values are in practice based on measurements of the latest full period of the alternating signal. For balanced systems, this effectively amounts to a filtering of an instantaneous RMS value. This filtering is approximated as a first-order low-pass filter, providing

$$\dot{v}_{rms} = \frac{1}{\tau_v} \sqrt{\frac{1}{2}\left(v_d^2 + v_q^2\right)} - \frac{1}{\tau_v} v_{rms}$$

where τ_v is the filter time constant of twice the per unit time period of the nominal frequency.

2.3 Electrical Load

The dynamics of an islanded DG are significantly impacted by the connected electrical load. In preparation for applying LQR, the electrical load is modeled as a pure resistance. The terminal voltages are then given by

$$\begin{bmatrix} v_d \\ v_q \end{bmatrix} = R_L \Lambda \begin{bmatrix} \psi_d & \psi_q & \psi_f & \psi_{1d} & \psi_{1q} \end{bmatrix}^T \tag{1}$$

where R_L is the per unit per phase load resistance and the non-zero elements of $\Lambda \in \mathbb{R}^{2\times 5}$ contain inductances [6].

2.4 Complete State-Space Model

Putting the above together, a tenth-order nonlinear state-space model on the form

$$\begin{aligned} \dot{x} &= A(x_2)x + B_1 w + B_2 \sqrt{\frac{1}{2}(w_1^2 + w_2^2)} + B_3(x_2)(r+u) \\ &\quad + x_1 F_1 x + x_3 F_3 x + x_4 F_4 x \\ y &= Cx \end{aligned}$$

is obtained, where x, w, r, u, and y are the state, terminal voltage, internal reference, supervisory control variable, and output vectors, respectively, given by

$$\begin{aligned} x &= \begin{bmatrix} \omega_m & T_m & \psi_d & \psi_q & \psi_f & \psi_{1d} & \psi_{1q} & e_{i\omega} & e_{iv} & v_{rms} \end{bmatrix}^T \\ w &= \begin{bmatrix} v_d & v_q \end{bmatrix}^T, \quad r = \begin{bmatrix} r_\omega & r_v \end{bmatrix}^T \\ u &= \begin{bmatrix} u_\omega & u_v \end{bmatrix}^T, \quad y = \begin{bmatrix} \omega_m & v_{rms} \end{bmatrix}^T \end{aligned}$$

and the matrices $A(x_2) \in \mathbb{R}^{10\times 10}$, $B_1 \in \mathbb{R}^{10\times 2}$, $B_2 \in \mathbb{R}^{10\times 1}$, $B_3(x_2) \in \mathbb{R}^{10\times 2}$, $C \in \mathbb{R}^{2\times 10}$, $F_1 \in \mathbb{R}^{10\times 10}$, $F_3 \in \mathbb{R}^{10\times 10}$, and $F_4 \in \mathbb{R}^{10\times 10}$ follow from the introduced relations.

Datasheet values are utilized for parameters concerning the system inertia, the torque bases, the armature resistance of the generator stator, and the self and mutual stator inductances. Alternatively, the system damping is determined in accordance with [22], while the generator rotor parameters are chosen to match the per unit values of the 'Synchronous Machine Salient Pole (fundamental)' block [25] from the Simscape Power Systems toolbox of MATLAB Simulink®, which are based on models described in [6, 26]. In general, parameters related to the rotor cannot be assumed available, since the standards applicable to the test procedures relevant for determining datasheet content do not include methods for determining all those parameters [27, 28]. Datasheets [29, 30] represent typical datasheets with the amount of content

that can be assumed available. Finally, τ_m, $k_{p\omega}$, $k_{i\omega}$, k_{pv}, and k_{iv} must be found based on system measurements using a parameter identification method. In the present work, the parameters were determined without much effort through trail and error; however, a more sophisticated approach would be beneficial for future implementations.

3 Automatic Genset Controller Design

Applying the traditional LQR method requires a linear model of the system and internal state information, which is not immediately measurable in typical DG systems. Thus, model linearization and state estimation is required before such a regulation scheme can be employed.

3.1 Model Linearization

The nonlinear DG model is linearized using first-order Taylor series expansion, treating R_L as a disturbance input rather than v_d and v_q, following the relation given by (1). Additionally, R_L is chosen as the variable that determines the active operating point; its value is found utilizing voltage and current measurements and will therefore at all times equal the true load resistance (within measurement accuracies) assuming a balanced three-phase load. The set of operating points is selected for a specific DG as detailed in Section 5. Derivations of the linear models are presented in [23].

3.2 Large-Signal State Estimation

In an effort to circumvent potential issues related to state discontinuities of classical Luenberger small-signal state estimators [31], a large-signal state estimator, as formulated in [23], is utilized. In the present work, the operating point values of the control variables u are at all times zero, because they represent offsets. The large-signal state estimator is given by

$$\dot{\hat{x}} = \bar{A}_i\hat{x} + \bar{B}_i u + \bar{B}_{di}\hat{d} + L_i(y - \bar{C}_i\hat{x}) - \bar{A}_i\bar{x}_i - \bar{B}_{di}\bar{d}_i$$

where $\hat{x}$ is the estimated large-signal per unit states, $\hat{d}$ is the estimated electrical load given by the calculated R_L, $\hat{y}$ is the estimated large-signal per unit output, L_i is the estimator gain matrix of the i-th operating point, $\bar{x}_i$ and $\bar{d}_i$ are the operating point values of the estimated states and electrical load for the i-th operating point, matrices $\bar{A}_i \in \mathbb{R}^{10\times10}$, $\bar{B}_i \in \mathbb{R}^{10\times2}$, $\bar{B}_{di} \in \mathbb{R}^{10\times1}$, and $\bar{C}_i \in \mathbb{R}^{2\times10}$ are the linearized system matrices of the i-th operating point, found according to the procedure shown in [23], and $i \in \{1, \ldots, n_{op}\}$ where n_{op} is the number of operating points for the specific DG.

3.3 Linear Quadratic Regulator

The theory of LQR state feedback is thoroughly described in literature and will, due to space considerations, not be presented here; instead, the reader is referred to [32, 33] for details. The AGC control law with state feedback of the large-signal estimated states $\hat{x}$ through the LQR state feedback matrix K_i of the i-th operating point is given by

$$u = -K_i\hat{x} + K_i\bar{x}_i, \qquad i \in \{1, \ldots, n_{op}\}$$

where the second term is included to accommodate the use of a large-signal state estimator.

The complete closed-loop AGC regulator design is shown in Fig. 2, where d is electrical load connected to the DG. Switching of i is implemented unfiltered; that is, without guarantees on, e.g., average dwell-time [34], which is very likely to be relevant in other implementations.

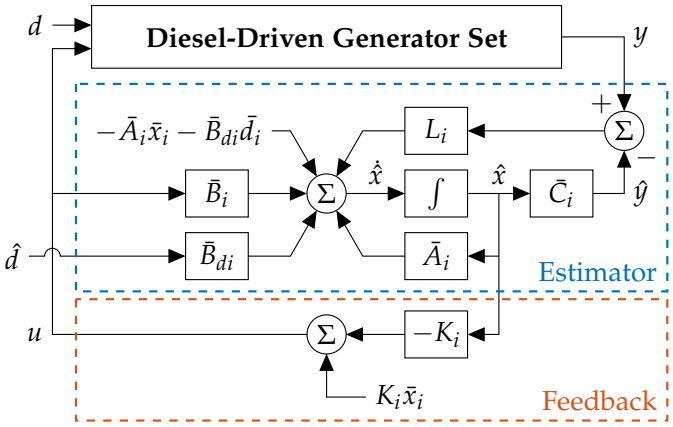

Fig. 2: Closed-loop AGC regulator design diagram, including large-signal state estimator and LQR state feedback. Note, all operating point discontinuities have been moved in front of the integration by the reformulation to a large-signal state estimator.

4 Experimental Setup

In this section, the physical setup used for model validation and to obtain the following implementation results is presented in detail. The experimental setup is located in a test room at the headquarters of DEIF in Skive, Denmark. The relevant elements and their interconnections are shown in Fig. 3 as a single-line diagram. Denoted DG 1, a 60 kVA DG, connects through Generator Breaker 1 to the load bank at the busbar. Denoted DG 2, a 40 kVA kW DG, similarly, connects through Generator Breaker 2 to the load bank at

the busbar. As the proposed regulator does not include synchronization and load-sharing capabilities, the two generator breakers are never closed at the same time while the proposed regulator is active.

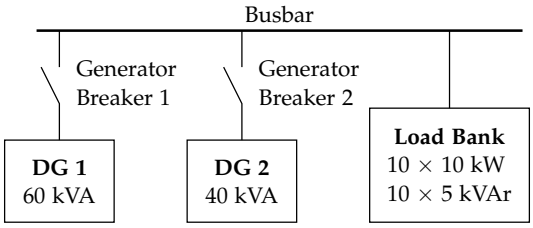

Fig. 3: Single-line diagram of the laboratory facilities, consisting of two diesel-driven generator sets connected through individual generator breakers to the load bank at the busbar.

DG 1 is made up of a turbocharged, four-stroke, four-cylinder Deutz BF4M2012 diesel engine and a salient four-pole, three-phase, brushless, synchronous, 60 kVA/48 kW at 50 Hz Leroy-Somer LSA 42.3 L9 C6/4 generator. The engine is controlled by a Deutz EMR 2 governor and the generator is controlled by a DEIF DVC310 AVR, with both the governor and the AVR set to run in isochronous regulation mode.

DG 2 consists of a turbocharged, four-stroke, four-cylinder Deutz BF4M-1011F diesel engine and a salient four-pole, three-phase, brushless, synchronous, 40 kVA/32 kW at 50 Hz Mecc Alte Spa ECO 32-3S/4 generator. The engine is controlled by a Huegli Tech HT-SG-100 governor while the generator is controlled by a DEIF DVC310 AVR; both operating in isochronous regulation mode.

The load bank is a system of active and reactive load elements, which can be connected in parallel. The load elements enable an applied active load from 0 to 100 kW in steps of 10 kW and reactive load from 0 to 50 kVAr in steps of 5 kVAr.

The proposed AGC regulator design is applied to the DG through a Rapid Control Prototyping (RCP) system based on a dSPACE DS1103-07 400 MHz PPC controller board [35]. The system has access to the frequency, which is obtained through a magnetic pick-up on the engine shaft, and all the three phase voltages and currents. The RCP is executed at a 10 kHz base frequency with measurement intervals determined by the rotational speed of the engine shaft to provide 16 samples per period. The control signal from the proposed regulator to the governor and AVR is sent as a 40 ms Controller Area Network (CAN) J1939 message, resembling a typical communication speed and protocol of industrial AGC units.

Measurements presented in Section 5 are collected using a HIOKI Memory HiCorder 8861 with High Resolution Unit 8957 input modules. All measurements from the HIOKI data collection system are taken at a 50 kHz sam-

pling rate.

5 Experimental Results

This section presents experimental results obtained implementing the proposed AGC LQR design; both on DG 1 and DG 2, to demonstrate the applicability of the design.

As DG 1 and DG 2 are given by different sets of model parameters, unique regulator and estimator gains have been calculated for every operating point of each DG. However, all those gains have been calculated using similar tuning parameter values. That is, the LQR feedback gain matrices K_i for all operating points i have been found by applying the diagonal weighting matrices

$$Q = \text{diag}\big(\begin{bmatrix}25 & 1 & 1 & 1 & 1 & 1 & 1 & 1 & 1 & 1\end{bmatrix}\big) \tag{2a}$$

$$R = \rho I_{2\times 2} \tag{2b}$$

which penalize deviations in the per unit mechanical angular velocity ω_m and, for $\rho > 1$, the two inputs higher than deviations in the remaining states. Further, calculation of the large-signal state estimator gain matrices L_i for all operating points i for both DGs has been done identically. That is, using MATLAB's implementation of the robust pole assignment algorithm presented in [36], i.e., the function `place()`, the poles of each $\bar{A}_i - L_i\bar{C}_i$ are placed at the values given by the multiplication of three with the pole values of the corresponding $\bar{A}_i - \bar{B}_i K_i$.

The operating point sets for DG 1 and DG 2 are chosen to coincide with the available resistive load elements, accommodating the rating of each DG. That is, the operating points for DG 1 are 10, 20, 30, 40, and 50 kW, while for DG 2 the operating points are 10, 20, and 30 kW.

The frequency and voltage transients in response to steps in active load are shown in Figs. 4 and 5 for DG 1 with $\rho = 200$. In these figures, measurements of an open-loop implementation, i.e., constant nominal references with no offset for the governor and AVR, and of an industry-standard PID regulator AGC implementation is provided for comparison.

In general, an improvement in transient response on the open-loop implementation is observed for the LQR implementation in both frequency and voltage on DG 1 with less overshoot and shorter settling times. Note that the PID implementation, according to most performance criteria, delivers worse transient responses than both the LQR and the open-loop implementations. However, the integral action of the PID regulator means the PID implementation is the only implementation able to sustain nominal frequency and voltage in any feasible steady-state condition; implying that the integral action of the governor and AVR is, in practice, insufficient.

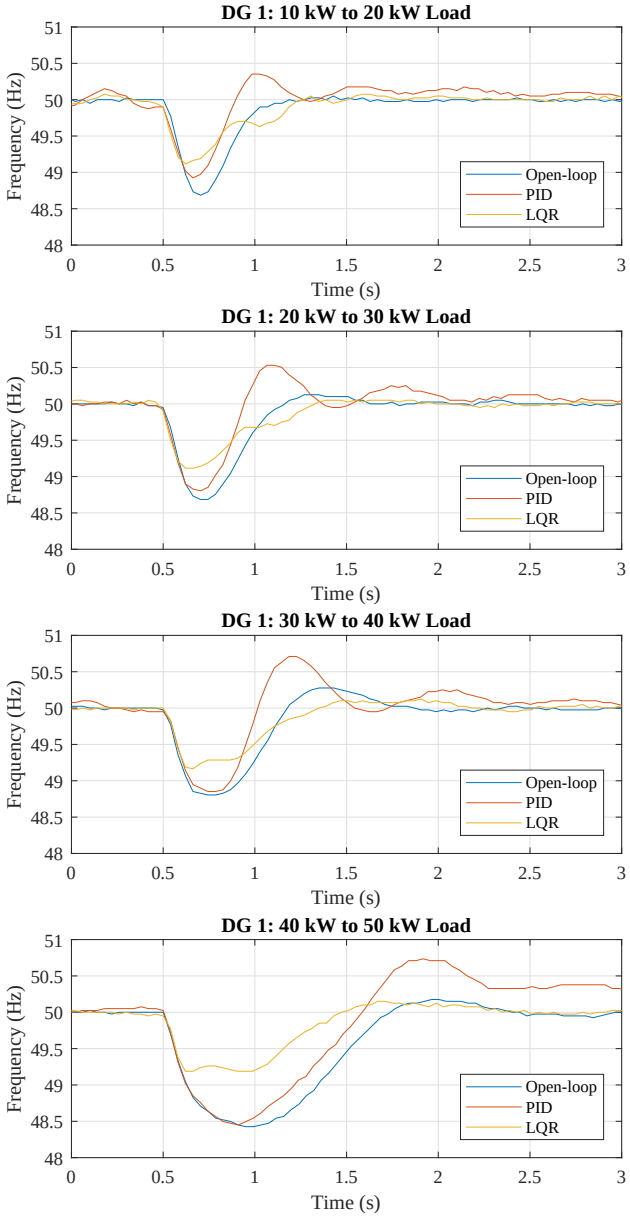

Fig. 4: Frequency transients following steps in active load with industry-standard PID, the proposed LQR, and no supervisory controller on the 60 kVA DG 1 with isochronous governor and AVR.

An additional objective of the proposed supervisory controller is to reduce tuning complexity. As demonstrated in Figs. 6 and 7, this is accom-

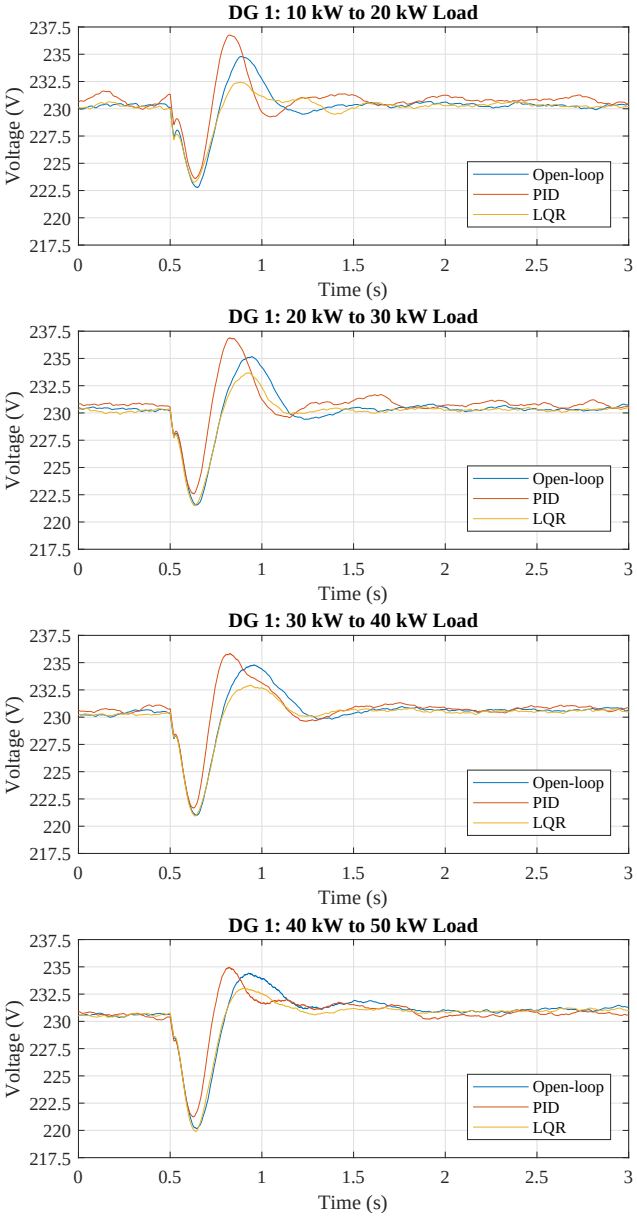

Fig. 5: Voltage transients following steps in active load with industry-standard PID, the proposed LQR, and no supervisory controller on the 60 kVA DG 1 with isochronous governor and AVR.

plished through one intuitive tuning handle; the parameter ρ in (2b). Alterations of R entail different deviation penalties on the inputs, which lead to

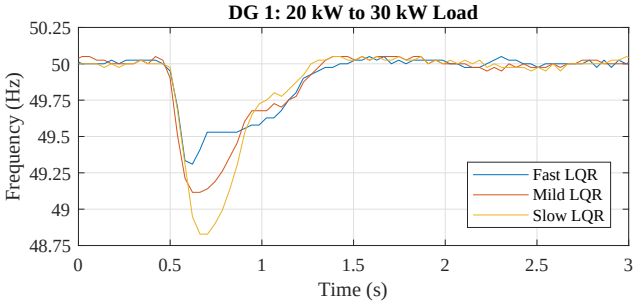

Fig. 6: Frequency transients following steps in active load using the proposed supervisory LQR design with Fast ($\rho = 100$), Mild ($\rho = 200$), and Slow ($\rho = 300$) tuning on the 60 kVA DG 1.

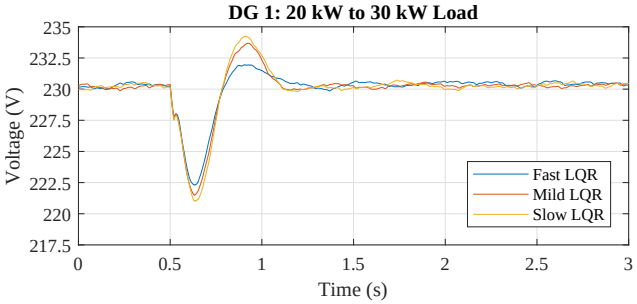

Fig. 7: Voltage transients following steps in active load using the proposed supervisory LQR design with Fast ($\rho = 100$), Mild ($\rho = 200$), and Slow ($\rho = 300$) tuning on the 60 kVA DG 1.

increased or reduced regulator activity. Utilizing $\rho = 100$ yields a more aggressive regulation, referred to as Fast LQR in Figs. 6 and 7. Using $\rho = 200$ obtains the regulation performance presented previously in Figs. 4 and 5, now referred to as Mild LQR. Finally, $\rho = 300$ yields the regulation referred to as Slow LQR in Figs. 6 and 7, which in general approaches the regulation performance of the open-loop implementation. Although demonstrated here only on DG 1, due to space considerations, the procedure has been applied equally successfully on DG 2 using a similar range of ρ.

As a part of the modeling and linearization approach presented in Sections 2.3 and 3.1, the effects of any non-resistive electrical load elements has been neglected. In an effort to challenge this approach, DG 2 has also been exposed to steps in apparent power, i.e., simultaneous steps in active and reactive load. Figs. 8 and 9 present the obtained frequency and voltage transients with the same LQR implementation for steps in load of active power and apparent power. The extraordinary initial drop in voltage for steps in apparent power is similar to the drops obtained with the industry-standard PID and open-loop implementations. These results clearly demonstrate the

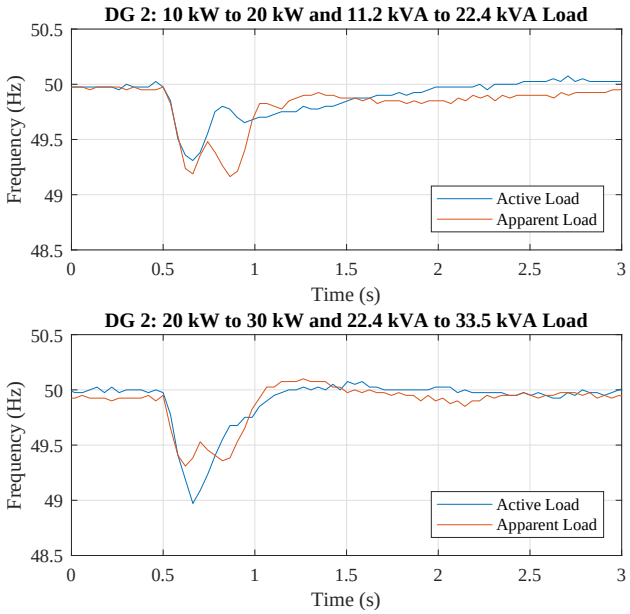

Fig. 8: Frequency transients following simultaneous steps in both active and reactive load elements with industry-standard PID, the proposed LQR, and no supervisory controller on the 40 kVA DG 2 with isochronous governor and AVR.

applicability of the proposed supervisory controller on differently rated DGs and during alternative load conditions not included in the model.

The final remarks on the results concern the complexity of DGs. The nature of DG 2, with all its components, is one that dictates a rather conservative regulation, something even a highly experienced commissioning engineer cannot know a priori, whereas DG 1 is more lenient towards aggressive regulation. Such observations encourage a self-tuning scheme that sets off from a conservative starting point. Lastly, comparing the open-loop measurements of Figs. 4 and 5 with the open-loop measurements presented from DG 1 in [22], a significant difference in the time it takes to return to nominal frequency following the step from 40 kW to 50 kW is noted. Possibly owing to general engine wear and tear, such variations in dynamic behavior occur frequently in real-life systems and must be anticipated. The current approach, evidently, has a certain robustness against this degree of parameter variation, since no adjustments were made to accommodate it. That is, the parameter identification was completed using the measurements in [22], while for the control design experiments presented here, which were carried out at a later point in time, the system exhibits different dynamics.

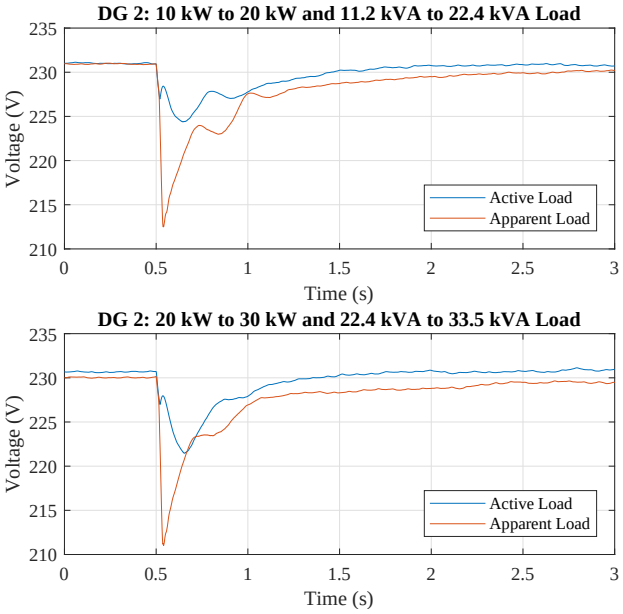

Fig. 9: Voltage transients following simultaneous steps in both active and reactive load elements with industry-standard PID, the proposed LQR, and no supervisory controller on the 40 kVA DG 2 with isochronous governor and AVR.

6 Conclusion

The model-based supervisory AGC design developed and experimentally demonstrated in this paper, shows promising features in terms of achieving improvements to the current industry-standard solutions. As shown in Section 5, replacing the current PID-based design with an LQR-based design can offer a simpler regulator tuning interface for commissioning engineers in addition to obtaining improved transient performance following changes of supplied electrical load.

Through the generic nature of the model and control design, the proposed supervisory control approach facilitates a self-tuning implementation; thus, designing a reliable automated parameter identification method would be a natural next step in any future development. Additional future work could include an investigation of, e.g., feedback linearization or genuine nonlinear control algorithms, in an attempt to remove the need for operating point specifications and calculations.

References

[1] G. Johnson, *Generator Sets Report*. Market Analysis, IHS Technology, 2014.

[2] ——, "Short-term headwinds, long-term growth for generator sets market," 2016. [Online]. Available: https://technology.ihs.com/582961/short-term-headwinds-long-term-growth-for-generator-sets-market

[3] Mordor Intelligence, *Global Diesel Generator Market - Analysis by Deployment Location - Growth Trends and Forecasts (2016 - 2021)*. Market Analysis, 2016.

[4] DEIF, *Land Power Application Guide*, 2016.

[5] ——, *Marine & Offshore Application Guide*, 2016.

[6] P. Kundur, *Power System Stability and Control*. McGraw-Hill, Inc., 1994.

[7] S. Roy, O. Malik, and G. Hope, "An adaptive control scheme for speed control of diesel driven power-plants," *IEEE Transactions on Energy Conversion*, vol. 6, no. 4, pp. 605–611, 1991.

[8] L. Guzzella and A. Amstutz, "Control of diesel engines," *IEEE Control Systems Magazine*, vol. 18, no. 5, pp. 53–71, 1998.

[9] K. B. Goh, S. K. Spurgeon, and N. Barrie Jones, "Higher-order sliding mode control of a diesel generator set," *Institution of Mechanical Engineers. Part I: Journal of Systems and Control Engineering*, vol. 217, no. 3, pp. 229–241, 2003.

[10] D. McGowan, D. Morrow, and M. McArdle, "A digital PID speed controller for a diesel generating set," in *IEEE Power Engineering Society General Meeting*, vol. 3, 2003, pp. 1472–1477.

[11] D. McGowan, D. Morrow, and B. Fox, "Integrated governor control for a diesel-generating set," *IEEE Transactions on Energy Conversion*, vol. 21, no. 2, pp. 476–483, 2006.

[12] R. J. Best, D. J. Morrow, D. J. McGowan, and P. A. Crossley, "Synchronous islanded operation of a diesel generator," *IEEE Transactions on Power Systems*, vol. 22, no. 4, pp. 2170–2176, 2007.

[13] D. McGowan, D. Morrow, and B. Fox, "Multiple input governor control for a diesel generating set," *IEEE Transactions on Energy Conversion*, vol. 23, no. 3, pp. 851–859, 2008.

[14] A. M. Kassem and A. M. Yousef, "Robust control of an isolated hybrid wind-diesel power system using Linear Quadratic Gaussian approach," *International Journal of Electrical Power and Energy Systems*, vol. 33, pp. 1092–1100, 2011.

[15] J. Mamboundou and N. Langlois, "Application of indirect adaptive model predictive control supervised by fuzzy logic to a diesel generator," in *IEEE International Conference on Control and Automation (ICCA)*, 2011, pp. 1037–1043.

[16] G. Zhang, "Marine diesel-generator excitation controller based on adaptive on-line GA tuning PID," in *Chinese Control Conference*, 2011, pp. 3868–3871.

[17] A. Cooper, D. McGowan, D. Morrow, and K. Chambers, "Temperature-dependant voltage regulator operation for optimal load acceptance of a diesel generator," *IET Electric Power Applications*, vol. 6, no. 8, pp. 553–560, 2012.

[18] M. Tuffaha and J. T. Gravdahl, "Modeling and Control of a Marine Diesel Engine driving a Synchronous machine and a Propeller," in *IEEE Conference on Control Applications (CCA)*, 2014, pp. 897–904.

[19] M. Guermouche, S. Ali, and N. Langlois, "Sliding Mode Control for Diesel Generator via Disturbance Observer," in *Mediterranean Conference on Control and Automation (MED)*, 2015, pp. 487–494.

[20] H. Hilal, M. Oktaufik, A. Prastawa, B. Prasetyo, and R. Hutahaean, "Smart diesel generator to compensate on-grid PV fluctuation: A case study in Sumba Island Indonesia," in *Conference on Power Engineering and Renewable Energy (ICPERE)*, 2016, pp. 33–37.

[21] T. Broomhead, C. Manzie, P. Hield, R. Shekhar, and M. Brear, "Economic model predictive control and applications for diesel generators," *IEEE Transactions on Control Systems Technology*, vol. 25, no. 2, pp. 388–400, 2017.

[22] J. Knudsen, J. Bendtsen, P. Andersen, K. Madsen, and C. Sterregaard, "Control-oriented first principles-based model of a diesel generator," in *European Control Conference*, 2016, pp. 321–327.

[23] J. Knudsen, J. Bendtsen, P. Andersen, and K. Madsen, "Self-tuning linear quadratic supervisory regulation of a diesel generator using large-signal state estimation," in *Australian Control Conference*, 2016, pp. 32–37.

[24] R. H. Park, "Two-Reaction Theory of Synchronous Machines - Generalized Method of Analysis - Part I," *Journal of the American Institute of Electrical Engineers*, vol. 48, no. 3, pp. 716–727, 1929.

[25] MathWorks, "Simscape Power Systems," 2017. [Online]. Available: https://se.mathworks.com/products/simpower.html

[26] S. E. Lyshevski, *Electromechanical Systems, Electric Machines, and Applied Mechatronics*. CRC Press, 1999.

[27] IEEE Power Engineering Society, "IEEE Guide: Test Procedures for Synchronous Machines," *IEEE Std 115-1983 (Revision of IEEE Std 115-1965)*, p. 87, 1983.

[28] ——, "IEEE Guide for Test Procedures for Synchronous Machines," *IEEE Std 115-2009 (Revision of IEEE Std 115-1995)*, p. 207, 2010.

[29] Mecc Alte, *Generator Type ECO 32-3S/4*. Datasheet, 2012.

[30] Leroy-Somer, *Low Voltage Alternators - 4 pole*. Datasheet, 2015.

[31] D. G. Luenberger, "Observers for Multivariable Systems," *IEEE Transactions on Automatic Control*, vol. 11, no. 2, pp. 190–197, 1966.

[32] B. D. O. Anderson and J. B. Moore, *Optimal Control: Linear Quadratic Methods*. Prentice-Hall, Inc., 1989.

[33] S. Skogestad and I. Postlethwaite, *Multivariable Feedback Control*. John Wiley & Sons, Inc., 1996.

[34] J. Hespanha and A. Morse, "Stability of Switched Systems with Average Dwell-Time," in *IEEE Conference on Decision and Control*, vol. 3, 1999, pp. 2655–2660.

[35] DSPACE, "DS1103," 2015. [Online]. Available: https://www.dspace.com/en/inc/home/support/pli/elas/elads1103.cfm

[36] J. Kautsky, N. K. Nichols, and P. Van Dooren, "Robust Pole Assignment in Linear State Feedback," *International Journal of Control*, vol. 41, no. 5, pp. 1129–1155, 1985.

Paper D

Fuel Optimization in Multiple Diesel Driven Generator Power Plants

Jesper Knudsen, Jan Bendtsen, Palle Andersen, Kjeld Madsen,
Claes Sterregaard, and Anthony Rossiter

The paper has been published in the
Proceedings of the IEEE Conference on Control Technology and Applications,
pp. 493–498, 2017.

The layout has been revised.

Abstract

This paper presents two fuel optimization approaches for independent power producer (IPP) power plants consisting of multiple diesel driven generator sets (DGs). The optimization approaches utilize assumed information about the fuel consumption characteristics of each DG in an effort to demonstrate the potential benefits of acquiring such information. Reasonable variations in fuel consumption characteristics are based on measurements of a DG during restricted air filter flow operation. The two approaches are: (i) a gradient search approach capable of finding the optimal power generation for each DG in a fixed selection of DGs accommodating a given plant power reference and (ii) a genetic algorithm approach further capable of determining the optimal selection of DGs to operate in an IPP power plant. Both approaches show notable potential benefits, in terms of fuel savings, compared to current market-leading solutions.

1 Introduction

Independent power producers (IPPs), supplying electric power under power purchase agreements (PPAs), have become integral parts of electric infrastructures worldwide due to ongoing deregulation. Whether providing temporary supply during, for example, musical festivals or sporting events, adding additional capacity in periodically overloaded grids, known as peak shaving, or establishing the main supply in an area without grid connection, IPP power plants must be highly reliable and flexible and provide a stable supply. Consequently, diesel driven generator sets (DGs) are widely used as the source of electric power generation by IPPs, providing the necessary overall plant capacity through a number of DGs [1, 2, 3, 4].

Under a PPA, an IPP has direct financial interest in maximizing the efficiency of its power plants as the payments relate to the delivered electric power. Therefore, successful IPPs maintain timely service of their DGs during plant operation. However, several elements affecting the efficiency of each individual DG are not handled by strict attention to service intervals. One such element is the ambient temperature, which may vary significantly across the area occupied by an entire power plant due to conditions like shade, wind direction or adjacent DGs. Besides influencing the quality of the combustion through the intake air temperature, power is also consumed by the cooling system of DGs. Cooling systems for power plant DGs often use electrically driven cooling fans as they offer higher flexibility in system design than belt driven fans. Electronic cooling systems often use around two to three percent of the rated power output, effectively reducing the DG efficiency [5, 6, 7]. If the cooling systems run constantly at maximum capacity, any efficiency optimization in that regard is inherently meaningless, whereas

regulated cooling systems will benefit from further efficiency optimization given ambient temperature differences across the plant.

Another element potentially affecting the efficiency of individual DGs across a power plant is the condition of air filters. Dust in the air caught by the filter builds up, eventually, clogging the filter which limits the air intake, causing decreased fuel efficiency of the diesel engine. This effect is confirmed in Section 3 by an experimental demonstration. Air filters are replaced or cleaned only as part of a routine service and according to the pressure drop across the filter. However, unless continuously monitored, clogging of air filters may occur suddenly, and unnoticed, due to, for example, a wind gust blowing sand onto a group of DGs in one area of the plant. Knowledge of such conditions could be used to optimize the efficiency by automatically redistributing the power demands for the DGs in the plant, until the filters can be replaced by a service engineer.

Current market-leading plant controller solutions have a user-specified power generation level for optimum fuel efficiency [8]. Assuming this specified level is valid, its usefulness is limited as it contains no information regarding the actual efficiency at that, or any other, power level. In an IPP power plant, the DGs are for practical reasons most often of the same make, type, and power rating which in turn implies that the user-specified power level for optimum fuel efficiency will be identical for all DGs in the plant. Therefore, each DG is indistinguishable from the next in a fuel optimization context. Thus, use of this value is rare. Instead, the number of operational DGs in a power plant is most often determined in order to guarantee a minimum of spinning reserve, to be able to cope with sudden unexpected load changes. In other words, more information would be needed for a plant-wide fuel optimization. Uncovering the potential benefit would allow IPPs or DG manufacturers to perform a cost-benefit analysis of the investment associated with the acquisition of additional information, e.g., installing additional sensors or developing identification methods.

Previous work on the area of DG plant optimization is surprisingly limited; however, similarities can be found in the area of wind farm control, see for example [9]. Within wind farm control many control approaches as well as modeling methods which could prove relevant for DG plant optimization have been investigated; this is demonstrated briefly by the following few examples. In [10], the authors present a fault tolerant wind farm controller whereas the authors of [11, 12, 13, 14] present various generation control approaches based on interior point, game theoretic, Bayesian ascent, and model predictive control methods, respectively.

In this paper, we propose two fuel optimization approaches for IPP power plants based on an assumed knowledge of the individual efficiency characteristics of each DG. The first approach uses a simple gradient search to determine the momentary optimal power distribution between a fixed selection

of DGs for a given plant power reference. The second approach is a genetic algorithm (GA) further able to determine the optimal choice of DGs to utilize in situations where the plant conditions, including the plant power reference, do not dictate a fixed selection of DGs in the plant.

The remainder of the paper is organized as follows. Section 2 briefly introduces the structure of IPP power plants and a sufficient, simple representation of individual DG fuel characteristics. In Section 3, experiments are conducted to acquire actual information regarding fuel efficiency changes caused by critical air filter conditions. Section 4 presents the two fuel optimization approaches, while Section 5 provides concluding remarks.

2 IPP Power Plants

Introducing the general structure of an IPP power plant, this section presents plant-wide efficiency considerations suggesting a rather simple efficiency representation for each individual DG in a plant.

2.1 Power Plant Structure

Generally, IPP power plants are structured such that DGs are arranged in so-called branches, connecting through circuit breakers and a power transformer to the grid. As illustrated in Fig. 1, with a four-branch example, power transformers can also be present in the branches, either at each DG or for a group of DGs, to increase the voltage and, thereby, reduce cable losses due to the lowered current level.

For a specific power plant, the use of power transformers will typically be identical in each branch. Further, for practical reasons, the branch power transformers will most often also be of the same make, type, and power rating. Depending on the application of the power plant, there might be more than one connection to the grid, or none at all. The power plant might simply supply the load directly, or in combination with delivering power to the grid.

2.2 Efficiency Representation

Looking at the fuel efficiency of each DG in an IPP power plant, a few reasonable assumptions allow a rather simple individual DG fuel efficiency representation.

Any loss inside the power plant is a direct financial cost to the IPP, hence, measures are taken to minimize those losses. Such measures include connecting DGs to nearby power transformers and using cable of sufficient rating and quality. Consequently, cable losses inside the power plant are very

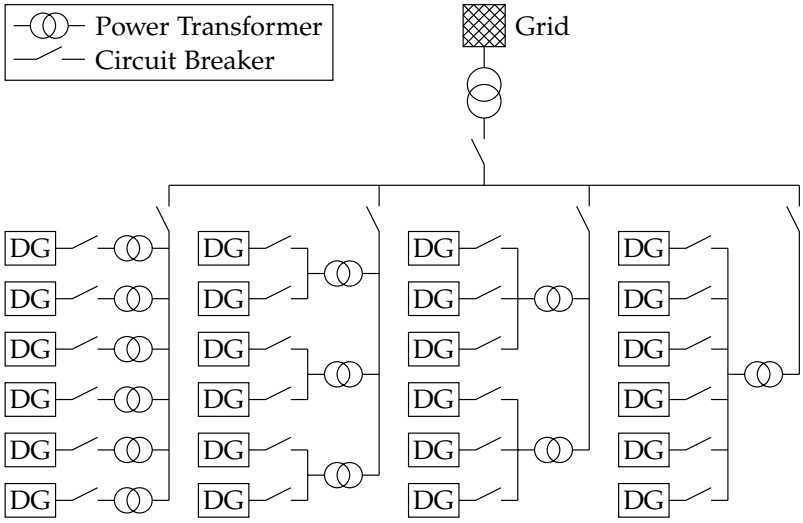

Fig. 1: Example diagram of an IPP power plant with four branches utilizing different branch constructions, in terms of transformer placement [1].

small and the difference in losses from one DG to another is negligible. Further, since all power transformers in the branches are in principle identical, the transformer efficiencies can be neglected in the context of plant-wide fuel optimization.

Following the above assumptions, each DG in the power plant can be represented simply by its individual fuel efficiency characteristics. A DG consists of a diesel engine and a synchronous generator. The efficiency of a generator is, for the purpose of this work, constant when avoiding operation at very low loads [15], leaving the engine as the dominant element in representation of efficiency characteristics.

Data sheets for DG engines provide sparse information about fuel consumption, typically, at three or four different generation levels, e.g., 25%, 50%, 75%, and 100% of rated generation. Fig. 2 presents data sheet fuel consumption information of four differently rated DG engines [16, 17, 5, 18]. Additionally, for each engine a least-square fit 2^{nd} degree polynomial obtained with the MATLAB® function `polyfit()` is shown. The 2^{nd} degree polynomials inherently match the data sheet information with only three values perfectly, whereas for data sheet information with four values small deviations between the polynomial and the values occur. However, in this work, 2^{nd} degree polynomials are considered sufficient fits to represent fuel consumption of each DG in a plant. Note, partly due to low efficiency, DGs in an IPP power plant generally never operate at power generation levels below 20% of rated generation.

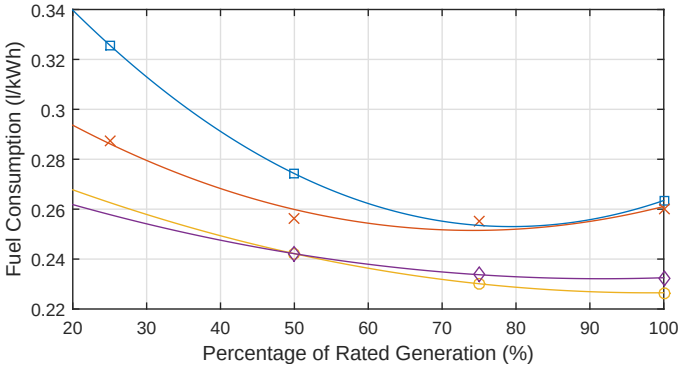

Fig. 2: Data sheet fuel consumption values of 54 kW [16] (blue squares), 71 kW [17] (red crosses), 1880 kW [5] (yellow circles), and 1575 kW [18] (purple diamonds) DG engines, with corresponding 2^{nd} degree polynomials.

3 Efficiency Variations

In an effort to demonstrate the potential efficiency variations on individual DGs in an IPP power plant and validate the use of least square fit 2^{nd} degree polynomial representations, this section presents measurement results obtained by limiting the flow through the air filter on a DG.

3.1 Experimental Setup

Fig. 3 shows a Titan/RS Pro OG1-SSS-SSQ-B oval gear flowmeter, mounted in the fuel supply path of a DG. The output of the flowmeter is sampled at 1 kHz by a HIOKI Memory HiCorder 8861 using a High Resolution Unit 8957 input module to collect fuel consumption information.

The DG consists of a Deutz BF4M2012 diesel engine driving a 60 kVA/48 kW Leroy-Somer LSA 42.3 L9 C6/4 synchronous generator. During experiments, the DG supplies a controllable load consisting of resistive JEVI heating elements mounted in a 10 m^3 water tank. With a 400 V phase-to-phase RMS voltage each heating element constitutes a 10 kW load. Multiple heating elements are coupled in parallel for increased load levels.

3.2 Experimental Procedure

The experiment is conducted as a two-part process. The conditions of the DG are, to the best of our ability, kept constant during both parts, except for the state of the air filter. Each part of the experiment is performed after an identical warm-up period of the DG from a cold starting point, i.e., both the DG and the ventilated room in which it is contained. Consumption measure-

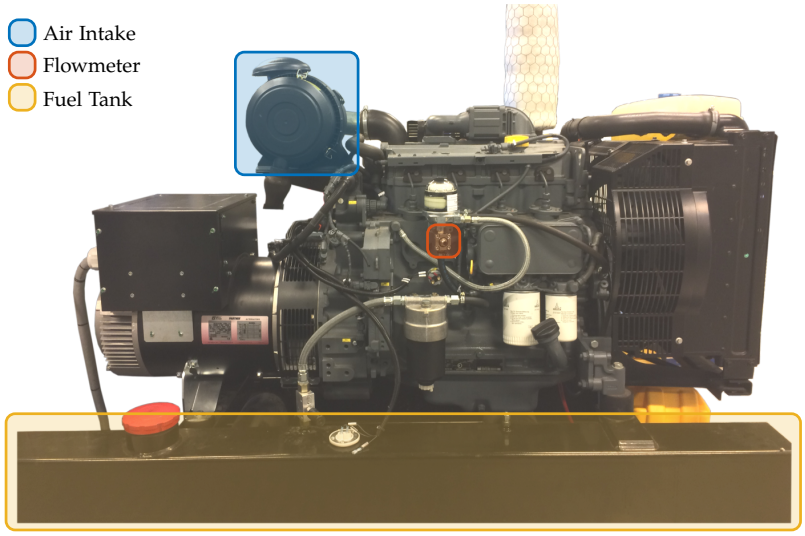

Fig. 3: Diesel driven generator set utilized during air filter experiments. The air filter is inside the air intake (blue), the burned fuel is pumped from the fuel tank (yellow) and measured by the flowmeter (red).

ments are then collected at various levels of constant load. These applied load levels are 20, 30, 40, and 50 kW.

A brand new air filter is fitted for one part of the experiment. For the other part of the experiment, a used air filter is covered in duct tape, to a state where the pressure drop across the filter reach service level at 50 kW load. Service level pressure drop is defined as the level of pressure drop across the filter for which the filter must be changed. For the utilized DG, service level pressure drop is 50 mbar.

3.3 Experimental Results

The presented measurements all represent average consumption values over 10-minute steady-state periods. Fig. 4 provides the results for both air filter conditions along with corresponding least-square fit 2^{nd} degree polynomials obtained with the MATLAB® function `polyfit()`.

Table 1 presents the fuel consumption results along with the corresponding air filter pressure drops. The pressure drops were observed using a Testo 435 multifunction meter.

We remind the reader that the absolute values of these experimental results should be analyzed with caution, both as a consequence of unavoidable measurement tolerances, the Titan/RS Pro OG1-SSS-SSQ-B has a documented accuracy of $\pm 0.5\%$, and the simplicity of the utilized experimental

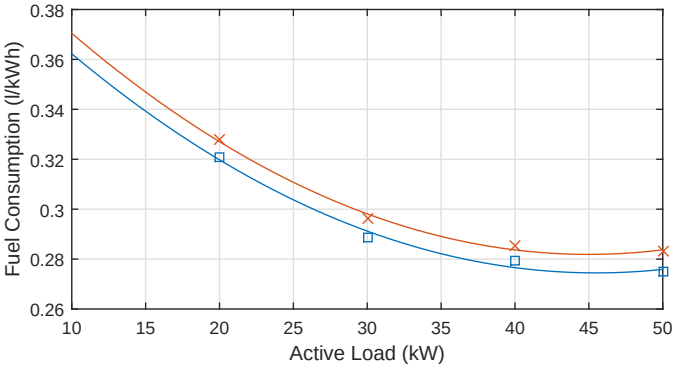

Fig. 4: Measured fuel consumption with new (blue squares) and taped (red crosses) air filter. Values are 10-minute steady-state averages, while the lines are corresponding least-square fit 2nd degree polynomials.

Table 1: Experimental data with new / taped air filter.

Load	Fuel Consumption	Air Filter Pressure Drop
20 kW	0.321 / 0.328 l/kWh	4 / 33 mbar
30 kW	0.289 / 0.296 l/kWh	5 / 39 mbar
40 kW	0.279 / 0.286 l/kWh	5 / 44 mbar
50 kW	0.275 / 0.283 l/kWh	6 / 51 mbar

setup. However, the key insight here is that these results do indeed confirm the influence of air filter conditions on the fuel consumption of a DG throughout its operating range and the suitability of 2nd degree polynomial representations.

4 Fuel Optimization

Utilizing assumed knowledge of individual DG fuel consumption characteristics as 2nd degree polynomials, this section presents two fuel optimization approaches to demonstrate the potential benefit of obtaining such information.

The fuel consumption curves in liters per kilowatt-hour are multiplied by the generated kilowatt to yield the consumption in liters per hour. The fuel consumption $f_i(x_i)$ in liters per hour of DG i with power generation x_i is, inherently, a strictly monotonic increasing 3rd degree polynomial. The fuel optimization problem, for a selection of n DGs and plant power reference r is given by

$$\min_{x} \quad \sum_{i=1}^{n} f_i(x_i) \tag{1a}$$

$$\text{s.t.} \quad 0 \leq x_i \leq \bar{x}_i \quad \forall i \tag{1b}$$

$$\sum_{i=1}^{n} x_i = r \tag{1c}$$

where $\bar{x}_i$ is the power generation rating of DG i, which for the typical IPP power plant is identical for all DGs. The inflection point of the 3rd degree polynomials lie around 50% of rated power generation. Hence, the polynomials are strictly convex functions for power generation above that point, which coincides with the region of highest efficiency. For n DGs with identical fuel consumption curves f operating in the strictly convex region of f, Proposition 1 shows that the plant power reference should be shared equally.

Proposition 1. *For any strictly convex function* $h(x_1, \ldots, x_n) = f(x_1) + \cdots + f(x_n)$*, where the function* $f : \mathbb{R} \to \mathbb{R}$ *is strictly convex, if* dom h *is constrained by* $x_1 + \cdots + x_n = r$*, the minimum of* $h(x_1, \ldots, x_n)$ *is at* $(x_1, \ldots, x_n) = (\frac{r}{n}, \ldots, \frac{r}{n})$.

Proof. By construction, the strictly convex level sets of $h(x_1, \ldots, x_n)$ are symmetric around the n-dimensional line $x_1 = \cdots = x_n$ and the unconstrained (global) minimum is on this n-dimensional line. If dom h is constrained by the surface $x_1 + \cdots + x_n = r$, the function $h(x_1, \ldots, x_n)$ attains a constrained minimum where the surface $x_1 + \cdots + x_n = r$ intersects the n-dimensional line $x_1 = \cdots = x_n$ which is at $(x_1, \ldots, x_n) = (\frac{r}{n}, \ldots, \frac{r}{n})$. ■

Presenting the proposition in a simple manner, Fig. 5 provides a sketch of the proof for $n = 2$.

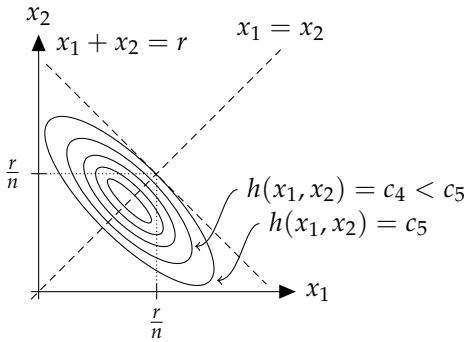

Fig. 5: Sketch of the constrained minimum for the strictly convex $h(x_1, x_2) = f(x_1) + f(x_2)$ where dom h is constrained by $x_1 + x_2 = r$.

Following the arguments in the Introduction and the confirming results shown in Section 3, we assume differences in fuel efficiency characteristics of the DGs in the plant. For simplicity, let each DG in the plant belong to one of five groups where the groups are distinguishable by their fuel efficiency

characteristics only. Fig. 6 presents five different fuel consumption curves which relate to DGs belonging to the corresponding group.

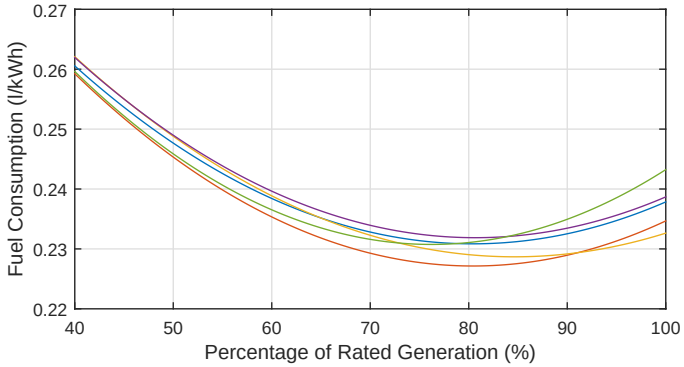

Fig. 6: Assumed fuel consumption curves of DGs in group 1 (blue), group 2 (red), group 3 (yellow), group 4 (purple), and group 5 (green), respectively.

4.1 Gradient Search Approach

For a given power reference to an IPP power plant, the optimum power distribution between a fixed selection of DGs with assumed 3rd degree polynomial fuel consumption characteristics can be found using a gradient search approach, if the selection of DGs meet one straightforward condition. Remember, the 3rd degree polynomial fuel consumption curves in liters per hour are strictly convex functions above their inflection points and a sum of convex functions is a convex function. The condition on the selection of DGs is therefore, that the selection must be one which allows every DG to operate in the convex region of fuel consumption while collectively accommodating the plant power reference.

We find the solution to this minimization problem (1) with the MATLAB® toolbox YALMIP [19], utilizing the interior-point method of the `fmincon` solver.

Case Study

With a selection of 30 DGs in total, consisting of six DGs belonging to each of the five groups, characterized by the fuel consumption shown in Fig. 6, we demonstrate the potential benefit of gradient search fuel optimization for a plant power reference of 55 MW when the power rating of each DG is 2 MW. Note, Proposition 1 extends to groups of identical fuel consumptions curves, that is, all six DGs of a group will generate the same amount of power in the optimal solution, whereas DGs of different groups will operate at different power generation levels.

Table 2 presents the power generation and fuel consumption results for the case described above. The optimal solution requires least power from DGs of group 5, which is in accordance with the fuel consumption curves in Fig. 6, where the green curve is the highest in the region of utilization for this specific plant power reference. Further, Table 2 presents the results for a solution where the plant power reference is distributed evenly among the 30 DGs, as current market-leading solutions do.

Table 2: Results utilizing the gradient search / even distribution approach for a fixed selection of 30 DGs.

Group	DGs†	Power Generation‡	Fuel Consumption‡
1	6	1.8341 / 1.8333 MW	427.68 / 427.46 l/h
2	6	1.8371 / 1.8333 MW	422.00 / 420.98 l/h
3	6	1.9376 / 1.8333 MW	447.95 / 420.76 l/h
4	6	1.8339 / 1.8333 MW	429.31 / 429.14 l/h
5	6	1.7239 / 1.8333 MW	401.59 / 432.71 l/h
Total	30	55 / 55 MW	12771.18 / 12786.35 l/h

†operational in Group, ‡per DG in Group

In comparison to the even distribution approach, the gradient search approach reduces the fuel consumption by approximately 15 liters per hour (0.1%) due to the simple redistribution of power generation among the DGs.

4.2 Genetic Algorithm Approach

If the selection of DGs operated to accommodate the plant power reference is *not* predetermined, the problem converts to a mixed-integer problem. To find the solution of this problem, a genetic algorithm approach is proposed, which is able to find the optimal selection of DGs to operate in an IPP power plant, when accommodating the plant power reference requires less than all the available DGs to optimize the total fuel consumption.

Generally, the structure of a GA is as shown in Fig. 7 [20, 21]. The only prerequisite for formulating a GA is the ability to find the fitness of any individual in the population, i.e., calculate the worth of any possible solution. In our particular case, this is the calculation of total fuel consumption of any possible power generation distribution, among the DGs in the plant, which accommodates the plant power reference. With the assumed 3rd degree polynomial fuel consumption information, that calculation is straightforward. GAs handle many possible solutions simultaneously and the collection of all these possible solution are denoted a population. The number of solutions in the population is a design parameter of the GA, referred to as the population size. Each successive repetition of evaluation, selection, crossover, and mutation is referred to as a generation. The following outlines the GA.

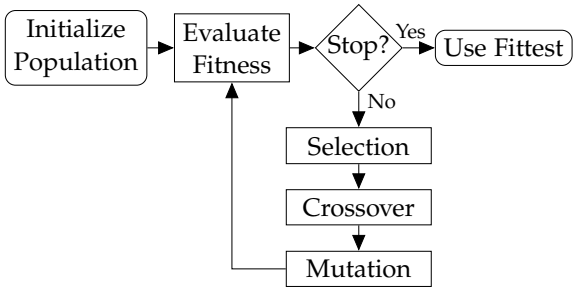

Fig. 7: General structure of a genetic algorithm [20, 21].

Initialize Population

The first element in the GA is to form an initial population, i.e., come up with a collection of possible solutions. In our GA, the initial population is formed by randomly assigning power to DGs in the plant. Until the total assigned power in a solution goes above the plant power reference, the power of randomly chosen DGs is selected uniformly in the range from the minimum allowable power to the DG rating. The minimum allowable power is defined as the average power needed from the remaining DGs during the forming of a solution to accommodate the plant power reference. Once the total assigned power goes above the plant power reference, that excess power is removed from the assigned power of the latest randomly chosen DG. The DGs without assigned power at this point, if any, will be part of the solution with zero power generation.

Evaluate Fitness

Each solution in the population can be evaluated by finding its total fuel consumption, utilizing the 3^{rd} degree polynomials.

Stop?

The stopping condition of the GA is set to a user-specified number of generations.

Selection

We utilize so-called tournament selection with replacement in which two solutions from the existing population are picked at random and the one with the best fitness is placed in the new population [20, 21]. This process is repeated until the new population is of the same size as the old population. Referred to as elitism [20, 21], a number of the most fit solutions are carried straight to the new population to guarantee survival of the fittest.

Crossover

Also known as mating, crossover is the process of mixing solutions in the population in hope of discovering solution with better fitness [20, 21]. The crossover in our GA takes its inspiration from the so-called single-point crossover [20, 21]. First, we pick two random solutions α and β from the population. With each solution containing the power generation of n DGs, we randomly choose a number γ between 1 and $n-1$. As a fifty-fifty chance, we choose whether to manipulate DGs 1 to γ or DGs $\gamma+1$ to n and denote the chosen set of DGs m. If the total power generation of the m DGs is zero in solution α or β, we choose a new random γ until this sum is non-zero in both α and β. We then calculate the power distribution of the m DGs for both α and β. Finally, we apply the power distribution of the m DGs in solution α to the m DGs in solution β while maintaining the total power generation of the m DGs in β, and vice versa, yielding two new solutions which both accommodate the plant power reference. However, some of the m DGs in the two new solutions might violate DG ratings due to the new combination of power distribution and total power generation. To prevent potential rating violations, the excess power of any such DG is removed and then added randomly to another of the m DGs until no violations occur in both of the two new solutions. Each α and β pair have a user-specified probability of going throug the entire crossover process, as described above, to form two new solutions. Alternatively, they go through the crossover process without manipulation. Random solutions are picked successively for crossover until a new population of the same size as before the crossover process began has been produced.

Mutation

To increase the diversity of the population, each solution in the population has user-specified probability of mutation [20, 21]. If a solution is subject to mutation, the power generation of a randomly picked DG in that solution is set to zero. The power removed by that mutation is added to the power generation of another randomly picked DG in the same solution. If this yields DG rating violations, the excess power is added randomly to another DG until no rating violations occur.

Case Study

For a 50 DG power plant, consisting of ten DGs belonging to each of the five groups shown in Fig. 6, we demonstrate the potential benefit of selecting the optimal DGs to operate for a 55 MW plant power reference when the power rating of each DG is 2 MW.

Table 3 presents the power generation and fuel consumption results using the GA with a population size of 1000, a crossover probability of 0.75, a mutation probability of 0.9, a stopping condition of 7500 generations, and carrying 10 solutions straight to the new population in accordance with the elitism principle. Table 4 presents the results for two solutions resembling current market-leading solutions with lack of individual fuel characteristic information. These two solutions determine the necessary number of operational DGs through a requirement for spinning reserve, set to 2 MW in this case. A spinning reserve matching the power rating of one DG is rather common for IPP power plants. For the case of a 55 MW plant power reference and 2 MW spinning reserve, a total capacity of 57 MW requires 29 operational 2 MW rated DGs. The two solutions differ by representing the most fortunate and most unfortunate selection of 29 DGs possible with respect to the fuel characteristics, which are unknown in current market-leading solutions.

Table 3: Fuel optimization results utilizing the genetic algorithm approach for a 50 DG power plant.

Group	DGs†	Power Generation‡	Fuel Consumption‡
1	5	1.6035 MW	370.17 l/h
2	10	1.6277 MW	369.76 l/h
3	10	1.7026 MW	389.36 l/h
4	0	0 MW	0 l/h
5	9	1.5200 MW	350.74 l/h
Total	34	55 MW	12598.58 l/h

†operational in Group, ‡per DG in Group

Table 4: Most fortunate / unfortunate even distribution approach results with 2 MW spinning reserve for a 50 DG power plant.

Group	DGs†	Power Generation‡	Fuel Consumption‡
1	9 / 9	1.8966 / 1.8966 MW	445.01 / 445.01 l/h
2	10 / 0	1.8966 / 0 MW	438.52 / 0 l/h
3	10 / 0	1.8966 / 0 MW	437.00 / 0 l/h
4	0 / 10	0 / 1.8966 MW	0 / 446.69 l/h
5	0 / 10	0 / 1.8966 MW	0 / 452.13 l/h
Total	29 / 29	55 / 55 MW	12760.29 / 12993.29 l/h

†operational in Group, ‡per DG in Group

The GA approach achieves fuel savings of 161 and 394 liters per hour (1.3% and 3.0%) compared to the most fortunate and most unfortunate choice of DGs, respectively, using the even distribution approach. Five additional DGs are operated by the GA approach, to achieve these fuel savings.

5 Conclusions

In this paper, two fuel optimization approaches for power plants consisting of multiple DGs have been presented.

1) A gradient search approach for a fixed selection of DGs.

2) A genetic algorithm approach for power plants where the selection of DGs is not predetermined.

Both optimization approaches utilize assumed information regarding individual DG fuel characteristics to demonstrate the potential fuel savings achievable by acquiring such information. In the two investigated case study scenarios, the potential savings range from 0.1% to 3%, which, in an "every bit counts"-industry, are indeed significant. Realistic variations in fuel characteristics have been found by measuring on a DG subject to critical air filter conditions. Further, these measurements confirm the air filter influence and the suitability of least square fit 2^{nd} degree polynomial fuel characteristic representations.

Genetic algorithms are well-established as an approach for finding solutions to non-convex problems; however, many different GA strategies exist, and there are no common methods that work well for all problems. The presented GA solves the investigated case in around eight minutes on a standard modern 2 GHz Intel® Core™ i5 laptop; in comparison, the simple gradient search approach solves its case in around three seconds. While the presented GA is rather consistent in terms of total fuel consumption, the power generation for individual DGs vary in tens of kW between consecutive GA runs. For the investigated case, we utilize Proposition 1 and assign the DGs of each group equal power generation, totaling the group power generation found by the GA. However, if each DG had unique fuel consumption characteristics, either designing alternative selection, crossover, or mutation methods, or combining the strengths of the GA with the gradient search approach could potentially work better.

Acknowledgment

The authors would like to thank Dr Robin Purshouse from the Department of Automatic Control and Systems Engineering at The University of Sheffield for inspirational discussions regarding genetic algorithms.

References

[1] DEIF, *Power & Control Technology: Independent Power Producers*, 2017.

[2] MAN Diesel & Turbo, *Power Solutions Independent Power Producers*, 2017.

[3] APR Energy, *Case Study: Peru | Peak Shaving*, 2017.

[4] ——, *Case Study: Argentina | Distributed Generation*, 2017.

[5] MTU Onsite Energy, *Diesel Generator Set MTU 16V4000 DS2250*. Datasheet, 2017.

[6] ——, *Diesel Generator Set MTU 16V4000 DS2500*. Datasheet, 2017.

[7] B. Kraemer, *Understanding Generator Set Ratings For Maximum Performance and Reliability*. Technical Article, MTU Onsite Energy, 2013.

[8] DEIF, *Land Power Application Guide*, 2016.

[9] C. F. Moyano and J. A. Peças Lopes, "An optimization approach for wind turbine commitment and dispatch in a wind park," *Electric Power Systems Research*, vol. 79, pp. 71–79, 2009.

[10] P. F. Odgaard and J. Stoustrup, "Fault Tolerant Wind Farm Control - a Benchmark Model," in *IEEE International Conference on Control Applications*, 2013, pp. 412–417.

[11] R. G. de Almeida, E. D. Castronuovo, and J. A. Peças Lopes, "Optimum Generation Control in Wind Parks When Carrying Out System Operator Requests," *IEEE Transactions on Power Systems*, vol. 21, no. 2, pp. 718–725, 2006.

[12] J. R. Marden, S. D. Ruben, and L. Y. Pao, "A Model-Free Approach to Wind Farm Control Using Game Theoretic Methods," *IEEE Transactions on Control Systems Technology*, vol. 21, no. 4, pp. 1207–1214, 2013.

[13] H. Zhao, Q. Wu, Q. Guo, H. Sun, and Y. Xue, "Distributed Model Predictive Control of a Wind Farm for Optimal Active Power Control - Part II: Implementation with Clustering-Based Piece-Wise Affine Wind Turbine Model," *IEEE Transactions on Sustainable Energy*, vol. 6, no. 3, pp. 840–849, 2015.

[14] J. Park, S.-D. Kwon, and K. H. Law, "A Data-Driven Approach for Cooperative Wind Farm Control," in *American Control Conference*, 2016, pp. 525–530.

[15] Leroy-Somer, *Low Voltage Alternators - 4 pole*. Datasheet, 2015.

[16] Deutz AG, *2012 The Genset Engine*, 2005.

[17] ——, *Genset Manual BF4M2012C*, 2015.

[18] MTU Onsite Energy, *Technical Engine Data 12V4000G23*. Datasheet, 2007.

[19] J. Löfberg, "YALMIP: A toolbox for modeling and optimization in MATLAB," in *IEEE International Conference on Computer Aided Control Systems Design*, 2004, pp. 284–289.

[20] D. E. Goldberg, *Genetic Algorithms in Search, Optimization and Machine Learning*, 1st ed. Addison-Wesley, 1989.

[21] K. Deb, *Multi-Objective Optimization using Evolutionary Algorithms*. John Wiley & Sons, Inc., 2001.

ISSN (online): 2446-1628
ISBN (online): 978-87-7210-117-0

AALBORG UNIVERSITY PRESS